School of Chemical and Petroleum Engineering

Department of Chemical Engineering

Degradation of organics from laundry water by photoelectrochemical and electrochemical processes on α-Fe$_2$O$_3$ nanostructure

Minh Hoang Nguyen

This thesis is presented for the degree of
Master of Philosophy

Of

Curtin University

December 2015

Declaration

To the best of my knowledge and belief this thesis contains no material previously published by any other person except where due acknowledgement has been made. This thesis contains no material which has been accepted for the award of any other degree or diploma in any university.

Signature: ....

Date: **01/12/2015**..

<u>Acknowledgement</u>

My great gratitude is dedicate to Australia Awards Scholarships program of Australia Government that gave me an unable better chance to study Master of Philosophy at Curtin University, and also two desirable years living in Australia.

My heartfelt gratitude must be presented to my supervisor Dr. Chi Phan for his continuous support of my Master study and research with extremely worthy instruction, patience and rigorous attitudes. Without his warm encouragement and thoughtful guidance, I had no chance to complete this thesis. I am also thankful for the excellent examples he has provided as how to be a successful scientist. It has been a great honor to be one of his students.

I owe a deep gratitude to my co-supervisor Associate Professor Tushar Sen. His knowledge always gives me inspiration. I also would like to thank to him for supporting to my study here continuously.

I am also grateful to Professor Vishnu Pareek being head of the school and my thesis chairman, who always encouraged me and praised my work, supported me morally and financially with great pleasure.

My sincere gratitude must go to Dr. Amir Memar, and laboratory technicians Guanliang Zhou, Andrew Chan, who gave me valuable helps for my experimental works, trainings on various equipment and software. They were not only the greatest demonstrators but also my dear friends and elder brothers.

To all of administration staffs, Julie Craig, Chris Kerin, Tracey, Hoa Pham, Araya Abera, Elaine Millers, and Tammy Atkins, I would like to express my gratitude for their help and kindness.

And last, but not the least, I would like to thank my parents, my beloved wife and my little daughter, who always give me their patience and unconditionally love. I truly thank them for sticking by my side, even when I was irritable and depressed.

Abstract

Recently, metal oxides, including α-Fe_2O_3 nanostructures have been widely used as a photocatalyst for wastewater purification owing to their cost-effectiveness, stability under deleterious chemical conditions, and environmental friendliness. This study concentrates on removing organic pollutants from laundry wastewater by employing electrochemical (EC) and photoelectrochemical (PEC) processes on α-Fe_2O_3 nanostructure.

Synthetic laundry water was prepared from commercial detergent powder and water. The applied voltage for the EC and PEC processes was between 1 and 3 V. α-Fe_2O_3 anodes were obtained by sol-gel spin coating method. The X-ray diffraction (XRD), Field emission scanning electronic microscopy (FESEM) was used to investigate morphology and crystalline of the α-Fe_2O_3 anode respectively. TOC removal testing was performed in the glass reactor with three-electrode system. For the PEC process, the reactor was irradiated under the solar simulator. Total organic compounds (TOC) were evaluated by the TOC analyzer. It was found that the PEC process showed higher efficiency than the EC method in all testing conditions. The higher the voltage, the higher TOC removal efficiency was. Lumped kinetic model was developed to simulate the kinetics of the degradation reactions. The model fitted experimental data well.

In the second part of the study, the same testing procedures were used to degrade sodium dodecyl sulfate (SDS), which is known as a most popular surfactant presented in laundry wastewater. In this case, the deposited substrates were annealed with a longer time. The highly porous α-Fe_2O_3 nanoflake structure was obtained. The disappearance of SDS after the first hour of treatment was observed via UV-Vis spectrum and Fourier transform infrared spectroscopy (FTIR). The different reactions and kinetics were also proposed, and they were numerically modelled. It was found that the degradation of SDS follows the first order kinetics, and it was also well simulated by ordinary different equations. In this work, the PEC method was more efficient than the EC process. The results showed that the simple PEC process can completely remove sulfate group from SDS, and reduce 90% of TOC. The

remaining organics contains hydroxyl and carboxylic groups are less harmful than SDS.

The results from this study present an economical and environmentally friendly method to reduce and remove pollutants from domestic laundry wastewater. The method is applicable to rural areas in developing countries where centralized wastewater facilities are not available.

Publications/ Presentations with Materials Produced in This Study

1. **Hoang M. Nguyen**, Chi M. Phan*, Tushar Sen, *Degradation of Sodium Dodecyl Sulfate by Photoelectrochemical and Electrochemical processes,* Chemical Engineering Journal, DOI: 10.1016/j.cej.2015.11.074.

2. **Hoang M. Nguyen**, Chi M. Phan*, Tushar Sen, Son A. Hoang, *TOC Removal from Laundry Wastewater by Photoelectrochemical Process on Fe_2O_3 Nanostructure*, Desalination and Water Treatment, DOI: 10.1080/19443994.2015.1064036.

3. **Hoang M. Nguyen**, Chi M. Phan*, Tushar Sen, *Photoelectrochemical degradation of Sodium dodecyl sulfate based on α-Fe_2O_3 nanostructure*, 4th European Conference on Environmental Applications of Advanced Oxidation Processes, 21-24 October, 2015, Athens Greece.

4. **Hoang M. Nguyen**, Chi M. Phan*, Tushar Sen, Son A. Hoang, *Degradation of organic compounds in laundry wastewater by photoelectrochemical process*, The 6th International Workshop on Advanced Materials Science and Nanotechnology (IWAMSN2014), 30 October - 02 November, 2014 Ha Long City, Vietnam.

Table of Contents

List of Figures

List of Tables

List of Abbreviations and Symbols

AOPs	Advanced oxidation processes	-
CMC	Critical micelle concentration	-
$C_{TOC}(0)$	The initial and transient TOC concentration	mg/L
$C_{TOC}(t)$	The TOC concentration at time t	mg/L
C_{SDS}	The concentration of SDS	mg/L
EC	Electrochemical	-
F	The Faraday constant	Ceq^{-1}
hv	Photon energy	eV
I	The current applied	A
Int	Intermediates generated during the degradation of SDS	-
$k_0, k_1, k_2, k_3, k_4, k_5$	The kinetic coefficients	min^{-1}
MCE	Mineralization current efficiency	-
MB	Methylene blue	-
PEC	Photoelectrochemical	-
Q_{SDS}	The TOC concentration corresponding to SDS	mg/L
Q_{ROH}	The TOC concentration corresponding to alcohols	mg/L
Q_{Int}	The TOC concentration corresponding intermediates	mg/L
R-H	Hydrocarbon	-
ROH	Alcohols formed during the degradation of SDS	-
SDS	Sodium dodecyl sulfate	-
SS	Stainless steel	-
TOC	Total organic carbon	-
V	The volume of solution	L

Chapter 1   Introduction

1.1.   Motivation

The rapid urbanization and the unceasing growing demand of water for drinking, industrial manufacture as well as daily activities cause the water scarcity in many countries throughout the world. This shortage constitutes a large number of severe consequences such as diseases, deaths, and pollution, particularly in arid, semi-arid areas, rural and remote areas, where centralized water treatment plants and technologies are limited. Meanwhile, the temporary solutions to tackle those challenges considerably rely on rivers, streams, groundwater and rain. These natured water sources, however, are depleting. Consequently, recycling or reusing wastewater is an important approach to encounter with this situation. However, these approaches have not been fully explored in many areas of the world [1]. The reason for this is the heavy financing investment required for wastewater treatment. Particularly in developing countries and rural areas, the water scarcity is very severe [2]. Surprisingly, the realistic reason is not only financial burden but also the ignorance of low - cost wastewater treatment technologies [3]. In other words, not only efficient water management but also extensive research is needed for sustainable water supply.

Recently, reusing domestic wastewater has been investigated in several developed countries. United States of America and Japan are two world leaders in reusing domestic water effectively [4, 5]. For developing countries, the reuse of domestic water is a relatively new concept [6]. Regulations and guidelines have only been developed recently, and still under modification in some areas [7]. Meanwhile, the benefits of treated domestic wastewater reuse for garden watering or general irrigation are obvious [8]. Domestic wastewater can be classified into two types: black water (from toilets), and grey water (from showers, dishwashers, laundries). Black water is much more polluted than grey water. Consequently, grey water is more attractive for reusing [9]. One of largest amount type of grey water is laundry wastewater. This wastewater is largely discharged every day (e.g., approximately 34% of the total water usage in Western Australia) [10]. The main ingredient of

laundry wastewater is synthetic surfactants. These chemicals are defined as the surface-active substances, which contain both hydrophobic and hydrophilic moieties, and can reduce the surface tension [11]. These synthesized surfactants are hard to be biodegraded in the environment [12]. Discharge of these apparently results in environmental pollution and threatens public health [13]. Consequently, removal of surfactants from laundry wastewater is a huge challenging for reusing purpose.

Moreover, among synthesis surfactants, sodium dodecyl sulfate (SDS), which is known as a strong surface – active anionic surfactant, is also the main ingredient of daily washing products such as shower soaps, gels, cosmetic as well as detergent. Due to its wide application, SDS has been considered as a major pollutant in wastewater. It has been pointed out that SDS in wastewater not only pollutes the environment, but also causes dangerous symptoms such as depression, labored breath, diarrhoea, and carbon metabolism disruption for animals [14]. Because of its extensive usage, SDS presents significantly in wastewater. For developing countries, where water treatment facilities are limited, the prolonged presence of SDS can have severe impacts on the environment.

The conventional techniques used to degrade synthesis surfactants, or SDS from laundry wastewater involve electrochemistry, adsorption, and various biological methods [15]. Recently, Advanced oxidation processes (AOPs) including photocatalytic, which oxidize organics from wastewater by generated hydroxyl radicals have been a special of interest, particularly when solar light is used [16]. In these processes, semiconductor photocatalysts, for example, α-Fe_2O_3, TiO_2, ZnO, or WO_3 are commonly used to oxidize organic contaminants [17]. Comparing with other photocatalysts, α-Fe_2O_3 exhibits superior properties such as affordability, and stability in chemical solution, environmental friendliness [18]. More importantly, this material has a suitable band gap (E_g = 2.2 eV) that is appropriate to be photo-excited by solar light [19]. α-Fe_2O_3 is thus utilized in a wide variety of applications such as water splitting, gas sensor, waste treatment [20].

The aim of this study is to explore the available energy (solar energy) to degrade synthesis organics from laundry water by photoelectrochemical and electrochemical

on α-Fe$_2$O$_3$ nanostructure. Particularly, this work focuses on the removal of a most widely used surfactant (SDS) from laundry water, which pollutes the environment, and is hard to be decomposed. The research is intended to apply to rural and remote areas, where technologies and budgets for wastewater treatment are limited.

1.2. Objectives of thesis

The main objectives of this research are:

- To synthesize α-Fe$_2$O$_3$ photocatalyst framework.
- To quantify the efficiency of photoelectrochemical and electrochemical processes for the removal of SDS and TOC.
- To quantify the kinetics of photoelectrochemical and electrochemical degradation of SDS and TOC from laundry water.
- To evaluate the stability of photocatalyst over the treatment time.

1.3. Thesis organization

Chapter 1: introduces the overall situation of the fresh water scarcity. The reasons for the need of laundry wastewater treatment were explained. The aims of this study are also presented.

Chapter 2: provides a comprehensive literature review on the physicochemical characteristics of laundry wastewater and SDS. Wastewater treatment technologies such as incineration, adsorption, chemical, biotechnology, electrochemical, advanced oxidation processes (AOPs) were discussed. The main objectives of this literature review were to: (i) provide an overview of different wastewater treatment technologies; (ii) select an appropriate method for laundry wastewater treatment.

Chapter 3: presents the methodology, materials, experimental setup of this study. Further, the analysis techniques were also introduced.

Chapter 4: discusses the removal of total organic compounds from laundry water by photoelectrochemical and electrochemical processes on α-Fe$_2$O$_3$ nanostructure. In this Chapter, α-Fe$_2$O$_3$ porous films were used as an anode for electrochemical and photoelectrochemical degradation of organic compounds from laundry water.

Lumped kinetic model was also proposed to describe the kinetics of these degradation processes.

Chapter 5: presents the degradation of SDS by photoelectrochemical and electrochemical processes. Two independently quantitative methods were used to quantify SDS and total organic compound concentration. The kinetics of the degradation reactions of SDS were numerically simulated by the different proposed models. Further, the presence of intermediates generated in the solution was also detected by Fourier transmission infrared spectroscopy.

Chapter 6: summarizes the study. This chapter is also devoted to the recommendations for future works.

Chapter 2   Literature review

2.1.   Introduction

Water is a fundamental resource for human need. It has been estimated that approximately 1.2 billion people are in the shortage drinkable water, 2.6 billion lack of sanitation [21], millions of people die every year from diseases related to contaminant water [22]. At this situation, a large number of people living under a stress of water shortage throughout the world is predicted to increase from half of billion to three billion in 2025 [23]. Particularly, about 900 million people living in remote and rural areas are forecasted to lack access to fresh water for their daily lives [24]. Moreover, food industrial manufacture, environment, energy and agriculture are also strongly impacted by water supply [25]. The demand for fresh water is thus predicted to increase with population growth and proposes further pressure to traditional sources such as rivers, dams, and streams, which, in turns, are depleting. For remote and rural areas, in which technologies and budgets for wastewater treatment are limited, water scarcity is much more unfavorable for daily livings of residents [26]. Apart from the increase in water demand, the adverse influence of contaminated water on both environment and human health is also of concern. It has been recognized that polluted water is the most serious risk associated with human health as well as animals [27]. Organic compounds in wastewater can be bio-accumulated in human bodies, and animal tissues, including reproductive and immune systems, endocrine disruption, and cancer. Consequently, wastewater treatment not only reduces water shortage and environmental pollution but also improves human health.

There are a large number of studies on wastewater treatment technologies such as adsorption, chemical, biological, and electrochemical processes. However, these techniques present several limitations including hazardous byproducts formation, high operation cost, and low treatment efficiency [28, 29]. As mentioned, research activities have centered on AOPs for degradation of organics from wastewater. Further, hematite nanostructure has also widely used in these technologies. However, this metal oxide has small hole diffusion length, and fast hole-pair recombination [30]. From these points of view, selecting an economical and

effective technology for wastewater treatment is a real challenge.

2.2.   Laundry wastewater

The treatment of largely discharged laundry wastewater is necessary for environmental and recycling purposes. To reuse this wastewater effectively, its properties such as ingredients, physical – chemical characteristics should be clarified. Laundry wastewater includes a wide range of components including organics from dirty clothes, metal ions, builders (sodium tripolyphosphate), or bleaching agents (sodium perborate), enzymes are also found [31]. However, the main ingredient is surfactants [32]. Surfactants are organic chemicals, synthesized via complex chemical reactions, from oil or fat raw materials [33]. They are wetting, emulsifying and dispersing which enable the removal of dirt from fabrics and keeping the soil suspended in the washing water [34]. Surfactants can be classified into three different groups: non-ionic, anionic and cationic surfactants [35]. Among these, anionic surfactants account for approximately 80% of the total surfactant production [36]. Anionic surfactants used in daily products such as detergent, soaps, shower gels usually include different types such as linear alkyl benzene sulfonates (LAS), alkyl sulfate (AS), alkyl ether sulfate (AES), alkyl ethoxylates (AE) [37].

In environmental aspects, the risk assessment of surfactants to terrestrial plants and animals was reported in several previous research works [38, 39]. The drainage of these types of chemical damages the ecosystem. In fact, the original soaps are very difficult to be degraded in the environment, and their residues remained in the waterway. Moreover, organic components presented in laundry wastewater are almost dissolved matters. Thus, a preferred technique used to treat this kind of water should be not only physical methods but also advanced oxidation processes.

2.3.   Sodium dodecyl sulfate

Sodium dodecyl sulfate (SDS) is known as a most widely used anionic surfactants in science, technology, and industry [40]. This is the most popular surfactant amongst alkyl sulfates presented in daily using products. With the average annual output of more than eight million tons of detergent products in both powder and

liquid forms [41], the accumulation of alkyl sulfate surfactants, including sodium dodecyl sulfate as a primary contaminant in municipal wastewater has been an environmental concern. Concerning chemical properties, SDS is monomeric form in both polar and nonpolar solvents at low concentration. When critical micelle concentration (CMC) is reached, regular micelles are formed [42]. At this stage, the hydrophobic chain of SDS heads to the bulk of the nonpolar solvents (i.e., oil). On contrast, the hydrophilic head group turns inside the micelles. Thus, water - in - oil emulsion is formed in this case [43]. In polar solvents, the situation is reversed: head group turns into the bulk of solvent while nonpolar hydrocarbon chain points to hydrophobic molecules and form micelles (oil - in - water emulsion).

Because of its favorable physicochemical characteristics, SDS is widely used in many industrial fields. However, it has been found that the amphoteric properties of SDS assist for the accumulation of SDS in living organisms [14]. The negatively charged head group can bind to the positively charged molecular substructures via electrostatic forces. While, the hydrophobic moiety may interact with the nonpolar parts of the target organs or organisms by hydrophobic forces [44]. Consequently, not only living species, or aquatic plants, but also human are adversely impacted by the presence of SDS in water [45]. The removal SDS from wastewater has thus been intensively investigated recently [46].

2.4. Wastewater treatment processes

This section reviews the current physical, chemical, biological and advanced oxidation processes technologies often used in wastewater treatment.

2.4.1. Incineration

This process is to combust contaminants in oxygen - rich environment at high temperature (over 800 ^{0}C). In this technique, innocuous carbon dioxide and water are formed. Incineration includes the following steps [47]:

$$R - H + O_2 \xrightarrow{T} CO_2 + H_2O \qquad\qquad 2\text{-}1$$

$$R - Cl + O_2 \xrightarrow{T} CO_2 + H_2O + HCl \qquad\qquad 2\text{-}2$$
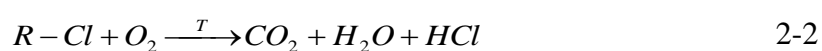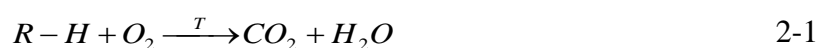
This conventional technique was widely used and successful. However, it is not

always a complete process [48]. In fact, byproducts such as hazardous solid waste, NO_x, chlorine, dioxin and other gasses are often generated during the combusting process [49]. These second pollutants can constitute more dangerous risks (cancer, or serious respiratory diseases) than the original wastes [50]. Moreover, this method apparently consumes higher energy, and usually requires further treatment steps, for instance, air treatment equipment [51]. The whole wastewater treatment is thus complicated and expensive.

2.4.2. Adsorption

Adsorption is known as a simple and economical technique for water purification. By comparing with another wastewater treatment technologies, adsorption displays cost - effective, flexible and simple for design [52]. Moreover, operating conditions and harmful byproducts generation are also excluded from this process. There are different adsorbents commonly used to remove organic pollutants from wastewater:

2.4.2.1. Activated carbon

Activated carbon has been widely used for removing pollutants from both liquid and gas phase in the industry [53]. The term "activated carbon" refers to a wide range of amorphous or random structures of carbon materials, which are porous and have a large surface area for organics to be absorbed [54]. During the treatment process, all molecules propose attractive forces driven stronger connections between organics and carbon molecules than those between organics in wastewater [55]. Accordingly, pollutants in wastewater are not only captured on the surface of carbon material, but they also penetrate into the pore channels to contact with the internal structures where the strongest attractive forces locate [56]. In this process, both physical and chemical adsorption may spontaneously occur on a carbon surface [57].

There are generally two size activated carbon: (1) powdered carbon (diameter < 200 mesh) and (2) granular carbon (diameter > 0.1 mm) [58]. Granular carbon is much more widely used in wastewater treatment, while powdered carbon is less used frequently owing to its relatively small particle size [59]. Activated carbon is made of different source materials such as coal, coconut, shells, wood. Coal is a

mixture of carbonaceous and mineral materials derived from the combustion of plants. El Quada et al. [52]; Tamai et al. [60]; Banat et al. [61]; have successfully used coal as an adsorbent for removing dye from wastewater. Moreover, biomass and other waste materials are also considered as the cost effective and renewable sources of activated carbon [62]. These disposed materials do not have much economic value and often pollute the environment. Reusing these wastes as an adsorbent for wastewater treatment is not only ideal for the cost reduction for wastewater treatment but also offers potentially inexpensive alternatives to existing commercial activated carbon [63].

2.4.2.2.   Clays

Natural clays minerals such as bentonite, kaolinite, diatomite have been used as an adsorbent for both inorganic ions and organic from wastewater because of their high sorption capacity. Moreover, the favorable layered structure and the ability to ion exchange with pollutants, and ions result in larger amount pollutants, and ions could be absorbed [64]. Particularly, the removal of methylene blue by adsorption on clays have been reported by many scientists such as A. Gurses et.al [65] Dipa Ghosh [66], Li Zhaohui et al. [67]. The adsorption of methylene blue on clay minerals is mainly owing to ion-exchange process. Meanwhile, Ferrero et al., [68] also indicated that the adsorption of dye onto clays is general because of physical adsorption (dominated by the particle size) and electrostatic interactions (dominated by the pH).

2.4.2.3.   Zeolites

By having favorable physicochemical properties such as porous structure, cation exchange, molecular sieving, catalysis and sorption, natural zeolites are at a great interest for environmental applications [69]. Natural zeolites such as chabazite, mordenite, clinoptilolite, analcime, phillipsite, stilbite, and laumontite are very common forms [70]. On contrast, barrerite, paulingite, and mazzite are much rarer [71]. Natural zeolites are highly porous aluminum silicates with various hollow and three - dimensional structures. Further, they also have a negatively charged lattice. For these reasons, natural zeolites possess the high ion-exchange capability,

relatively high specific surface areas. More importantly, these materials are affordable, and thus, natural zeolites are to be more attractive adsorbents [72].

Natural zeolites have been proposed for methylene blue removal. Han et al., indicated that approximately 98% methylene blue could be removed by natural zeolites [73]. As for these materials, the increase in sorption capacity is mainly at the result of the increase in the surface area rather than a specific interaction [74]. Consequently, the overall removal efficiency of pollutants from wastewater by natural zeolites may not be as high as that of clay materials. However, theses associated limitations may be compensated by their availability and inexpensive cost.

In summary, the efficiency removal of pollutants from wastewater by adsorption apparently heavily depends on parameters such as temperature, pH, interface contacting time, and the absorbent assay pore size [75]. However, it should be pointed out that contaminants in wastewater include dissolved organics or smaller size than that of the carbon pore openings. Moreover, some constituents in glycol, amine, can cause foaming or fouling of equipment [76]. Thus, organics cannot be completely collected on and inside absorbents [77]. Consequently, adsorption methods should be combined with other advanced processes to remove both undissolved and soluble contaminants efficiently.

2.4.3. Chemical oxidation

Chemical oxidation is another simple technique used to transfer organic compounds from wastewater to less harmful components by oxidizing agents. In this operation, one, or more electron is transferred from the oxidants to the targeted pollutants producing the degradation of these contaminants [78]. The capacity of the oxidation of chemical compounds against pollutants in the wastewater depends on reduction - oxidation (redox) potential of each oxidizing agent [79]. The larger redox potential of the oxidant is, the higher the oxidizing ability of oxidants is. The standard redox potential of commonly used oxidants is shown in the following table.

Table 2-1. Oxidation potential of different oxidants [80].

Oxidants	Redox Potential E^O (eV)
Fluorine	3.03
Hydroxl radical	2.70
Sulfate radical	2.60
Atomic oxygen	2.42
Ozone	2.07
Persulfate	2.01
Hydrogen peroxide	1.78
Permanganate	1.68
Chlorine dioxide	1.57
Hypochlorous acid	1.49
Chlorine	1.36

Persulfate, peroxide, ozone, and permanganate are widely used as oxidizing agents for wastewater treatment [81]. One another common oxidant of chemical oxidation is alkaline chlorination. Accordingly, chlorine under alkaline conditions can effectively destruct contaminants such as pesticide, cyanide [82]. However, chemical oxidation is a selective oxidizing method for a few pollutants, and it may generate second contaminated products such as chloroform and its derivatives [83]. Potassium permanganate considered as an eco-friendly oxidant is also commonly used for water purification. In the permanganate ion, manganese has an oxidation state of +7, and it can form series of oxidation state in wastewater solution such as MnO_4^-, $HMnO_4$, MnO_3^+, $H_2MnO_4^+$ [84]. The change of these intermediate oxidation states depends upon various reaction conditions, types of substrate and their stability [85]. Potassium permanganate can be effectively used to destroy a wide range of organic compounds in wastewater such as acids and alcohols. However, this technique generates precipitations in magnesium oxide forms [86]. Consequently, it needs further treatment processes.
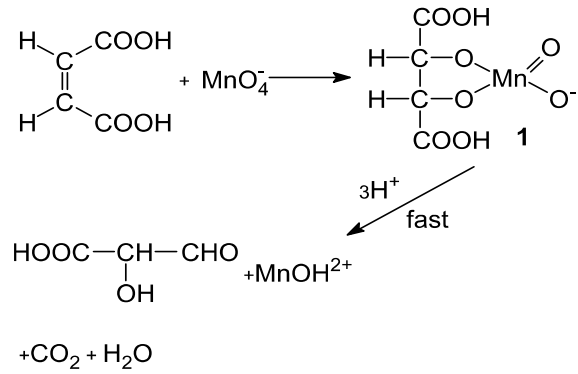
Figure 2-1. A diagram of oxidizing process by potassium permanganate [86].

One another oxidizing method widely used in wastewater treatment is ozone method. Ozone is known as a vigorous oxidant including both single and one double oxygen bond [87]. The double bonds are inactive while single bonds are straightforward to be released. Hence, free OH^* radicals in water oxidizing pollutants can be formed easily by these single attacks.
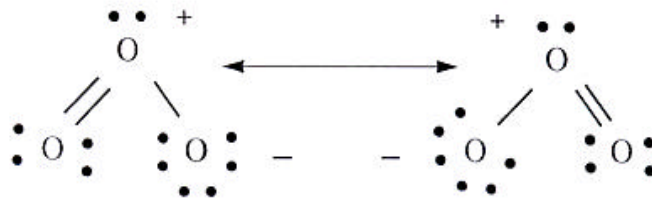
Figure 2-2. Resonant structure of ozone [88].

Ozone is a highly reactive chemical that can quickly react with many organic compounds, particularly for substances having C=C, N=N, C=N bonds [89]. However, this treatment process is only effectively used to degrade minerals and salts [89]. Moreover, ozone is also high energy consumption.

Chemical oxidation can be effectively used to remove dissolved pollutants from wastewater. Nevertheless, this method produces harmful byproducts, and exhibits lower rates of organic degradation compare to other techniques based on the free radicals [90].

2.4.4. Biological degradation

Biological processes have been widely used in wastewater treatment. The visible

advantages of this method compared to other techniques are operating cost and capital investment [91]. Biological degradation can take place in two ways: aerobic and anaerobic. In aerobic biological treatment, microorganisms (called aerobes) operating as catalysts are used to decompose organics in oxygen - riched environment [92]. By contrast, when those pollutants are degraded by anaerobes without free oxygen surrounding is anaerobic treatment technique [93]. In general, the final products of these two processes are CO_2, biomass, and methane (anaerobic process) [94].

In the aerobic biological process, activated sludge system is commonly used to remove organic compounds. This system includes an aeration tank where reactions take place, an aeration source (mixed liquor suspended solids or mixed liquor volatile suspended solids) that supplies dissolved oxygen [95]. Aerobic bacteria thrive, and move around the aeration tank. These microorganisms multiply rapidly with sufficient food and oxygen from aeration source. Subsequently, they use most of the organic matter to produce new cells, and eventually settle to the bottom of the clarifier tank, separating from the clean water [96].

Anaerobic methods are also appropriate techniques for removing surfactants from daily laundry wastewater. By comparing with aerobic processes, they exhibit higher performance in treating industrial and agricultural effluents [97]. In this process, anaerobic filters, hybrid digesters, upflow anaerobic sludge blanket, and anaerobic sequencing batch reactors are also employed for treating dairy effluents (**Figure 2-3**).
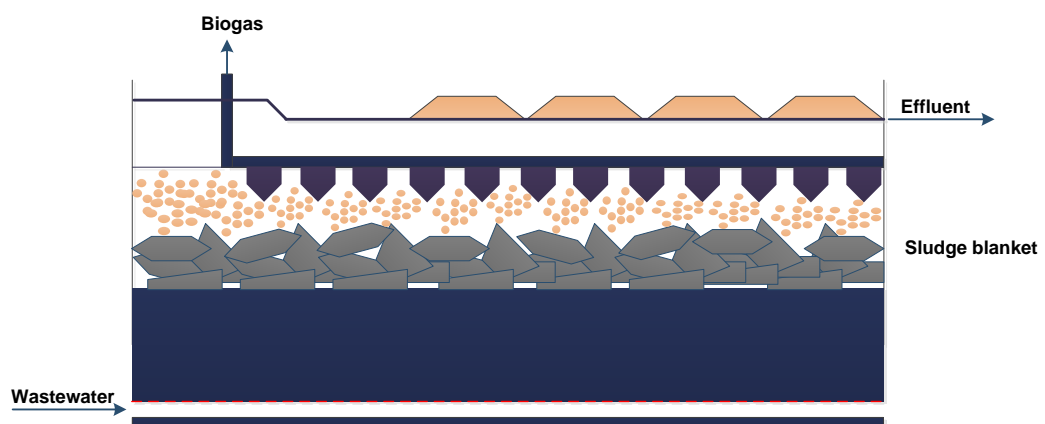
Figure 2-3. Upflow anaerobic sludge (UASB) blanket [98].

There are two types of anaerobic processes: single – and two – phase. The performance of these processes generally can be up to 97 % [99]. Original objectives of these two techniques are to obtain a high degree of wastewater stabilization, and a high conversion of effluents to methane [100]. Whereby, anaerobic filter reactors are used in single – phase methods. By contrast, the acid reactor is utilized to provide the appropriate substrate for the subsequent methane phase reactor in two – phase operation [101]. The second anaerobic process is considered higher efficacy than conventional single – phase design [99]. Moreover, two – phase anaerobic treatment system are particularly suitable for treating wastewater containing high concentrations of organic suspended solids [102].

Recently, membrane bioreactor (MBR) has been known as the latest technology of biological wastewater treatment for removal of contaminants from wastewater [103]. This technique is widely applied in domestic wastewater treatment. The membrane bioreactor process is almost similar to the activated sludge processes in terms of liquor solids mixed in suspension in an aeration tank [104]. However, in the MBR process, the bio-solids are separated employing a polymeric membrane based on microfiltration or ultrafiltration unit, as against the gravity settling process in the secondary clarifier in conventional activated sludge process [105]. As a consequence, membrane bioreactor has more benefits than the activated sludge process regarding higher bio-solid concentration, occupied space (aeration tank in this method is smaller than that in activated sludge process) [106].

Overall, biological technologies can be utilized to remove synthetic surfactants from wastewater. However, these methods need additional treatment steps to remove suspended contaminants [107]. Moreover, they are unfriendly to operate.

2.4.5. Electrochemical technologies

Wastewater treatment by electrochemical processes was first proposed in the UK in 1889 [108]. These methods have been intensively investigated and developed. Electrochemical technologies can be classified into two main different methods such as electrocoagulation, electro - oxidation.

2.4.5.1. Electrocoagulation

Electrocoagulation, sometimes named as electro - flocculation, has been widely utilized for wastewater treatment on an industrial scale. This technology has early illustrated its superior efficiency in removing wastewater containing suspended solids, oil, and grease [109]. Furthermore, inorganic or organic pollutants, which can be flocculated, can also effectively be removed by this technique.

Coagulants in electrocoagulation are generated by dissolving either aluminum or iron ions from respectively aluminum or iron electrodes electrically. The metal ions formation occurs at the anode. Meanwhile, at the cathode, H_2 gas is released. This gas also assists to float the particles out of the water. The reaction pathways are as the following equations [108].

At aluminum anode:

$$Al - 3e \rightarrow Al^{3+} \qquad \text{2-3}$$

In alkaline conditions:

$$Al^{3+} + 3OH^- \rightarrow Al(OH)_3 \qquad \text{2-4}$$

In acidic conditions:

$$Al^{3+} + 3H_2O \rightarrow Al(OH)_3 + 3H^+ \qquad \text{2-5}$$

In case of iron anode used:

$$Fe - 2e \rightarrow Fe^{2+} \qquad \text{2-6}$$

In alkaline conditions:

$$Fe^{2+} + 2OH^- \rightarrow Fe(OH)_2 \qquad \text{2-7}$$

In alkaline conditions:

$$4Fe^{2+} + O_2 + 2H_2O \rightarrow 4Fe^{3+} + 4OH^- \qquad \text{2-8}$$
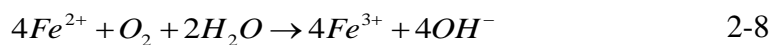
The oxygen evolution reaction is:

$$H_2O - 4e \rightarrow O_2 + 4H^+ \qquad\qquad 2\text{-}9$$

Meanwhile, at the cathode, hydrogen gas is released:

$$2H_2O + 2e \rightarrow H_2 + 4OH^- \qquad\qquad 2\text{-}10$$

In the simplest configuration, an electrocoagulation reactor may include an electrolytic cell with cathode and anode. However, this reactor is not appropriate for wastewater treatment due to metal dissolution (the anode is corroded, and the cathode is passive). This issue has been overcome by monopolar electrodes either in parallel or in series connections for the reactor shown in the following figure.
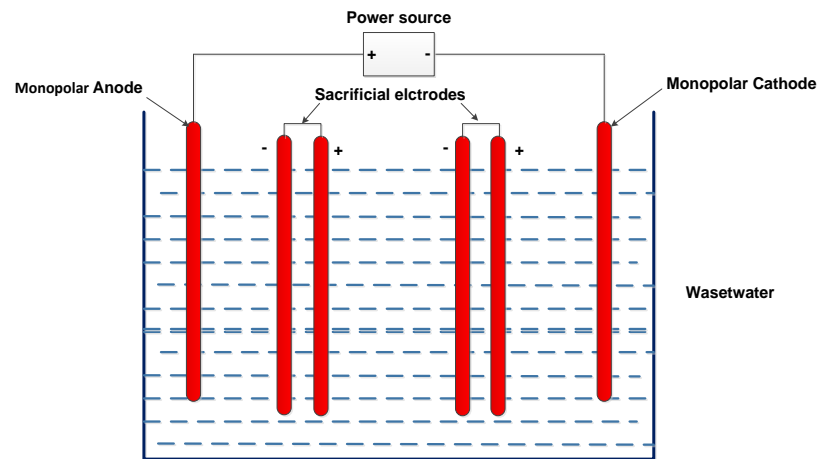
Figure 2-4. The electro-coagulation reactor [110].

In this configuration, when the current crossing between anode and cathode, the neutral sides will be transformed to charged sides of the conductive plate. Accordingly, these charged sides will have opposite charge respect to the parallel side [111]. At this stage, the sacrificial electrodes are used as bipolar electrodes. Consequently, anodic reactions occur on the positive sides. On contrast, cathodic reactions are encountered on the negative sides. Iron or aluminum is normally utilized as sacrificial electrodes [112]. These materials also continuously produce ions for the electrocoagulation system. Moreover, coagulation is initiated while the charges of the particles are also neutralized by generated ions [113]. Pollutants from wastewater can also be removed by these free ions via the chemical reaction and precipitation [114].

In summary, electrocoagulation requires simple equipment, and it is easy to operate. However, the high conductivity of wastewater suspension is required. Furthermore, gelatinous hydroxide may tend to solubilize in some cases. More importantly, the physicochemical properties of both water and pollutants may be altered by interactions between applied current and colloidal, oils moving through the system.

2.4.5.2.   Electro-oxidation

Electro-oxidation science was investigated from the 19th century when cyanide electrochemical decomposition was conducted [115]. The intensive investigations on this technology have started since the late 1970s. Electrochemical processes have recently drawn large interests for the treatment of polluted waters. In comparison with other wastewater treatment processes, electrochemical oxidation has been considered as an effective technology, which can be able to decompose non-biodegradable organic pollutants, and remove nitrogen species from wastewater [108]. Electrochemical oxidation of organic pollutants can occur through two different oxidizing mechanisms as shown in **Figure 2-5**:

(i) Decomposing organic pollutants at the anode surface. This process is called direct oxidation (**Figure 2-5a**).

(ii) A mediator (HClO, $H_2S_2O_8$) is used to electrochemically oxide pollutants under electrochemical activities. It is indirect oxidation (**Figure 2-5b**).
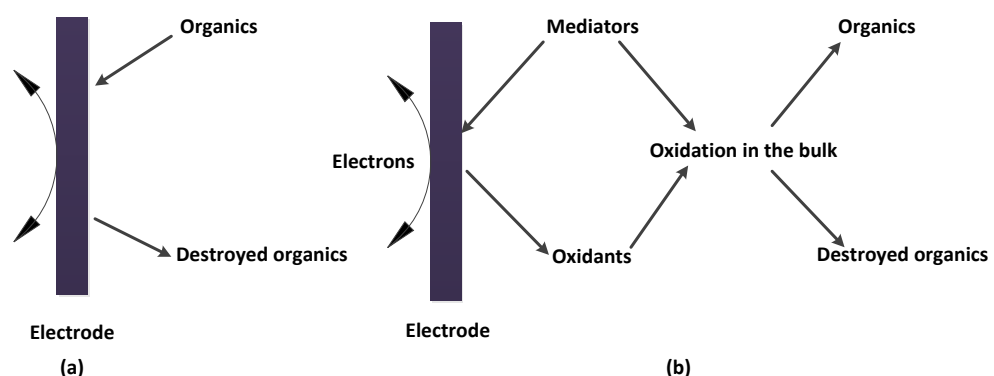
Figure 2-5. Diagram of (a) direct and (b) indirect oxidation treatment of pollutants [116].

Direct electrochemical oxidation requires adsorption of contaminants onto the electrode surface. This process can occur at relatively low potentials. On contrast, indirect electrolysis depends on oxidizing species generated at the electrode that can mediate the transformation of pollutants.

2.4.5.2a.   Direct oxidation

Direct anodic oxidation is the simplest form of electrochemical technologies for water purification. Direct oxidation of pollutants occurs as two following steps [117]:

- Pollutants diffuse from the bulk solution to the anode surface.
- Pollutants are oxidized at the anode surface. This oxidizing process occurs though physically adsorbed "active oxygen" (adsorbed hydroxyl radical, *OH) or chemisorbed "active oxygen" MO_{x+1}).

The efficiency of this technique depends on three factors: (i) The anode material; (ii) the generation of adsorbed hydroxyl radicals; and (iii) the competition with the oxygen evolution reaction [118]. During anodic oxidation process, there are two different ways can be followed [119]:

- Electrochemical conversion: In this period, partial oxidization of organics occurs, whereby, toxic, non-biocompatible contaminants are oxidized and transformed to biocompatible organics.

$$R \rightarrow RO + e^- \hspace{4cm} 2\text{-}11$$

- Electrochemical combustion: Organics are transferred to innocuous carbon dioxide, water, and salts, and thus, no post-treated process is necessary.

$$R \rightarrow CO_2 + H_2O + Salts + e^- \hspace{3cm} 2\text{-}12$$
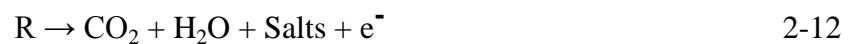
The anodic oxidation does not require a lot of chemicals added to wastewater, or even to provide oxygen to cathodes [120]. Apparently, these advantages contribute to the larger attraction of direct oxidation compared to other electro-oxidation processes [121]. For this process, the important factor is undoubtedly the anode material. There have been many types of anode materials such as boron-doped diamond electrodes [122], diamond [123] or metal oxides RuO_2[124], IrO_2 [125],

TiO$_2$ [126]. However, they are either expensive or not efficient enough. Developing an alternative anode material for wastewater treatment is thus a part of this study work.

2.4.5.2b.   Indirect oxidation

In this technique, peroxide, Fenton's reagent, Cl$_2$, hypochlorite, peroxidisulfate, and ozone are used as mediators to decompose organics in wastewater. Among these, chlorine is commonly used electrochemical oxidant to destroy pollutants because of its ubiquitous character of Cl$^-$ ion in wastewater. The efficiency of this method depends on the diffusion of oxidants in wastewater treatment, temperature and pH [127]. Chlorine and hypochlorite generated at the anode can be used to destruct contaminants [128]. In fact, this method is more effective than direct oxidation in preventing electrode corrosion [129]. However, it also should be considered the formation of halogenated byproducts. Moreover, to maintain the efficiency of the process, the concentration of chlorine in solution must not be decreased [130]. As a result, a large amount of salt has to be periodically supplemented. This issue limits the wider applications of indirect oxidation in the industry. In spite of concerns about chlorine intermediates and complicated facilities required, but indirect oxidation is an applicable process to treat wastewater containing toxic or bio - refractory pollutants.

In summary, electrochemical oxidations can be effectively used for decentralized gray water treatment owing to their high efficiency, operation at ambient temperature and pressure. Furthermore, the influent composition and flow rate can also be able to be the adjusted to variations. More importantly, electrochemical processes can be adapted to various applications, and can be easily combined with other existing treatment techniques [120]. However, the high cost of electrodes and energy consumption limit the wider application of electrochemical process [131].

2.4.6. Advanced oxidation processes

Advanced oxidation technologies for wastewater treatment have recently drawn many attentions from scientists and researchers. These methods are cost - effective, highly efficient and environmentally friendly [132]. These techniques include

different processes such as Fenton's reagent, photocatalytic oxidation. Their oxidizing efficacy mainly depends on the hydroxyl radicals (*OH) generated oxidizing reagent or photocatalysts under illumination. Free radicals are reactive and none - selective, and can oxidize a large number of pollutants [133].

2.4.6.1.   Fenton processes

2.4.6.1a.   Fenton reagent

The mixing ability of hydrogen peroxide and iron (II) to destroy tartaric acid was first discovered in 1876 [134]. After the next eighteen years, this Fenton's chemistry study was officially published [16]. Hydrogen peroxide is decomposed by ferrous ions used as a catalyst. The Fenton reactions are continued by Fe^{2+} regeneration that can occur by the reduction of Fe^{3+} with H_2O_2 as shown in the following equations [135]:

$$Fe^{2+} + H_2O_2 \rightarrow Fe^{3+} + {}^*OH + OH^-$$
2-13

$$Fe^{3+} + H_2O_2 \rightarrow Fe^{2+} + HO_2^* + H^+$$
2-14
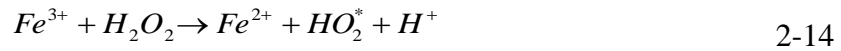
Moreover, in the condition of a proper pH condition (2.8 - 3.0), the activity of oxidizing radicals via the catalytic properties of Fe^{3+}/Fe^{2+} couple can be thrust [136].

$$Fe^{2+} + H_2O_2 \rightarrow Fe(OOH)^{2+} + {}^*H^+$$
2-15

$$Fe(OOH)^{2+} \rightarrow Fe^{2+} + {}^*HO_2^*$$
2-16

$$Fe^{3+} + HO_2^* \rightarrow Fe^{2+} + O_2 + H^+$$
2-17
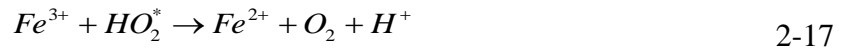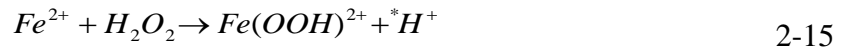
Organic compounds (RH) are mainly oxidized by hydroxyl radicals as presented as the following equation [137]:

$$^*OH + RH \rightarrow H_2O + R*$$
2-18
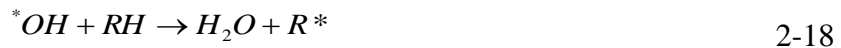
The produced intermediate organic radicals (R^*) can react with Fe^{3+} and H_2O_2, forming R^+ and ROH that can be further oxidized as in the **Eq.2-19** to the **Eq.2-21**

[138, 139]. Finally, innocuous carbon dioxide and water are produced from (**Eq.2-22**) reaction:

$$Fe^{3+} + R^* \rightarrow Fe^{2+} + R^+$$ 2-19

$$R^+ + OH \rightarrow ROH$$ 2-20

$$R^* + H_2O_2 \rightarrow ROH + {}^*OH$$ 2-21

$$ROH + {}^*OH \rightarrow CO_2 + H_2O$$ 2-22

The performance of this process depends upon different parameters such as pH, temperature, concentration of peroxide and catalyst. Particularly, a careful pH control is needed to operate this method properly [140]. At low pH value, for example, 2.8, the concentration of Fe^{2+} available in the system is high, and it thus boosts Fenton's reaction rate. Conversely, $Fe(OH)_3$ begins to accumulate when pH value > 5.0, and thus, decreases catalyst activity. Likewise, the temperature is also an important factor. When the temperature increases, the kinetics of the reactions are enhanced. However, oxygen and water are also largely formed by the vigorous decomposition of hydrogen peroxide. These species diminish the oxidizing efficiency.

2.4.6.1b. Photo-Fenton reaction

In this process, ultraviolet or solar light illumination is used to support the oxidizing reactions of Fenton's reagent. Accordingly, this combination generates much more reactive radicals than only Fenton reactions. In this case, hydroxyl radicals are generated by the reaction between hydrogen peroxide and UV light ($\lambda <$ 285 nm) as shown in the **Eq.2-23** [141, 142].

$$H_2O_2 \xrightarrow{h\nu} ROH + {}^*OH$$ 2-23

Photo-reduction reactions, which reproduce Fe^{2+} from the **Eq.2-23** of aqueous ferric ions also occurs [143]. Apparently, photon activities in this process are boosted since hydroxyl radicals are both generated from Fenton's reactions and photon excitation. However, the precipitation of Fe (III) species decreases the treatment efficiency.

Overall, Fenton processes are effective techniques for decomposing a wide range of organic pollutants such as anilines, toluene, herbicides, phenols, anilines, and toluene from wastewater [144]. However, several drawbacks of these processes such as highly remained iron concentration, manpower requirement for removing sludge, and catalysts recycling should also be taken into account [145, 146].

2.4.6.2. Photocatalysis technologies

Among advanced oxidation processes, photocatalysis methods such as photochemical, photoelectrochemical techniques have early exhibited their high performance for wastewater treatment. These techniques have been widely used to treat both dissolved and solved organics from wastewater since nineteenth century [147].

2.4.6.2a. Photocatalysis mechanism

Photocatalysis processes have been considered as the effective and inexpensive methods for the removal of organic pollutants from wastewater [148]. Many semiconductor metal oxides such as Fe_2O_3, TiO_2, ZnO have been utilized for photocatalytic oxidation. The commonly - used photocatalysts are listed in the following table.

Table 2-2. List of band gap energy and adsorption threshold of various semiconductor photocatalysts [149].

Semiconductor	Band Gap Energy (eV)	Wavelength Sensitivity
TiO_2 (anatase)	3.2	388
TiO_2 (rutile)	3.0	413
ZnO	3.2	388
ZnS	3.6	344
Fe_2O_3	2.3	539
$SrTiO_3$	3.2	388
WO_3	2.8	443

When photon energy (hv) from the illuminated light is greater than or equal to the band gap energy of semiconductor (as 2.3 eV for α-Fe$_2$O$_3$), the electrons are photo-excited to the empty conduction band in femtoseconds. Empty unfilled valence band is left, and hence creating the electron-hole pair (e$^-$ - h$^+$) (**Eq.2-24**) [150].

$$Fe_2O_3 + hv \rightarrow e^- + h^+ \tag{2-24}$$

$$e^-_{CB} \rightarrow e^-_{TR} \tag{2-25}$$

$$h^-_{VB} \rightarrow e^-_{TR} \tag{2-26}$$
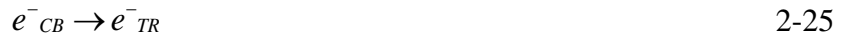
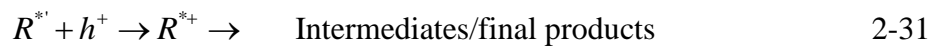The generated holes escape direct recombination (**Eq.2-27**) to reach the surface of α-Fe$_2$O$_3$. They react with surface adsorbed hydroxyl groups, or water to form adsorbed *OH radicals as shown in the **Eq.2-28, Eq. 2-29** [147].

$$e^-_{TR} + h^+_{VB}(h^+_{TR}) \rightarrow e^-_{CB} + heat \tag{2-27}$$

$$O_2 + e^- \rightarrow O_2^{*-} \tag{2-28}$$

$$OH^- + h^+ \rightarrow OH^* \tag{2-29}$$

Organic contaminants (R-H) are photo-oxidized by OH* as shown in the following equations [148, 151]:

$$RH + OH^* \rightarrow R^{*'} + H_2O \tag{2-30}$$

$$R^{*'} + h^+ \rightarrow R^{*+} \rightarrow \quad \text{Intermediates/final products} \tag{2-31}$$

In this process, oxidative species such as O$_2$$^{*-}$ and H$_2$O$_2$, which are generated from the reduction sites, and radical reactions, are given in the following reactions [152]:

$$O_2^{*-} + OH^* \rightarrow HOO^* \tag{2-32}$$

$$HOO^* + e^- \rightarrow HO_2^- \tag{2-33}$$

$$HOO^* + h^+ \rightarrow H_2O_2 \tag{2-34}$$

Overall, photocatalytic removal of organic pollutants from wastewater can be summarized as the following:

$$\text{Organic contaminants} \xrightarrow{\alpha\text{-}Fe_2O_3/hv} \text{Intermediates} \rightarrow CO_2 + H_2O \tag{2-35}$$

Or,

$$\text{Organic Contaminants} \xrightarrow{\alpha\text{-Fe}_2O_3/h\nu} CO_2 + H_2O \qquad\qquad 2\text{-}36$$

This process can be theoretically divided into five following independent steps [153]: (i) mass transfer of the organic pollutants in the liquid phase to the photocatalyst surface such as α-Fe$_2$O$_3$; (ii) adsorption of the organic contaminants onto the photon activated α-Fe$_2$O$_3$ surface; (iii) photocatalysis reactions for the adsorbed phases on the α-Fe$_2$O$_3$ surface; (iv) desorption of generated intermediates from the α-Fe$_2$O$_3$ surface; (v) transfer of these intermediates to the bulk. The reaction rate of this process heavily depends on mass transfer speed, surface interact between the catalyst and pollutants as well as photocatalyst itself (**Figure 2-6**).
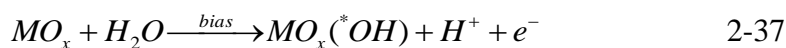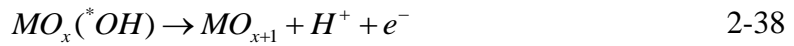

Figure 2-6. Schematic diagram of photocatalytic mechanism [153].

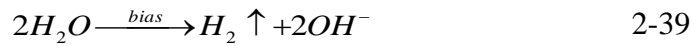### 2.4.6.2b. Photoelectrochemical mechanism

Likewise to electrochemical process, under applied voltage, oxidizing species are generated as the following equations:
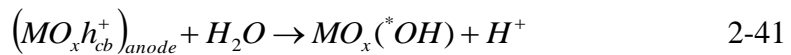
At the anode:

$$MO_x + H_2O \xrightarrow{bias} MO_x(^*OH) + H^+ + e^- \qquad\qquad 2\text{-}37$$

$$MO_x(^*OH) \rightarrow MO_{x+1} + H^+ + e^- \qquad \text{2-38}$$

At the cathode, the counter reaction is:

$$2H_2O \xrightarrow{bias} H_2 \uparrow + 2OH^- \qquad \text{2-39}$$

By applying a potential to photoanode, both anode reactions occur in the PEC process. Under illumination, photo-energy further generates holes and electrons on the photoanode as the following equations:

$$MO_x \xrightarrow{hv} \left(MO_x e_{cb}^-\right)_{anode} + \left(MO_x h_{cb}^+\right)_{anode} \qquad \text{2-40}$$

$$\left(MO_x h_{cb}^+\right)_{anode} + H_2O \rightarrow MO_x(^*OH) + H^+ \qquad \text{2-41}$$

The electrons on photoanode are withdrawn by the applying bias potential and transfer through external circuit to the cathode (**Figure 2-7**).

Figure 2-7. Photoelectrochemical mechanism.

It should be also noted that electron and holes can be recombined within photoanode:

$$\left(MO_x e_{cb}^-\right)_{anode} + \left(MO_x h_{cb}^+\right)_{anode} \rightarrow MO_x + heat \qquad \text{2-42}$$
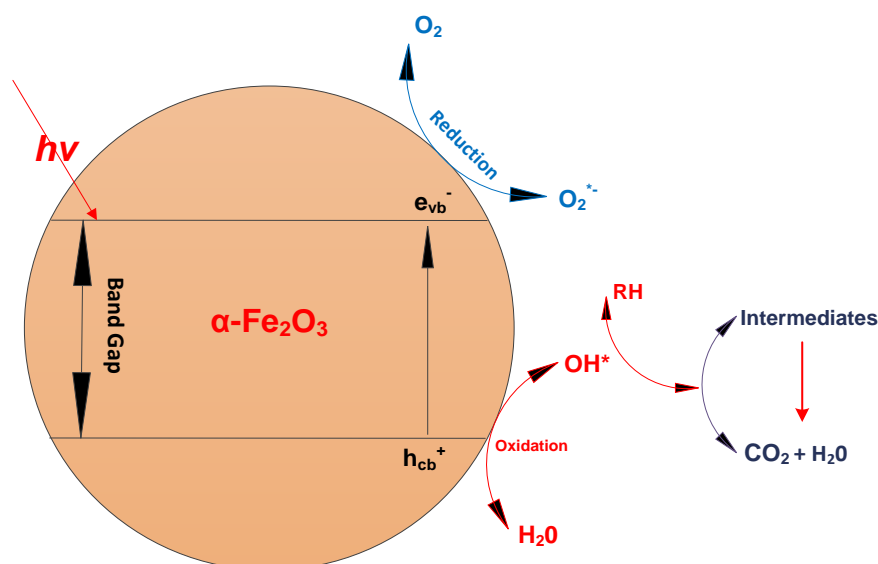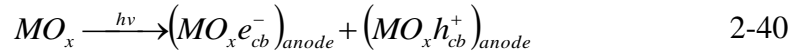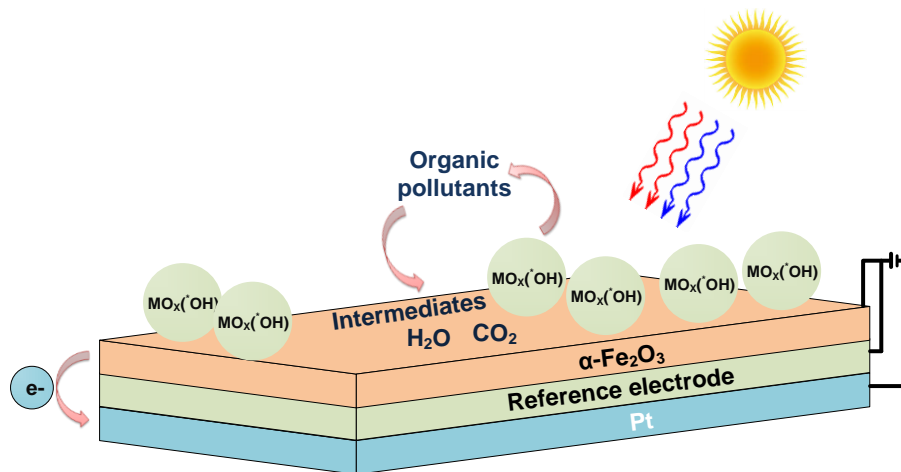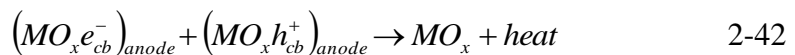
At high applied bias, the movement of electrons to cathode is very fast and thus the electron − hole recombination is hindered. Overall, with the presence of photo-energy, the PEC will generate more MO_{x+1} and $MO_x(^*OH)$ than the EC process.

2.4.6.2c.   Photocatalysts

In both photocatalytic and photoelectrochemical processes, photocatalyst material is an important factor contributing to the whole efficiency of wastewater treatment [154]. Many important characteristics of these photocatalyst materials have determined their feasible applications in wastewater treatment including [155]:

- Ambient operating temperature and pressure.
- No harmful byproduct generation.
- Long stability.
- Affordable and environmentally friendly.

In fact, none of photocatalyst material can satisfy all the mentioned features. Some photocatalysts are affordable and can work at normal thermodynamic conditions (room temperature and atmosphere pressure) [156]. However, they are only activated by UV illumination resulting in high operating cost [157]. While, others materials exhibit low resistant ability to corrosion [158]. Commonly, nanostructured metal oxides such as TiO_2, ZnO, and Fe_2O_3 have been widely used for environmental applications.

-    **TiO_2**

TiO_2 photocatalysis has been widely used for the degradation of organic pollutants from wastewater since the 19th century [159]. TiO_2 photocatalyst can be activated under the photon energy of 300 nm $< \lambda <$ 390 nm [160]. Other than that, TiO_2 possesses multi-faceted functional properties such as chemical and photochemical stability [161], biological inertness [162]. More importantly, this material is inexpensive. Because of these, TiO_2 has been used as an effective photocatalyst not only in wastewater treatment but also in water splitting [163]. Liu Zhaoyue et al., illustrated that TiO_2 can remove 80 % phenol from water [164], while Juan Yang indicated that 90 % of rhodamine-B dye (RhB) and sulforhodamine B dye (SRB) could be removed after three hours of treatment [165]. TiO_2 has band gap energy of 3.02 eV that is at near ultraviolet radiation (300 nm) [166]. Moreover, TiO_2 absorbs only 5% energy of the visible wavelength [167]. Consequently, UV excitation source is needed for activating TiO_2, and it results in high operation cost.

Many intensive researches have been conducted to develop a TiO_2 photocatalyst that can be activated by solar energy with high catalytic efficiency [168]. Most of these works are to modify TiO_2 structure with other elements such as metals and others. Modification TiO_2 with noble metals, such as Au, is of largest interest because the high photocatalytic efficiency of TiO_2 is achieved [169]. The overall performance of this modification heavily depends on content, type of TiO_2 and selected noble metal [170]. Apart from photocatalytic improvement, TiO_2 modified with this kind of metal can be able to absorb visible wavelength. Likewise, transition metals such as Co [171], Cr [172], Zr [173] have been replaced for noble metals to modify titan dioxide structure. This alternative is due to the expensive cost of noble metals. Far from that, TiO_2 doped transition metals presents relatively high catalytic activity, and stability [174]. However, metal doping requires expensive facilities. Moreover, electrons generated during the wastewater treatment process are often trapped by the metal centers. These mentioned drawbacks can be overcome by using none - metal materials [175]. Carbon nanotubes can be effectively used to obtain highly active TiO_2 photocatalyst [176]. Other, the photocatalyst can also be achieved by hydrolysis of titanium precursors in the presence of dopant such as acidic sulfuric [177]. Further, by modifying with none – metal materials, the generations of various impure phases, for example, metal oxides at high temperatures, which lead to the decrease of TiO_2 activity, are eliminated [178].

Overall, TiO_2 photocatalytic is still of high interest for environmental applications owing to its mentioned superior properties. However, the required UV illumination has challenged practical applications of this process on an industrial scale. Undoubtedly, aforementioned modification methods can make TiO_2 to response to visible light. However, these steps apparently require facilities and capital investments.

- **ZnO**

Likewise to TiO_2, ZnO is also a common photocatalyst for the degradation of organics from wastewater. Particularly, ZnO is preferred for photocatalytic degradation of phenol due to reductive and oxidative reactions on its surface. In

fact, ZnO has a few advantages over TiO_2 such as higher quantum efficiency and catalytic efficiency [179]. Other than that, TiO_2 absorb a smaller fraction of solar spectrum than ZnO [180]. For this advantages, ZnO has also been used for dye degradation [181].

However, ZnO remains drawbacks: (i) large band gap as often necessitating near UV light ($\lambda < 400$ nm) to induce electron photoexcitation; (ii) instability in an aqueous medium, leading to photocatalyst decomposition; (iii) high electron - hole recombination rates [155]. For instance, ZnO shows photo - corrosion effects resulting in ZnO self - deactivate by forming Zn^{2+} ions when it reacts with photo-generated holes in the water. Finally, it is dissolved into solution [182]. Therefore, photocatalysts required for wastewater treatment should be photo-stable, feasible under visible light, and more efficient.

- **α-Fe$_2$O$_3$**

By comparing to TiO_2 and ZnO, α-Fe_2O_3 is a higher stable photocatalyst under ambient conditions [183]. Further, hematite is also considered as an environmentally friendly semiconductor because it is less harmful, chemical inertness and ability to combine with biological technology [184]. Additionally, α-Fe_2O_3 can be used for wastewater treatment at a large volume and easy to be magnetic separation [185]. Previously, α-Fe_2O_3 was most interested in heavy metal treatment [186]. However, it has been recently used for photocatalytic degradation of organics from wastewater [187]. By having a suitable band – gap (2.2 eV), which can be excited by visible light, α-Fe_2O_3 is believed to be an economical and sustainable photocatalyst for wastewater treatment [188, 189].

Nevertheless, the fast recombination of electron - hole pairs (within nanoseconds) is a real challenge for using α-Fe_2O_3 in environmental applications. A large number of intensive researches have been done to overcome this obstacle. Accordingly, doping hematite nanostructure with metals is considered as a most effective method. At this stage, noble metals such as Pt [190], Cr and Mo [191] could generate the faster transfer of surface electrons. [192]. Moreover, the better separation between electrons and holes would allow a better photocatalytic activities [193]. However, these means of doping are expensive owing to high cost

of doped metals. Relatively cheaper metals such as Al, Si have been used [194], however, these methods to prepare α-Fe_2O_3 anode are complicated and time - consuming. Amir et al., has been successfully and effectively controlled morphology and photocatalytic activities of α-Fe_2O_3 by cationic surfactants [195]. This work also utilizes this technique combining with a voltage applied crossing α-Fe_2O_3 surface to optimize its photooxidation activities. Iron oxide is normally used in the form of thin films for almost its applications. Many different methods can be used to synthesize α-Fe_2O_3 thin films such as Vapor Phase Deposition (VPD), Chemical Vapor Deposition (CVD), Electrochemical Deposition [196-198].

+ *Chemical deposition.* The chemical deposition methods have been considered as the simple, economical and effective ways to fabricate nanostructured films, with various morphologies such as nanoparticles, nanowires, nanotubes, hollow spheres, and nanoflowers [199-202]. This method includes different techniques such as hydrothermal, solvothermal and sol–gel [203-206]. Among these, the sol–gel method, for example, the spin coating (**Figure 2-8**) is known as a simple and highly efficient method. This technique is operated at low temperature (the highest calcining temperature is always below 1000 $^\circ$C) and can easily control the nanostructured crystallinity [219]. Moreover, no expensive equipment is required, and the process can be controlled easily and accurately. The sol–gel process can also be applied to deposit a film having a complex geometry onto a substrate [207, 208].
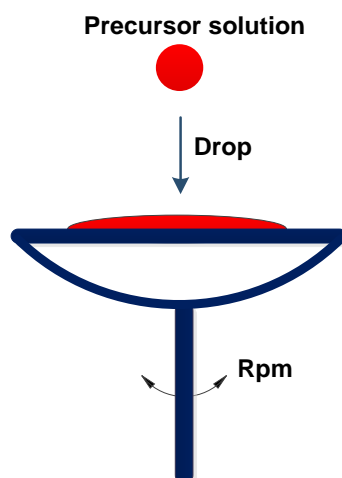
**Figure 2-8**. The spin coating method [219].

+ *Vapor phase deposition.* Gas deposition method includes physical vapor evaporation, atomic layer deposition and chemical vapor deposition (**Figure 2-9**).
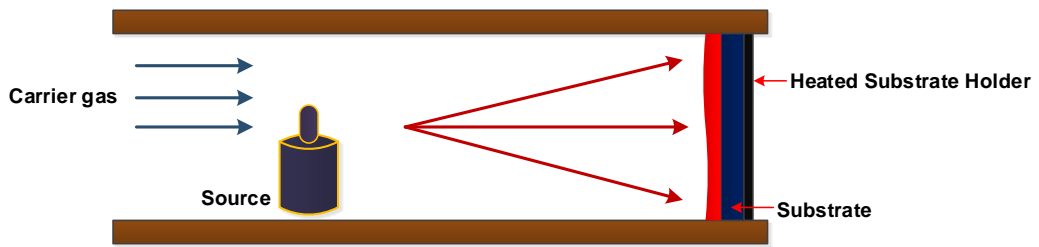
Figure 2-9. Vapor phase deposition method [209].

This method has been extensively used in various nanostructured film preparations. Quian et al., [210] has used this method to synthesize nanowire while Glasscock et al., [211] and Lin et al., [212] have illustrated its efficiency for hematite nanostructured thin films. α-Fe$_2$O$_3$, which has various morphologies such as nanowires, nano - dendritic structures, nanorod arrays, and thin films could be fabricated by gas phase deposition [213]. However, this technique operation is toxic and flammable. Meanwhile, atomic layer deposition also requires a higher cost of operation than that of the solution - based methods [214].

+ *Thermal pyrolysis.* Thermal pyrolysis are also promising method for the synthesis of nanostructured α-Fe$_2$O$_3$ films. These films can be directly obtained by oxidizing iron metal [215, 216]. Moreover, hematite thin films can be fabricated by spray pyrolysis (**Figure 2-10**).
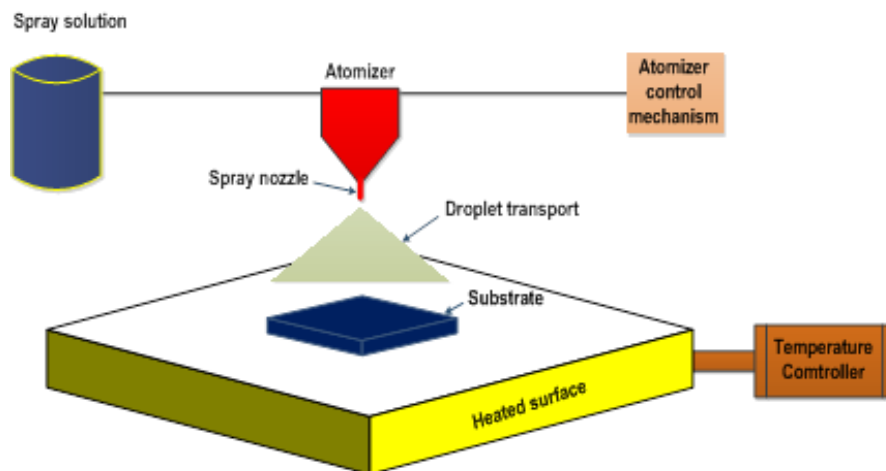
Figure 2-10. Thermal spray pyrolysis for α-Fe$_2$O$_3$ films [217].

The iron precursor can be sprayed onto the substrate surface that was annealed [217]. The properties of the thin film mainly depend on operating parameters such as annealing temperature or precursor solution. While iron oxide with various morphologies such as nanowire, nanorod arrays are likely more appropriate to be prepared by a vapor phase deposition method, thermal pyrolysis is mainly used for the growth of nanoparticle thin film.

+ *Electrochemical deposition.* The electrochemical deposition also has been used to fabricated hematite nanostructures, especially highly porous morphologies. Hua Yang et al., [218] and Alan Kleiman-Shwarsctein et al., [194] have also used electrochemical technology for α-Fe_2O_3 nanostructure film deposition. By comparing with other methods, this technique can precisely control the microstructure and the potential of co-depositing dopants [219]. Further, it operates at low temperature.
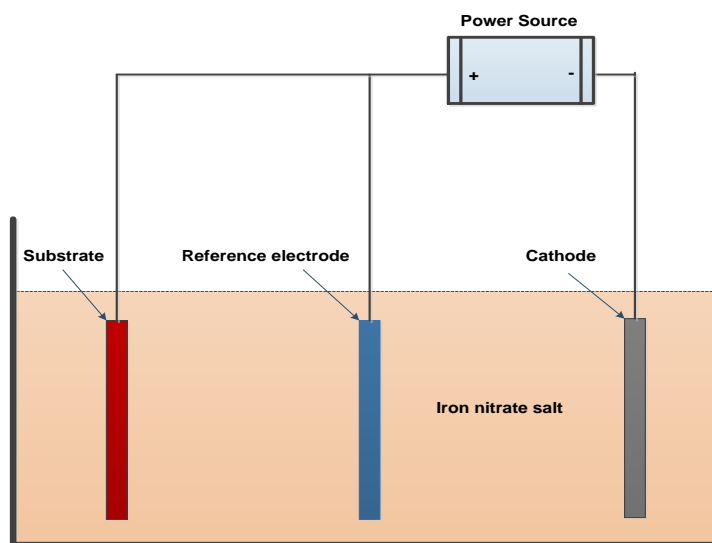
Figure 2-11. Electrochemical deposition of α-Fe_2O_3 thin film [220].

The three - electrodes system, which includes working electrode (substrate), reference (Ag/AgCl) and counter electrode (Pt plate), is usually used for electrochemical deposition (**Figure 2-11**). The film thickness and morphology can easily be managed by controlling the concentration of precursor salt, depositing time as well as applied voltage. However, this method is higher energy consumption and much more time – consuming than the spin coating method.

Page | 31

+ *Glancing angle deposition.* This method has also been received attention to preparing the α-Fe_2O_3 nanostructured film for photoelectrochemical applications.
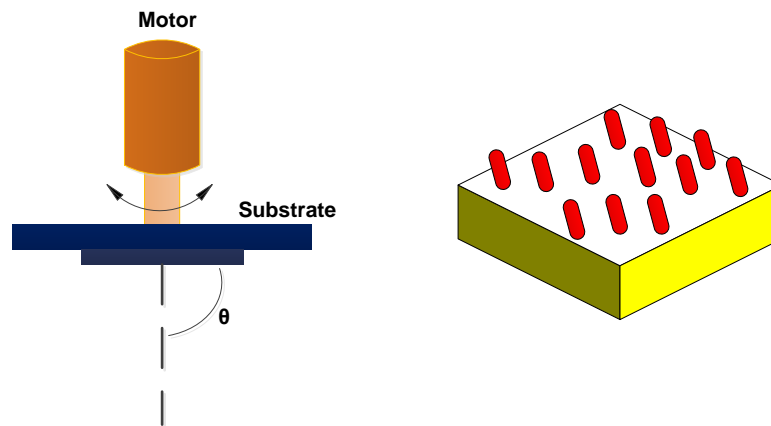
Figure 2-12. Glancing angle deposition technique for α-Fe_2O_3.

Glancing angle deposition (**Figure 2-12**) relies on ballistic shadowing phenomenon happening when a material is directionally deposited onto a relatively cool substrate at a glancing angle. Separated nano - columns can be achieved by increasing deposition angle [189]. However, this process is complicated and time - consuming.

2.5. Conclusion

From the aforementioned analysis, it could be found that synthesized surfactants including sodium dodecyl sulfate from laundry wastewater not only damage the environment but also cause dangerous symptoms for both animals and human. Many technologies can be utilized for degraded these kinds of organic from laundry wastewater such as incineration, adsorption, electrochemistry, biological and advanced oxidation processes. The main advantages of adsorption and electrochemical techniques are high performance, simple to operate and easy to control the whole system. Physical adsorptions, however, are not the continuous processes, and they cannot be effectively used to treat contaminants, which are both dissolved in water and smaller than the size of the filter pore openings. Meanwhile, electrode stability is a huge challenge to apply practically electrochemical process due to corrosive reactions occurring at electrode surface over treating time, especially metal electrodes such as Cu, Fe. In fact, several kinds of the electrode such as boron - doped diamond, or gold can be stable longer over treating time.

However, they are expensive. In the meanwhile, incineration and biotechnology are considered as ineffective method owing to high energy consumption and hard to be controlled the operation respectively. Among advanced oxidation processes, Fenton technologies possess high oxidizing ability owing to strong radical oxidizing species. However, likewise to chemical oxidation processes, Fenton methods generate harmful byproducts. Conversely, photocatalysis processes have been illustrated as the innovative and effective water treatment technologies. Further, from the economical and practical perspective, α-Fe_2O_3 has been widely recognized as a highly effective photocatalyst for environmental applications.

In this study, α-Fe_2O_3 anode prepared by the simple sol - gel spin coating method was used to degrade synthetic organics from laundry water. The voltage was also applied crossing iron oxide anode to enhance photocatalytic efficiency. The study ultimately aims to treat wastewater containing surfactants, particularly in rural and remote areas where technologies and budgets for wastewater treatment are limited.

Chapter 3   Methodology

3.1.   Materials

3.1.1. Chemicals

All chemicals used in this study were purchased from Sigma - Aldrich (**Table 3-1**). Stainless steel substrates with the dimension of 25 mm $\times$ 75 mm $\times$ 2 mm (width/length/thickness) were ordered from Haynes Educational (Australia). This study used a commercial detergent FAB™ (Unilever, Australia) to prepare laundry water.

Table 3-1. List of the chemicals used in the study.

Name	Formula	Assay (%)
Sodium dodecyl sulfate	$CH_3(CH_2)_{11}SO_4Na$	≥ 90
Iron (III) nitrate	$Fe(NO_3)_3.9H_2O$	≥ 99.95
Tetramethylammonium bromide (TMAB)	$C_4H_{12}BrN$	≥ 98
Ethanol	C_2H_5OH	≥ 95

3.1.2. Electrodes

3.1.2.1.   Cathode

By having superior hydrogen evolving behaviors, platinum has been of interest as a cathode. Moreover, platinum is also an effective catalyst for H^+ in electrochemical operations. There are many different types of platinum electrodes for quantitative electrochemical analysis in laboratory scale such as a rod, coil, plate. In this work, the coiled platinum was used as the counter cathode (**Figure 3-1**).

Figure 3-1. The platinum electrode.

This coiled platinum wire with high purification covered by the epoxy rod. The surface area of this coiled platinum is about 4.7 cm^2 while its diameter is about 9 mm. The black epoxy rod (6.9 mm OD) is 150 mm long. The overall length of the rod and the coil is approximately 180 mm. On the top, one small metal head is used to connect with the electric power.

3.1.2.2.   Reference electrode

A reference electrode is needed to maintain a constant voltage and thus ensure all experiments are consistent. In this study, Ag/AgCl immersed in KCl 3M was used as the reference electrode, and its constitution is showed in **Figure 3-2**. Glass tube is used to contain a silver wire that is coated with a thin layer of silver chloride and isolate the electrode from the solution. A nearly saturated solution of KCl 3 M, which the concentration can be reproducible, is filled into the glass tube.

Figure 3-2. The constitution of the reference electrode.

3.1.2.3.   α-Fe₂O₃ anode

The stainless steel substrates with the dimension of 25 mm × 75 mm × 2 mm (width/ length/ thickness) had been subsequently rinsed in the ultrasonic bath with deionized water, ethanol before being dried with nitrogen for 10 minutes. The spin coating method was selected to prepare α-Fe_2O_3 thin film.

Figure 3-3. The spin coater.

Two different procedures were used to prepare the anodes as the following:

- (I): TMAB (0.5 g) was mixed with 5 ml deionized water. The solution was stirred for 30 minutes, before adding 4g Iron (III) nitrate, and then stirring for more 2 hours. The sample deposition was as the following steps: (i) Drop prepared solution onto the stainless steel substrate that tightly held on the chuck of spin coater (**Figure 3-3**), (ii) two fixed speeds (200 rpm, 300 rpm) used to spin the substrate for 1 minute in total, (iii) the samples was heated on a ceramic plate at 80 ^{0}C for 15 minutes before placing into the furnace (**Figure 3-4**) at 450 ± 1 ^{0}C, for 2 hours, in air, with fixed heating and cooling rate of ~ 4 ^{0}C/min. The prepared anodes were used to remove organic compounds from laundry water.

- (II): TMAB (1 g) was added into 5 ml deionized water. The solution was stirred for 30 minutes. 4 g Iron (III) nitrate was added into this mixture, and then also stirred for next 2 hours. The same sol-gel procedure was repeated to deposit the thin film onto the stainless steel substrate. However, these samples were annealed in the furnace at 450 ± 1 ^{0}C for 8 hours, in air, with fixed heating and cooling rate of ~ 1 ^{0}C/min.


Figure 3-4. The furnace.

3.2. Preparation

3.2.1. Aqueous solution

The synthetic laundry was prepared by dissolving 5 g of detergent powder in 500 ml water. This study used a commercial detergent FAB™ (Unilever, Australia). The solution was magnetically stirred for 2 hours before leaving for two more hours in room temperature. It was then transferred to vacuum membrane filtration system with Polycarbonate membrane filter with pore size of 0.1 μm (SterliTech Corporation, USA). This filtration step represents the physical removal, which is often applied in the commercially available units. In the meanwhile, SDS solution with 100 mg/L of concentration was prepared by dissolving SDS powder in water. The solution was magnetically stirred at room temperature for 30 minutes.

3.2.2. Reactor setup

TOC removal and SDS degradation were performed in the circular-shaped reactor (500 mL). The reactor was covered by quartz and placed under a solar simulator (**Figure 3-5**). The α-Fe_2O_3 anodes had an apparent surface area of 18.75 cm^2. For the removal of SDS, because of ionic nature of sulfate head group, the evaluation of physical adsorption of SDS on hydrophilic anode surface was performed in this reactor without voltage applied.
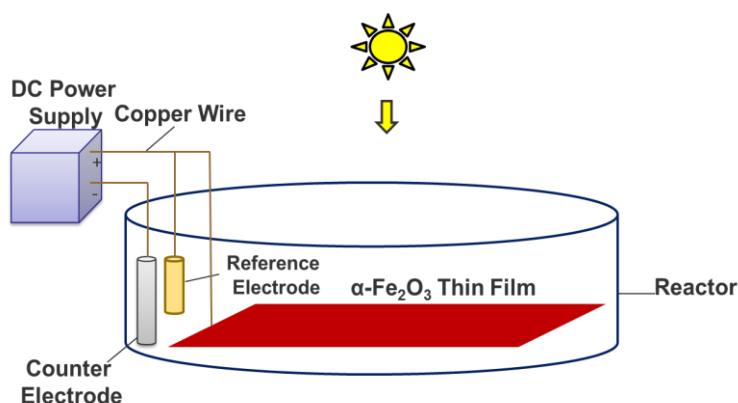
Figure 3-5. Reactor setup.

On contrast, to evaluate TOC removal efficiency as a result of an applied electric field, this study applied different combinations: (i) electrochemical (EC) and (ii) photoelectrochemical (PEC) process. The reference electrode was used to maintain

a constant voltage, and thus ensure all experiments are reproducible. Three different combinations of power were employed: 1V; 2 V; and 3 V. The forward bias values to the working electrode were generated by the DC power supply (**Figure 3-6**) (QJ3003XC DC Regulated Power Supply 30V-3A LCD, Australia).

Figure 3-6. The DC supply power.

For PEC processes, all non-semiconductor parts such as the substrate, wire were covered by the none - conductive plastic film to prevent exposure of the solution to these components. The system was illuminated under 500 W Xenon lamp (100 mWcm^{-2}, 25 ^{0}C) solar simulator (Abet Teachnologies, Model 11016A Sun 3000).

Figure 3-7. Solar simulator.

3.3. Sample characterization

3.3.1. Anode morphology and crystalline

3.3.1.1. Scanning electron microscope (SEM)

A scanning electron microscope (SEM) is a type of microscope that produces images of a sample by scanning it with a focused beam of electrons. The resolution of an SEM is given by the minimal spot size. Meanwhile, the Field emission SEM (FESEM) uses a field emission gun, also called a cold cathode field emitter, to produce the electrons from a much smaller area than a thermionic gun of conventional SEM. In other words, FESEM can deliver the high – quality imaging resolution in the field of nanotechnology. Consequently, FESEM, Tescan Mira3 was utilized in this study for characterization of α-Fe_2O_3 nanostructure (**Figure 3-8**).
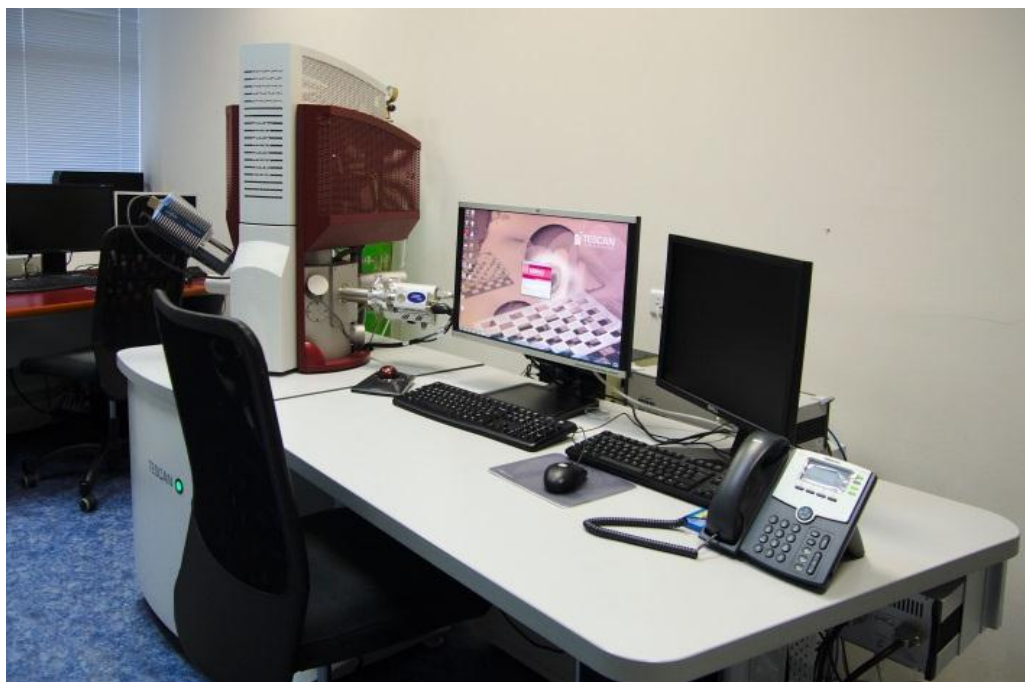
Figure 3-8. SEM equipment.

3.3.1.2.   X – Ray diffraction

X-ray crystallography is a common technique used for characterizing the atomic and molecular structure of a crystal. Whereby, the X-rays are beamed to crystalline atoms of the material, and cause diffracted beams following specific directions. The angles and intensities of these diffracted beams are measured to produce crystalline characteristics of the material. Furthermore, the mean positions of the atoms in the crystal can be determined, as well as their chemical bonds, their disorder, and various other characteristics. In this study, XRD, Bruker D8 Advance with Cu Kα radiation (λ=0.15418 nm) was used. For qualitative analysis, XRD diagrams were recorded in the interval $20^0 \leq 2\theta \leq 80^0$ at a scan rate of 0.01^0 s^{-1}.

3.3.2.   Total organic compounds analysis

Treated solution samples (1 ml) were periodically transferred from the reactor to test tubes after every 15 minutes. Afterward, the samples were analyzed by the TOC analyzer (TOC-VWS/TOC-VWP, Shimadzu, Japan) using wet oxidation method [221].
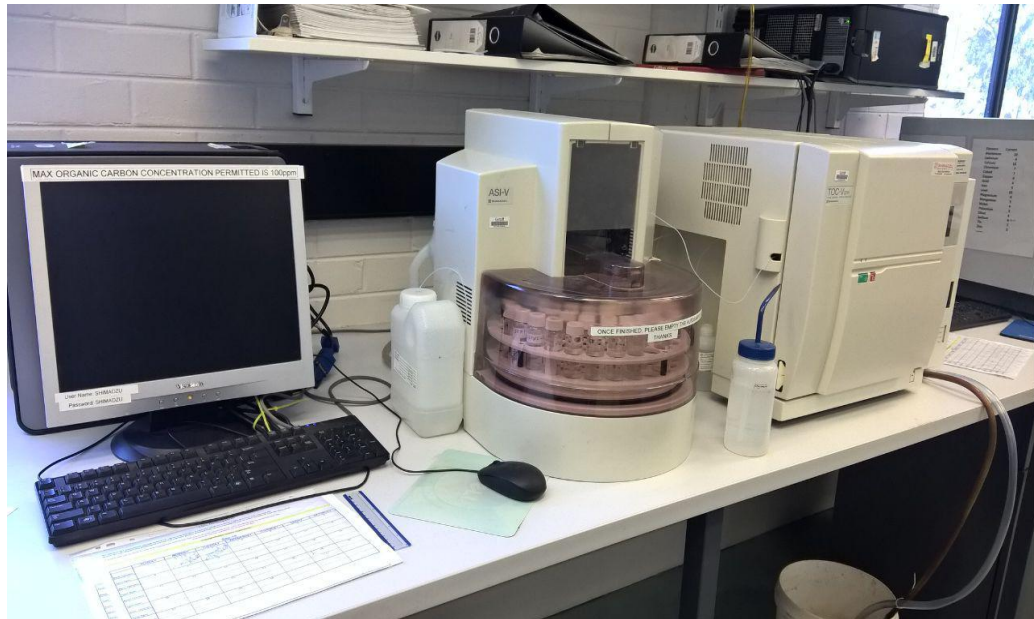
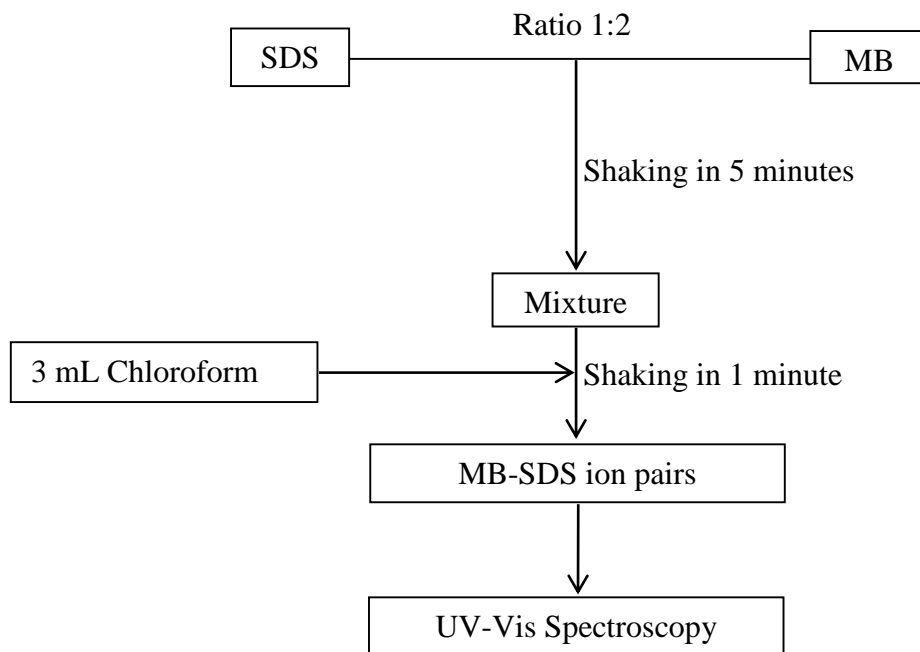**Figure 3-9.** TOC analyzer.

Moreover, the same TOC analysis procedures were used to evaluate the TOC reduction during the degradation of sodium dodecyl sulfate.

3.3.3. Determination of SDS concentration

The variation of SDS concentration was determined via methylene blue active substance (MBAS) method as in **Figure 3-10** [222].

Figure 3-10. MBAS method for SDS concentration determination.

The concentration ratio of SDS and methylene blue used is 1:2 to make sure that the reactions to form SDS - MB ion pairs are completely occurred. Chloroform was used to extract generated ion – pairs from the separatory funnel. The absorbance of SDS - MB ion pairs formed was determined via UV - Vis Spectrophotometer (JASCO, V-670 spectrophotometer). The standard solution equivalent from 0 – 100 mg/L of SDS was prepared to get the calibration curve. From this calibration curve, the variation SDS concentration against time under treatment processes was calculated.

Figure 3-11. UV - Vis Spectrophotometer.

3.3.4. Intermediate verification

Organics presented in the SDS solution were detected by Fourier transform infrared spectroscopy (Perkin Elmer Spectrum 100 FT-IR). Accordingly, the sample compartment was cleaned with acetone and water. The FTIR calibration curve of pure water was performed to ensure the accuracy of the analysis. Testing samples in liquid form were gently dropped onto the sample compartment to prevent air bubble formation. The FTIR spectrum software was used to analyze the samples automatically.

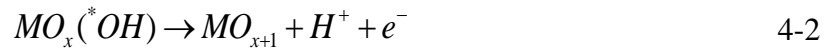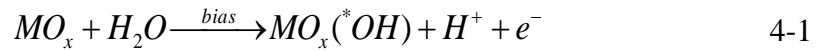**Figure 3-12.** Fourier transform infrared spectroscopy (FTIR).

Chapter 4

Experimental study on TOC removal from laundry water

This chapter discusses the removal of TOC from laundry water. Organic compounds in laundry water were degraded by photoelectrochemical (PEC) and electrochemical (EC) processes on α-Fe$_2$O$_3$ anode. The applied voltage was between 1 and 3 V. Moreover, lumped kinetic was developed to describe the kinetics of TOC removal.
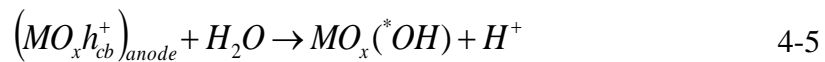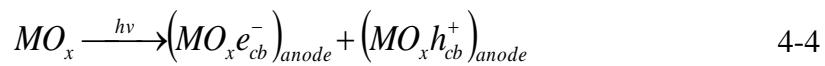
4.1. Mechanism

The decomposition of organic compounds on the metal oxide anode via EC process can be illustrated by the formation of adsorbed hydroxyl radicals (**Eq.4-1**) or adsorbed oxygen (**Eq.4-2**) or both [129]:

$$MO_x + H_2O \xrightarrow{\ bias\ } MO_x(^*OH) + H^+ + e^- \qquad \text{4-1}$$

$$MO_x(^*OH) \rightarrow MO_{x+1} + H^+ + e^- \qquad \text{4-2}$$

At the cathode, the counter reaction is:

$$2H_2O \xrightarrow{\ bias\ } H_2 \uparrow + 2OH^- \qquad \text{4-3}$$

By applying a potential to photoanode, both anode reactions occur in the PEC process. Under illumination, photo-energy further generates holes and electrons on the photoanode as the following equations:

$$MO_x \xrightarrow{\ hv\ } \left(MO_x e_{cb}^-\right)_{anode} + \left(MO_x h_{cb}^+\right)_{anode} \qquad \text{4-4}$$

$$\left(MO_x h_{cb}^+\right)_{anode} + H_2O \rightarrow MO_x(^*OH) + H^+ \qquad \text{4-5}$$

The electrons on photoanode are withdrawn by the applying bias potential and transfer through external circuit to the cathode. It should be also noted that electron and holes can be recombined within photoanode:
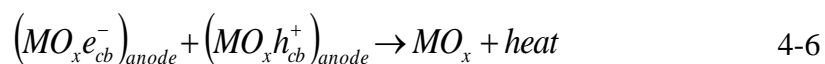
$$\left(MO_x e_{cb}^-\right)_{anode} + \left(MO_x h_{cb}^+\right)_{anode} \rightarrow MO_x + heat \qquad \text{4-6}$$

At high applied bias, the movement of electrons to cathode is very fast and thus the electron - hole recombination is hindered. Overall, with the presence of photo-energy, the PEC will generate more MO_{x+1} and $MO_x(^*OH)$ than the EC process.
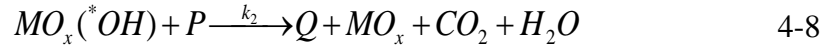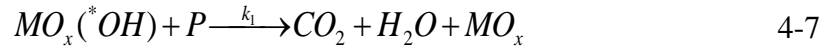
4.2. Kinetics of TOC removal from laundry water

The produced hydroxyl radicals can oxidize the organic compounds adsorbed on anode. The laundry wastewater contains a wide range of dissolved organics, with complex oxidation steps. Consequently, lumped kinetics is required [223]. Generally, the organics can be oxidized completely or partially as the following:

$$MO_x(^*OH) + P \xrightarrow{k_1} CO_2 + H_2O + MO_x \qquad \text{4-7}$$

$$MO_x(^*OH) + P \xrightarrow{k_2} Q + MO_x + CO_2 + H_2O \qquad \text{4-8}$$

Where, P is the original organics, Q is product of the partial oxidation.

It can be assumed that Q comprises of the organic compounds that are not adsorbed into the anode and hence cannot be oxidized by PEC process. The TOC of solution equals to the sum of P and Q. Hence, the initial and the dynamic TOC concentration (mg/L) at time (t) are given as $C_{TOC}(0)=C_P(0)$ and $C_{TOC}(t)=C_P(t)+C_Q(t)$.

During the PEC and EC processes, the produced rate of free radicals is assumed constant. Assuming both oxidizing reactions are first-order kinetic, the rate of equations of lumped kinetics can be written as [224]:

$$\frac{dC_P}{dt} = -(k_1 C_P + k_2 C_P) \qquad \text{4-9}$$

$$\frac{dC_Q}{dt} = k_2 C_P \qquad \text{4-10}$$

Integrating the above system yields:

$$\frac{C_{TOC}(t)}{C_{TOC}(0)} = \left\{ \frac{k_2}{k_1 + k_2} + \frac{k_1}{k_1 + k_2} \exp[-(k_1 + k_2)t] \right\} \qquad \text{4-11}$$

It should be noted that the above differentiate equation is the simplest form of the lumped kinetics. More complicated forms, involving three or more different steps,

have also been developed in the literature [223]. Nevertheless, the binary system has been successfully verified for the TOC degradation of an industrial bleaching effluent [224]. The above equation, **Eq.4-11**, will be used to model the TOC removal in this study.

4.3. Results and Discussion

4.3.1. Anode characterization

The morphology of α-Fe$_2$O$_3$ anode was examined. As shown in **Figure 4-1,** the deposited film consists of α-Fe$_2$O$_3$ nano-tuft structure. This film presented a highly porous structure illustrated to have the larger adsorption capacity than that of particle films [225].
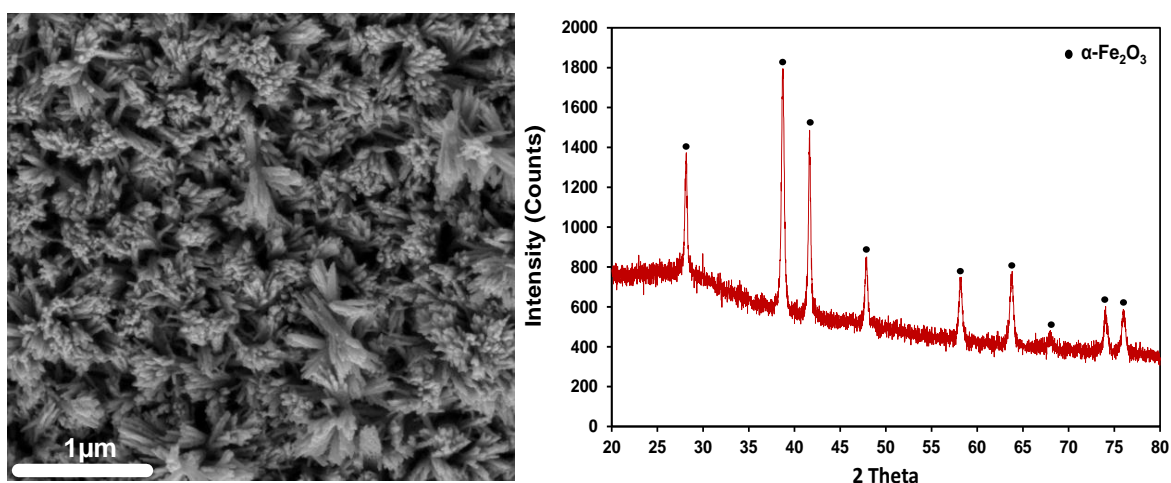
Figure 4-1. SEM image and X-ray diffraction of nanostructured α-Fe$_2$O$_3$ prepared by the procedure I.

Crystalline properties and the phase formation of α-Fe$_2$O$_3$ film were verified by X-ray diffraction analysis **(Figure 4-1)**. The α-Fe$_2$O$_3$ peaks and their corresponding facets were observed at 28.09^0 {012}, 38.65^0 {110}, 42.44^0 {113}, 47.86^0 {024}, 58.08^0 {122}, 64.72^0 {300}, 67.65^0 {208}, 74.84^0 {1010}, 76.85^0 {220}. The results indicate the position of the standard peaks of hematite α-Fe$_2$O$_3$ with a rhombohedral structure (JCPDS 33 - 0664). Thus, it can be concluded that a complete of hematite phase was formed by annealing process. A similar prevalence of the peaks has also been observed for α-Fe$_2$O$_3$ film previously [195, 226].

4.3.2. Overall TOC removal

TOC removal analysis was performed by analyzer wet oxidation method. The TOC removal efficiency was defined as the following equation:

$$TOC(\%) = \frac{C_{TOC}(0) - C_{TOC}(t)}{C_{TOC}(0)} 100 \qquad \text{4-12}$$

Where $C_{TOC}(0)$ and $C_{TOC}(t)$ are the initial and transient TOC concentration (mg/L) respectively.

Besides, the comparative oxidation power of PEC system can also be explained from its mineralization current efficiency (MCE) [227]:

$$MCE = \frac{C_{TOC}(0) - C_{TOC}(t)}{8I \, \Delta t} FV \qquad \text{4-13}$$

Where F is the Faraday constant (96.487 Ceq^{-1}), I is the current applied (A), and V is the volume of solution (L).

Table 4-1. TOC removal by α-Fe$_2$O$_3$ under various conditions.

DC bias	Solar Simulator	Total degradation rate, %	MCE at 180 mins
1 V	**On**	**68.78**	**5.05**
1 V	Off	68	4.98
2 V	**On**	**74.68**	**5.48**
2 V	Off	73.1	5.36
3 V	**On**	**77.47**	**5.68**
3 V	Off	74.7	5.48

For the EC system, increasing the applied bias increased the TOC removal. At 1 V the total degradation rate was 68 % at 180 minutes, and MCE was 4.98. By comparing to higher power (2 V), a much considerable improvement in the

degradation of organics was observed (73.1 % at 180 minutes, MCE = 5.36). Likewise, when a further higher current (3 V) was applied, a larger TOC removal efficiency via α-Fe$_2$O$_3$ was obtained via the PEC reaction (74.7 % at 180 minutes, MCE = 5.48). This gradually increasing trend was repeated in EC processes under the same bias values used. A good agreement between these results and reported values in the literature for pentachlorophenol [228]. Overall, the PEC process had higher removal efficiency than the EC method.

4.3.3. Reaction kinetics

The modelling, **Eq.4-11,** was fitted against experimental data (**Figure 4-2**) to obtain kinetics constants. It can be seen that the binary model fitted well all experimental data. The obtained kinetics coefficients, k_1 and k_2, reflected the efficiencies of different treating processes. Generally, when a higher bias applied crossing electrodes, the rate constants of completed oxidizing reactions were higher for both EC and PEC processes. For PEC treatment, the rate constants of the completed oxidation, k_1, was almost proportional to the applied voltage.
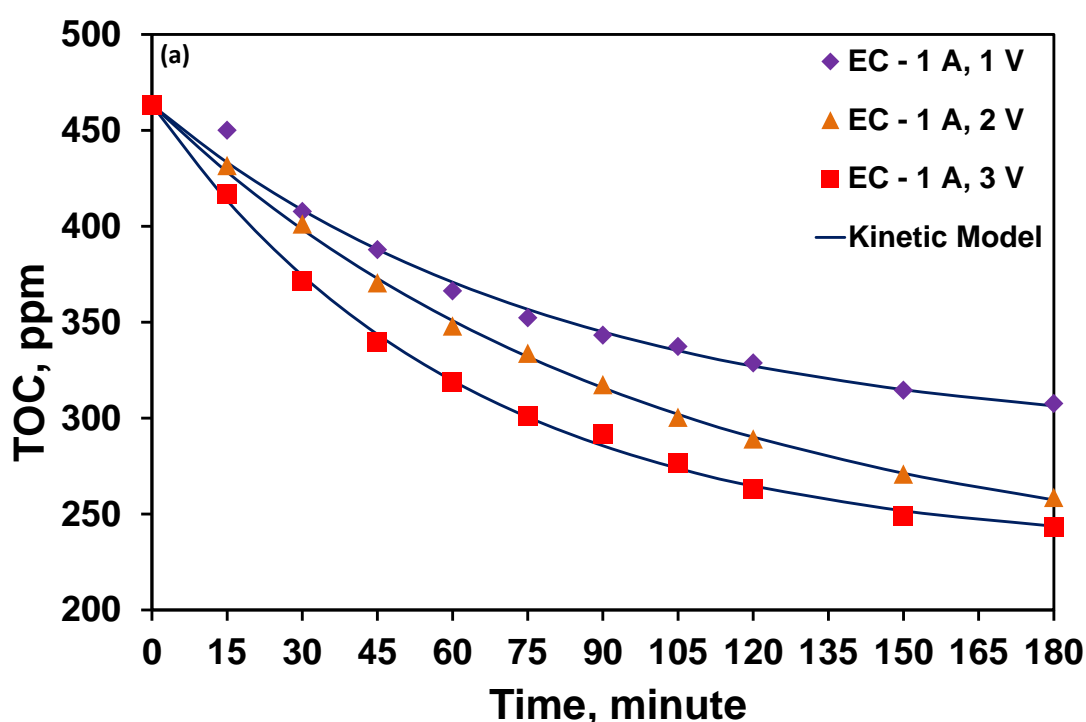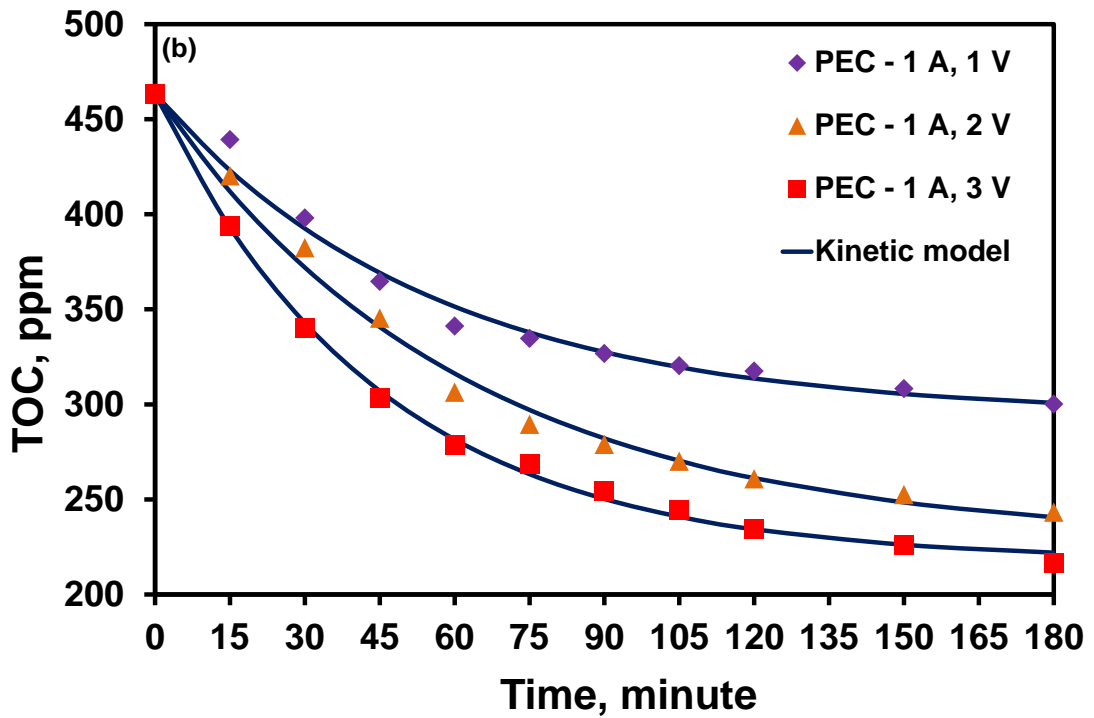
Figure 4-2. TOC removal under different processes: (a) EC; (b) PEC.

As anodic bias increases, a large amount of current carrier (photoelectrons) passes through the anode, and photocurrent excited holes and electrons used to oxidize organics. Consequently, the higher the bias the larger TOC is removed.

Table 4-2. Kinetic parameters of TOC removal.

DC bias	Solar Simulator	k_1, min^{-1}	k_2, min^{-1}
1 V	**On**	6.5×10^{-3}	1.1×10^{-2}
1 V	Off	4.7×10^{-3}	7.7×10^{-3}
2 V	**On**	8.1×10^{-3}	7.8×10^{-3}
2 V	Off	5.2×10^{-2}	4.4×10^{-3}
3 V	**On**	1.2×10^{-2}	1.1×10^{-2}
3 V	Off	8.0×10^{-3}	7.9×10^{-3}

In **Table 4-2**, it can be seen that at the low bias value (1 V), the partial oxidization (k_2) were higher than those of complete oxidation (k_1). This phenomenon can be explained via the role of electric power applied. It is well-known that laundry

wastewater includes a wide range of organic compounds, mainly including polar (anionic, cationic) and non-polar (non-ionic) surfactants [229]. When these surfactants are brought into contact, polar surfactants form aggregates at α-Fe_2O_3 surface on account of electrostatic interactions between separately charged species and the oppositely charged α-Fe_2O_3 surface [230].

The degradation kinetics of organics occurred via two mechanisms: (i) complete oxidation to form CO_2 and water, and (ii) break-down to shorter chains [152]. These intermediates were less oxidized by generated holes, but often by electrons running from anode to cathode [231, 232]. Therefore, when a relatively low bias was applied, the produced electrons were not enough to keep the organics close to the surface. Consequently, partial oxidizing is the dominant ($k_2 > k_1$), and the remaining organic compounds were suspended within the solution. With the increasing voltage (e.g., 3 V), however, the rate coefficients of the completely oxidizing reactions, k_1, was higher than that of the partial ones. In this instance, organics were much more prone to complete oxidation. While the molecular nature of the original and remaining organics is not known, it is expected that most of the surfactant "heads" were oxidized (since they have strong surface adsorption). Hence, the remaining TOC should contain mostly non-ionic compounds, such as alcohols, which are less harmful than the original compounds.

4.3.4. Stability of the electrodes

The stability of the α-Fe_2O_3 electrodes was clarified via FESEM. Generally, the α-Fe_2O_3 electrodes showed a good stability over three hours of reactions in both EC and PEC processes (**Figure 4-3**). Furthermore, in comparison with untreated anodes (Figure 4-1), treated α-Fe_2O_3 surfaces were changed by electrochemical reactions. Accordingly, the corrosion of α-Fe_2O_3 surface resulted in formation of smaller nano-tufts in EC (**Figure 4-3a, Figure 4-3b, Figure 4-3c**), and vigorous deformation by PEC process (**Figure 4-3d, Figure 4-3e, Figure 4-3f**). The deformation is expectedly increased with increasing voltage.
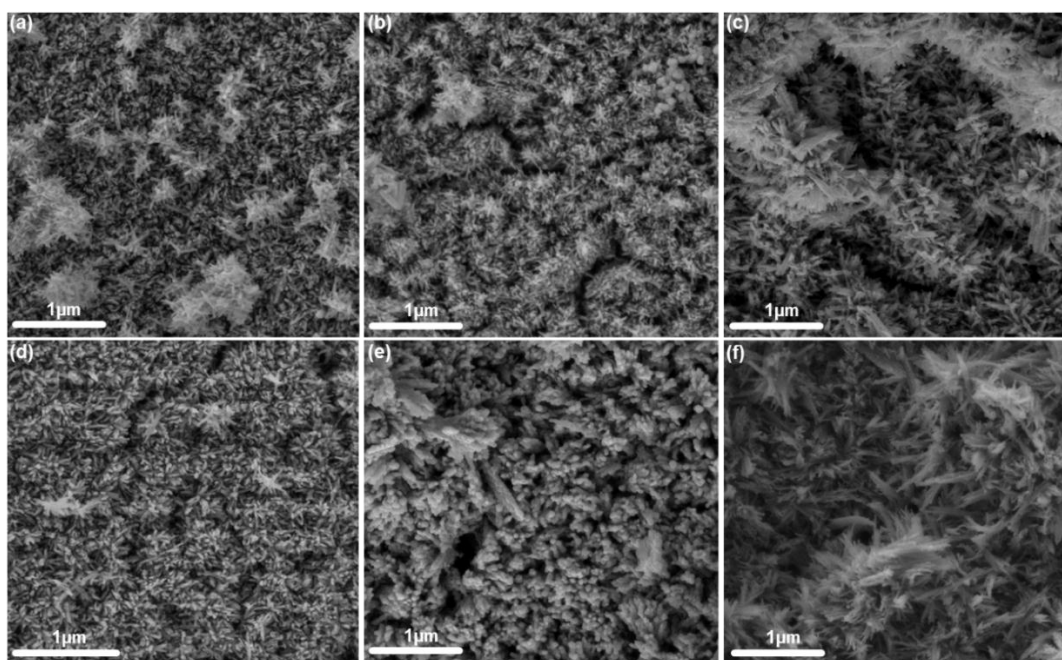
Figure 4-3. SEM images of α-Fe$_2$O$_3$ surface after EC treatment at: (a) 1 A, 1 V; (b) 1 A, 2 V; (c) 1 A, 3 V; and PEC treatment at: (d) 1 A, 1 V; (e) 1 A, 2 V; (f) 1 A, 3 V.

The PEC process had more noticeable impact on α-Fe$_2$O$_3$ films more than EC process. This is due to the larger adsorption capacity, and higher catalysis activity under solar illumination. These were consistent with the higher TOC removal, i.e. the oxidation of organics on the α-Fe$_2$O$_3$ surface. Nevertheless, α-Fe$_2$O$_3$ thin films used in this study generally exhibits a good stable under bias applied over treating time. The results provide important foundation for further scaling up for practical applications.

4.4. Summary

Organic compounds in laundry water were degraded by photoelectrochemical (PEC) and electrochemical (EC) processes on α-Fe$_2$O$_3$ anode. The EC process exhibited lower TOC removal rate than PEC process for all testing conditions. α-Fe$_2$O$_3$ anodes were still stable over three hours treatment time. Further, the experimental data were successfully described by the proposed lumped kinetic model. Accordingly, the degradation of organics from laundry water occurred by

both complete and partial oxidation. It was also found that the kinetic constants were influenced by the applied voltage.

Chapter 5

Experimental study on degradation of sodium dodecyl sulfate

This Chapter presents the degradation of SDS, which is one of the most common anionic surfactants in daily products such as detergent powder, soaps, shower gels and cosmetic. The photoelectrochemical (PEC) and electrochemical in dark (EC − dark) processes were used to decompose SDS from the water. For analysis, the presence of - OSO_3 group was monitored via UV-Vis spectrum and Fourier transform infrared spectroscopy (FTIR). Moreover, methylene blue active substance method and TOC analyzer were also used to qualify the variation of SDS and total organic compound concentration against treatment time. Different numerical models were developed to simulate the kinetics of both SDS degradation and TOC reduction simultaneously.

5.1. Kinetic models

The formation mechanism of oxidizing hydro radicals by EC and PEC processes is similar to the mechanism presented in Chapter 4 (**Eq.4-1** to **Eq.4-6**). Because of the hydrophilic behavior of SDS head group, SDS degradation from water occurred via the hydrolysis reaction of SDS to form dodecanol ($C_{12}H_{25}OH$) [233]. This reaction is very slow at normal thermodynamic conditions, i.e. atmosphere pressure and room temperature [233]. On contrast, in the presence of applied voltage and photocatalyst, the hydrolysis of SDS is accelerated by oxidizing species. Consequently, this study proposes four numerical models to simulate the kinetic characteristics of SDS degradation and TOC reduction:

5.1.1. Model P_1

The detail pathways of the Model P_1 are shown as below:

$$\text{ROSO}_3^-\text{Na}^+ \xrightarrow{\quad k_0 \quad} \text{ROH} \xrightarrow{\quad k_1 \quad} \text{CO}_2 + \text{H}_2\text{O}$$

This study employed two independent methods to quantify experimentally the kinetics: (i) UV-Vis spectroscopy to quantify SDS concentration; (ii) TOC analyzer to evaluate all organics presented in bulk solution. By assuming that all reaction follows pseudo – fist order kinetic, the first method gives kinetics of SDS removal, and the TOC measurement describes kinetic reactions of all organics, yields:

$$\frac{dC_{SDS}}{dt} = -k_0 C_{SDS} \tag{5-1}$$

For TOC reductions, we have:

$$\frac{dQ_{SDS}}{dt} = -k_0 Q_{SDS} \tag{5-2}$$

$$\frac{dQ_{ROH}}{dt} = k_0 Q_{SDS} - k_1 Q_{ROH} \tag{5-3}$$

Where, k_0, k_1 (min^{-1}) is the kinetic coefficients, C_{SDS} is the concentration of SDS (mg/L), Q_{SDS}, Q_{ROH} are the TOC concentrations corresponding to SDS, alcohols generated (mg/L), respectively. The degradation kinetic of SDS, **Eq.5-1**, is the same for all proposals from the model P$_1$ to the model P$_4$. For the model P$_1$, the **Eq. 5-1** the kinetics of SDS removal is equal to kinetics of SDS oxidation, i.e. k_0 as in the **Eq.5-3**. At this stage, the TOC of the solution is the sum of all organic presenting in solution i.e., SDS and ROH, thus:
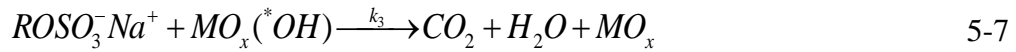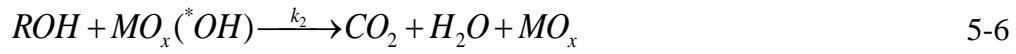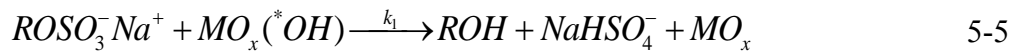
$$\frac{dTOC}{dt} = \frac{dQ_{SDS}}{dt} + \frac{dQ_{ROH}}{dt} \tag{5-4}$$

The above system of ordinary different equations could be solved and fitted against experimental data simultaneously by a numerical model developed in MATLAB (ODE45 and curve fitting). The kinetic rates can be obtained from fitting to transient data in two steps. First, k_0 was obtained from SDS transient concentration. Consequently, k_1 was obtained simultaneously from TOC data.

Likewise, we also have kinetic equations for other proposals:

5.1.2. Model P₂

The Model P_2 can be presented as the following:

$$CO_2 + H_2O$$

$$ROSO_3^-Na^+ \xrightarrow{k_2} \qquad \uparrow k_3$$

$$ROSO_3^-Na^+ \xrightarrow{k_1} ROH$$

$$ROSO_3^-Na^+ + MO_x(^*OH) \xrightarrow{k_1} ROH + NaHSO_4^- + MO_x \qquad \text{5-5}$$

$$ROH + MO_x(^*OH) \xrightarrow{k_2} CO_2 + H_2O + MO_x \qquad \text{5-6}$$

$$ROSO_3^-Na^+ + MO_x(^*OH) \xrightarrow{k_3} CO_2 + H_2O + MO_x \qquad \text{5-7}$$
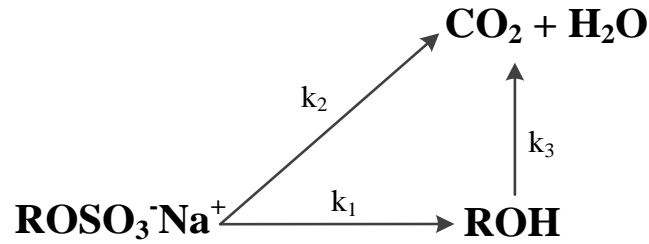
And the kinetic equations:

$$\frac{dQ_{SDS}}{dt} = -(k_1 + k_2)Q_{SDS} \qquad \text{5-8}$$
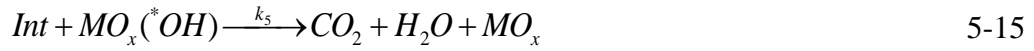
$$\frac{dQ_{ROH}}{dt} = k_1 Q_{SDS} - k_3 Q_{ROH} \qquad \text{5-9}$$

Where, k_0, k_1, $(k_1 = k_0 - k_2)$, k_2, k_3 (min^{-1}) is the kinetic coefficients. C_{SDS} is the concentration of SDS (mg/L), Q_{SDS}, Q_{ROH} are the TOC concentrations corresponding to SDS, alcohols generated (mg/L), respectively.

TOC reduction in this case is defined as the following equation:

$$\frac{dTOC}{dt} = \frac{dQ_{SDS}}{dt} + \frac{dQ_{ROH}}{dt} \qquad \text{5-10}$$

5.1.3. Model P₃

The reactions following the model P_3 can be described as below:

$$ROSO_3^-Na^+ + MO_x(^*OH) \xrightarrow{k_1} ROH + NaHSO_4^- + MO_x \qquad \text{5-11}$$

$$ROSO_3^-Na^+ + MO_x(^*OH) \xrightarrow{k_2} CO_2 + H_2O + MO_x \qquad \text{5-12}$$

$$ROH + MO_x(^*OH) \xrightarrow{k_3} Int + CO_2 + H_2O + MO_x \qquad \text{5-13}$$

$$ROH + MO_x(^*OH) \xrightarrow{k_4} CO_2 + H_2O + MO_x \qquad \text{5-14}$$

$$Int + MO_x(^*OH) \xrightarrow{k_5} CO_2 + H_2O + MO_x \qquad \text{5-15}$$

Where, *Int* refers to intermediates of partial oxidation i.e., shorter-chain alcohols, or acids.

And the kinetic equations:

$$\frac{dQ_{SDS}}{dt} = -(k_1 + k_2)Q_{SDS} \qquad \text{5-16}$$

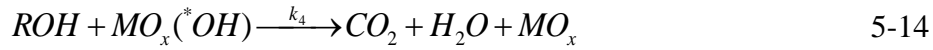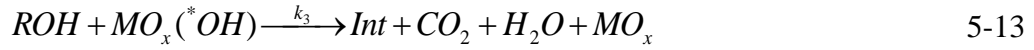$$\frac{dQ_{ROH}}{dt} = k_1 Q_{SDS} - (k_3 + k_4)Q_{ROH} \qquad \text{5-17}$$

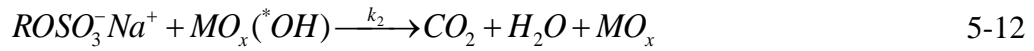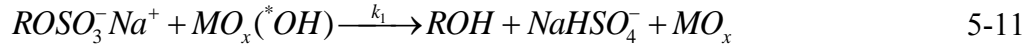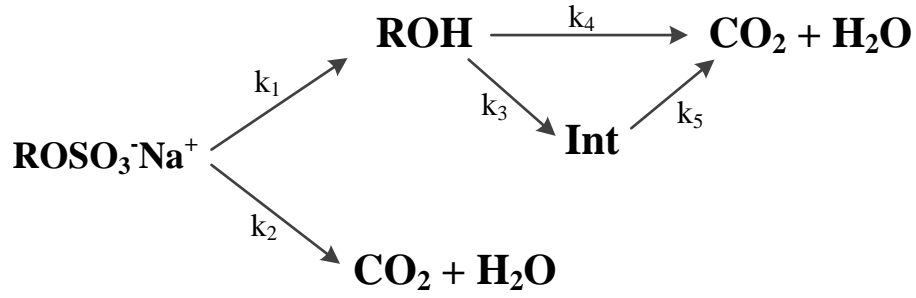$$\frac{dQ_{Ints}}{dt} = k_3 Q_{ROH} - k_5 Q_{Ints} \qquad \text{5-18}$$

Where, k_1, k_2 ($k_2 = k_0 - k_1$), k_3, k_4, k_5 (min^{-1}) is the kinetic coefficients. C_{SDS} is the concentration of SDS (mg/L), Q_{SDS}, Q_{ROH}, Q_{Int} are the TOC concentrations corresponding to SDS, alcohols and intermediate compounds (mg/L), respectively. At this stage, the TOC of the solution is also the sum of all organics presenting in solution i.e., SDS, ROH, and Int, thus:

$$\frac{dTOC}{dt} = \frac{dQ_{SDS}}{dt} + \frac{dQ_{ROH}}{dt} + \frac{dQ_{Int}}{dt}$$ 5-19

5.1.4. Model P₄

For this model, the reactions of SDS degradation are assumed as the following reactions:
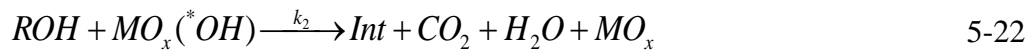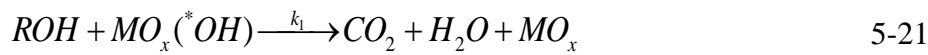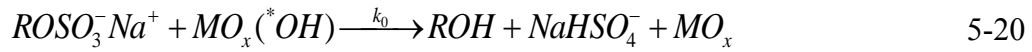
$$ROSO_3^-Na^+ \xrightarrow{k_0} ROH \xrightarrow{k_1} CO_2 + H_2O$$

with $ROH \xrightarrow{k_2} Int$ and $Int \xrightarrow{k_3}$

$$ROSO_3^-Na^+ + MO_x(^*OH)\xrightarrow{k_0}ROH + NaHSO_4^- + MO_x$$ 5-20

$$ROH + MO_x(^*OH)\xrightarrow{k_1}CO_2 + H_2O + MO_x$$ 5-21

$$ROH + MO_x(^*OH)\xrightarrow{k_2}Int + CO_2 + H_2O + MO_x$$ 5-22

$$Int + MO_x(^*OH)\xrightarrow{k_3}CO_2 + H_2O + MO_x$$ 5-23

Where, *Int* refers to intermediates of partial oxidation i.e., shorter-chain alcohols, or acids.

Thus, the kinetic equations of TOC reduction in this case are:

$$\frac{dQ_{SDS}}{dt} = -k_0Q_{SDS}$$ 5-24

$$\frac{dQ_{ROH}}{dt} = k_0Q_{SDS} - (k_1 + k_2)Q_{ROH}$$ 5-25

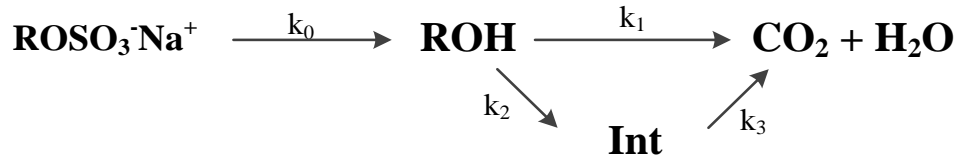$$\frac{dQ_{Int}}{dt} = k_2Q_{ROH} - k_3Q_{Int}$$ 5-26

Where, k_1, k_2, k_3 (min^{-1}) is the kinetic coefficients. C_{SDS} is the concentration of SDS (mg/L), Q_{SDS}, Q_{ROH}, Q_{Int} are the TOC concentrations corresponding to SDS, alcohols and intermediate compounds (mg/L), respectively. For the model P₄, the TOC of the solution is the sum of all organic presenting in solution i.e., SDS, ROH, and *Int*, thus:

$$\frac{dTOC}{dt} = \frac{dQ_{SDS}}{dt} + \frac{dQ_{ROH}}{dt} + \frac{dQ_{Int}}{dt}$$

5-27

It can be seen that the model P_1, model P_2, model P_3, and the model P_4 has 2, 3, 5, 4 parameters, respectively. This study employs these models to fit experimental data. The effectiveness of these models is hence verified.

5.2. Results and Discussion

5.2.1. Surface morphology and crystalline of photoanode

The morphology and crystalline of α-Fe$_2$O$_3$ anode are showed in **Figure 5-1**. Whereby, α-Fe$_2$O$_3$ nanoflake structured film illustrated to have the larger adsorption capacity than that of particle films [234] was found. While, crystalline properties and the phase formation of α-Fe$_2$O$_3$ photoanode were investigated by X-ray diffraction analysis (**Figure 5-1**). The α-Fe$_2$O$_3$ peaks were observed at 28.09^0, 38.65^0, 42.44^0, 47.86^0, 58.08^0, 64.72^0, 67.65^0 74.84^0, 76.85^0. Apparently, only hematite phase was formed after the annealing process, since no any related-impurity peak was observed. A similar prevalence of the peaks has also been observed for α-Fe$_2$O$_3$ film in the study carried out by sol-gel method [195].
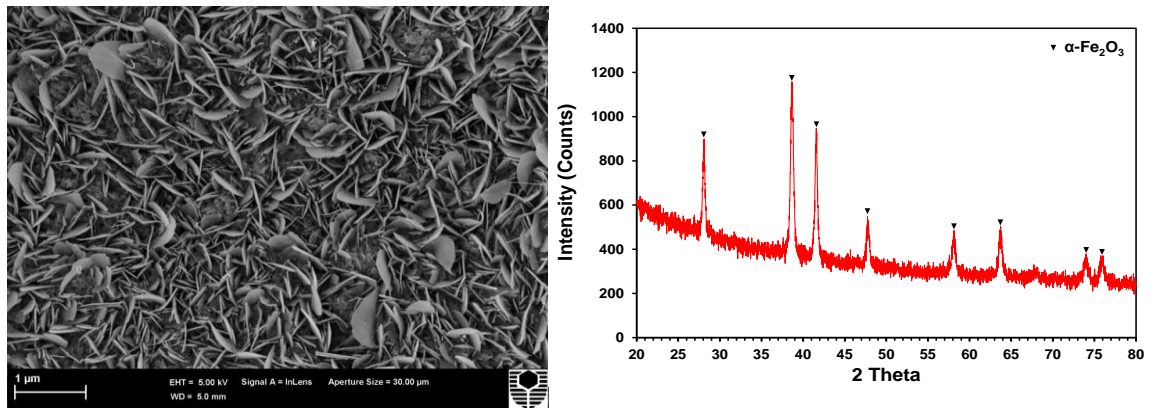
Figure 5-1. SEM and XRD of α-Fe$_2$O$_3$ anode prepared by the procedure II.

5.2.2. UV – Vis Spectra

The UV-Vis adsorption spectra of MB-SDS ion pairs in aqueous solutions are presented in **Figure 5-2**. The maximum adsorption of ion-pairs is at 653 nm, and a negligible shoulder at 612 nm. A good agreement between these observations and

reported values of Zaghbani et.al., [235], and Hayashi [236]. No any peak corresponding to $-SO_3$ group was observed after 1 hour of treatment with both PEC and EC – dark processes, which illustrated the complete decomposition of SDS from solution.
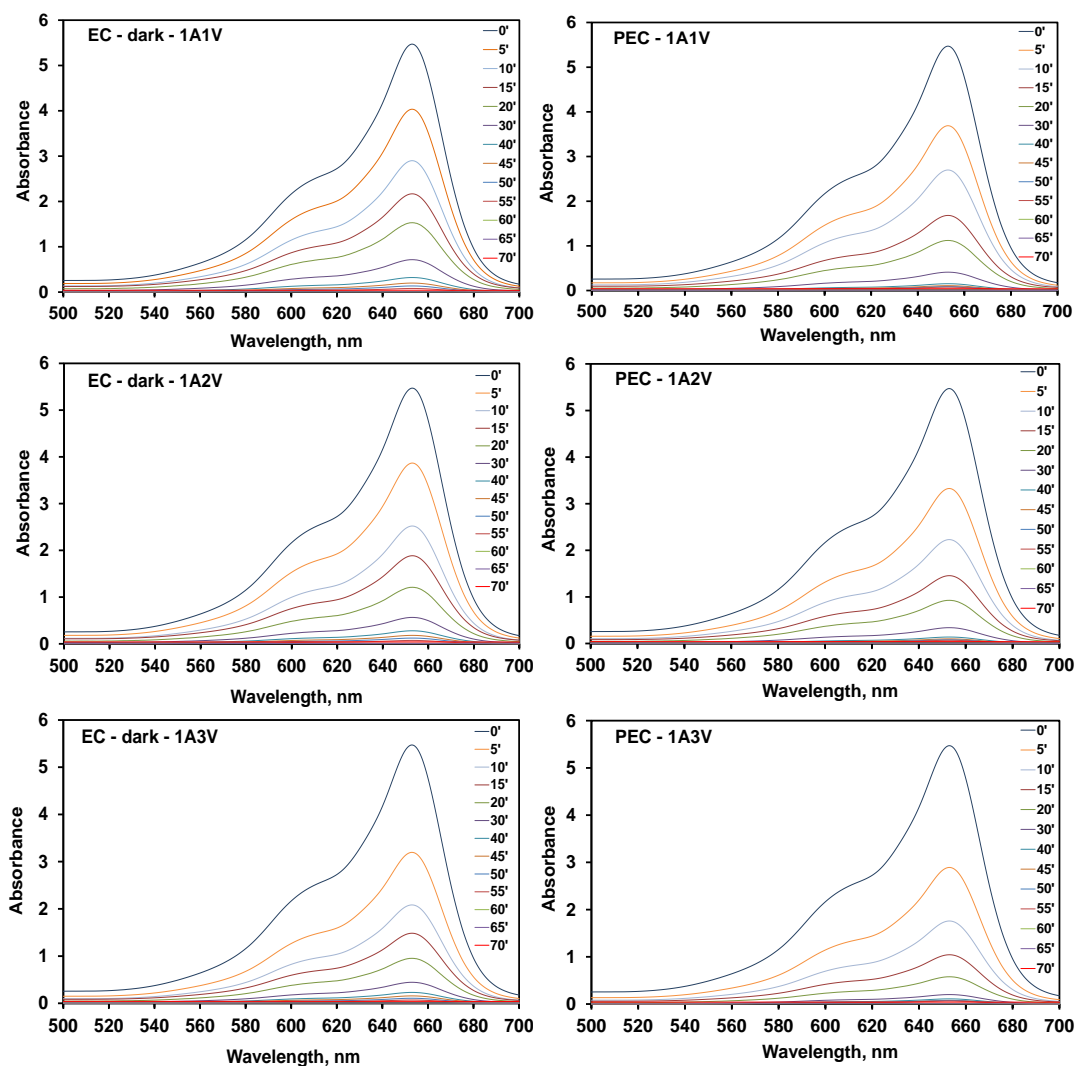
Figure 5-2. UV-Vis spectra of SDS-MB ion pairs.

5.2.3. SDS degradation and kinetics

SDS was completely removed after one hour of treatment by both PEC and EC – dark processes under all testing conditions (**Figure 5-3**). Without applied current, on contrast, only 1 % was removed after three hours **(Figure 5-3a)**, due to physical adsorption. Being an anionic surfactant, the adsorption of SDS reached equilibrium rapidly owing to the strong attractive interaction between α-Fe$_2$O$_3$ photocatalyst

and polar head group [237]. Thus, α-Fe$_2$O$_3$ surface was covered by SDS molecules. The adsorption along was insignificant comparing to the soluble SDS.
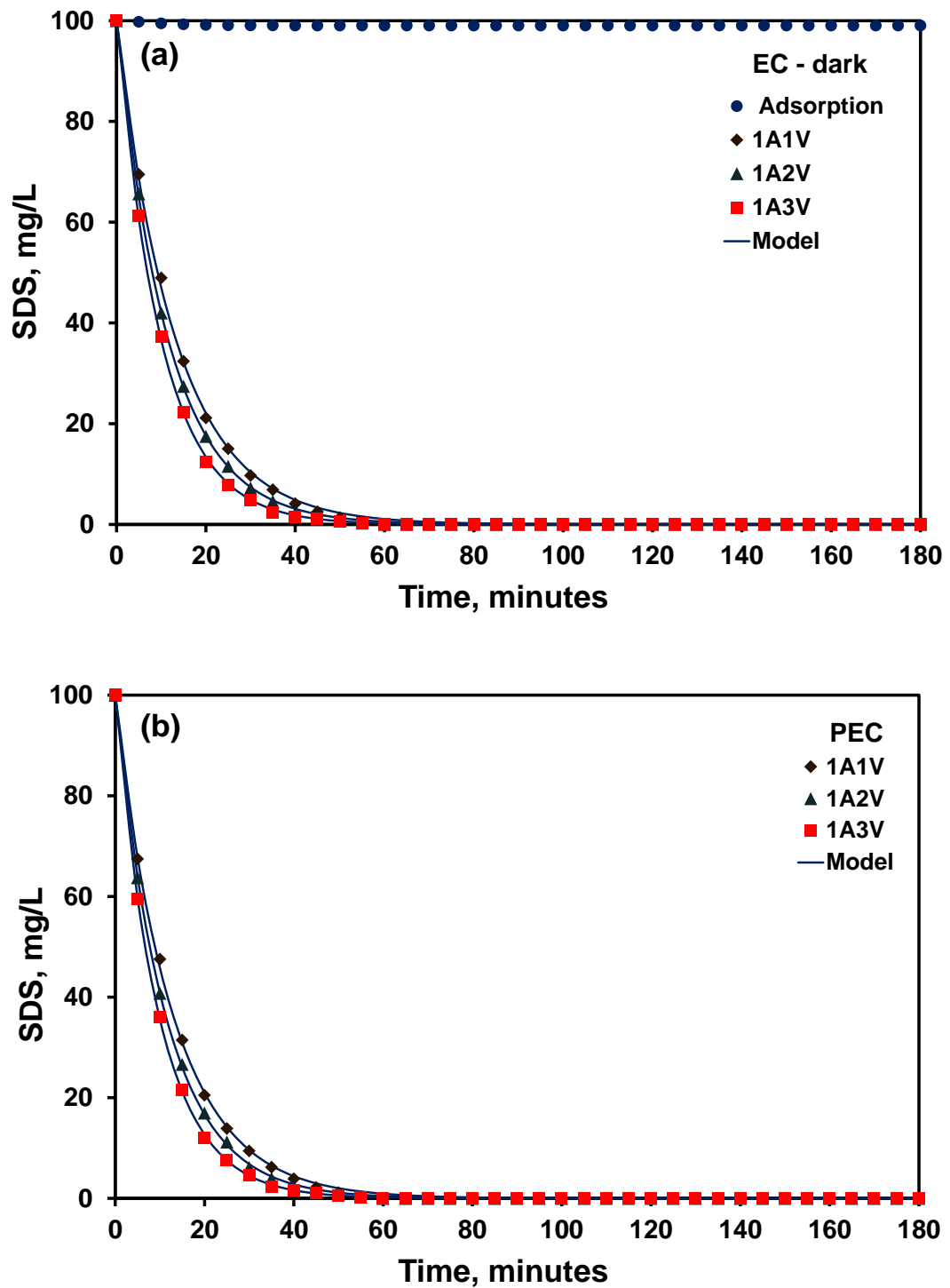
Figure 5-3. SDS concentration determined via MBAS method: (a) EC - dark and (b) PEC process. Model is taken from the Eq. 5-1.

By applying voltage crossing α-Fe_2O_3 anode, adsorbed SDS molecules were rapidly degraded to dodecanol or intermediates. The proposed model, **Eq.5-1**, fitted the experimental data of EC – dark and PEC treatment very well. The kinetic constant, k_0, was slightly different between the two processes. Hence, SDS removal was dominated by the applied current due to its ionic nature. In other words, the light had a minimal effect on SDS degradation.

Table 5-1. Kinetic coefficients of SDS degradation.

Process	DC bias	k_0, min^{-1}
EC – dark	1 A, 1 V	7.5×10^{-2}
	1 A, 2 V	8.6×10^{-2}
	1 A, 3 V	10.0×10^{-2}
PEC	1 A, 1 V	7.8×10^{-2}
	1 A, 2 V	9.0×10^{-2}
	1 A, 3 V	10.3×10^{-2}

The degradation of SDS via these processes is superior to those of other methods such as Fenton-liked advanced oxidation (63% at 1 hour) [238], natural hydrolysis SDS in acid environment (100% hydrolysis of SDS after 12 hours) [233], or biodegradation with bacteria (almost 97% after 10 days) [239].

5.2.4. TOC reduction

To simplify, the study first simulates the TOC reduction kinetics of the PEC process at 1 A, 1 V. This experimental data were fitted by the model P_1 to the model P_4 (**Figure 5-4**). As can be seen that the experimental data were not well simulated by the model P_1, model P_2, and model P_3. On contrast, the proposed the model P_4 fitted the experimental data very well.
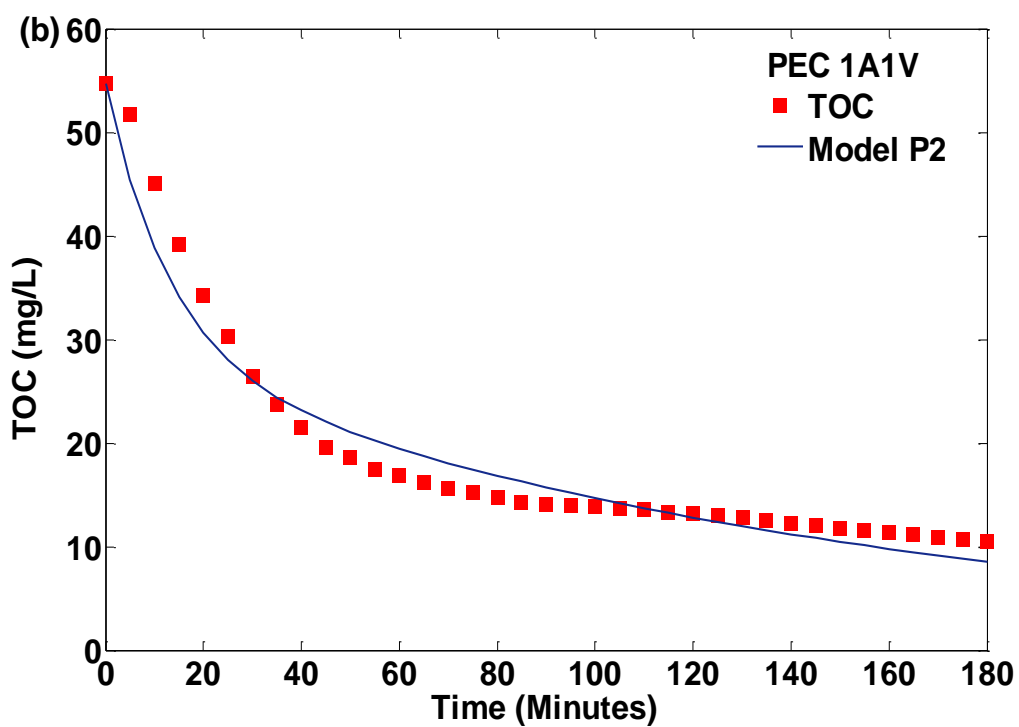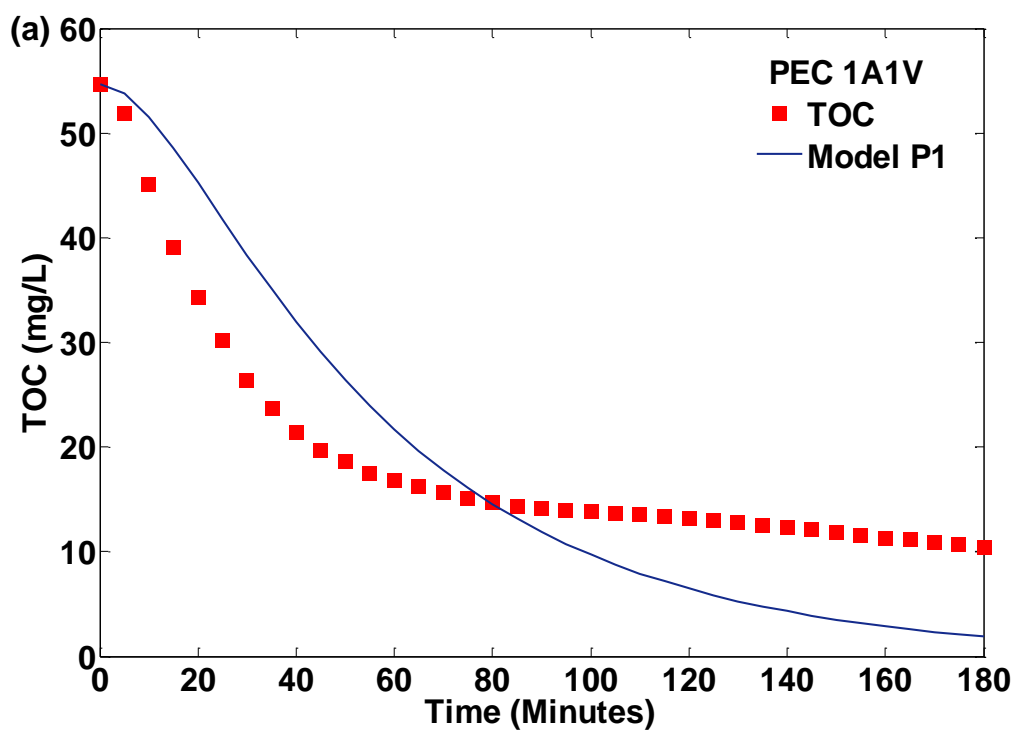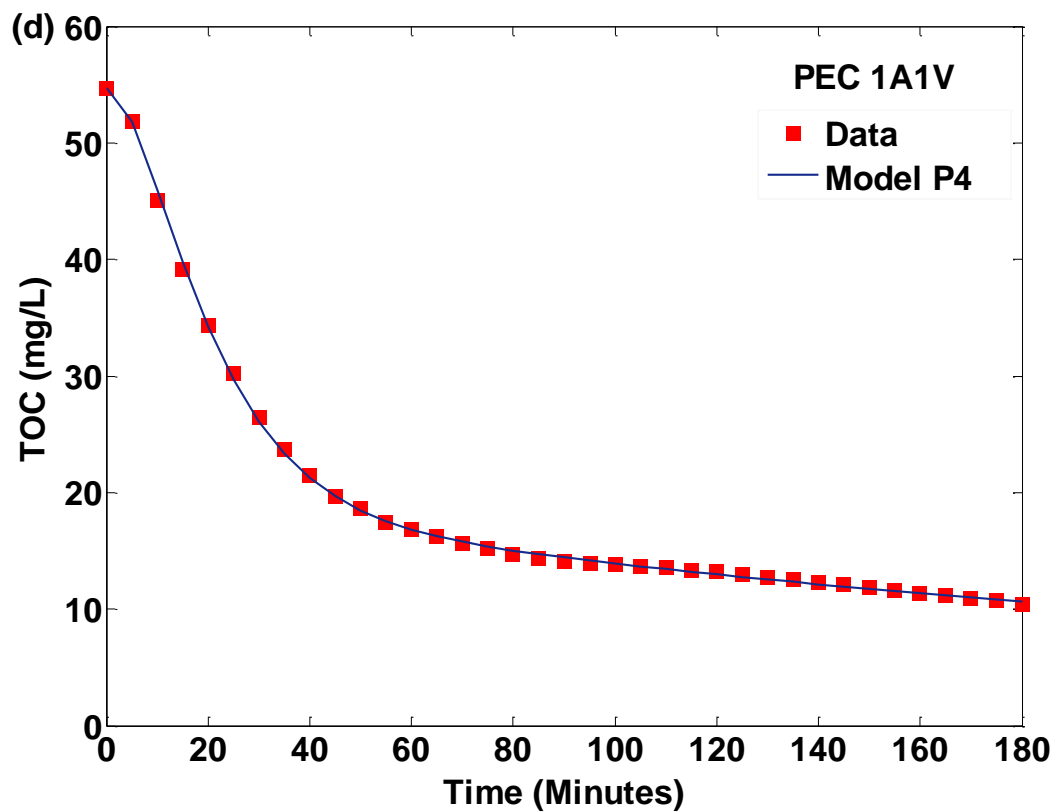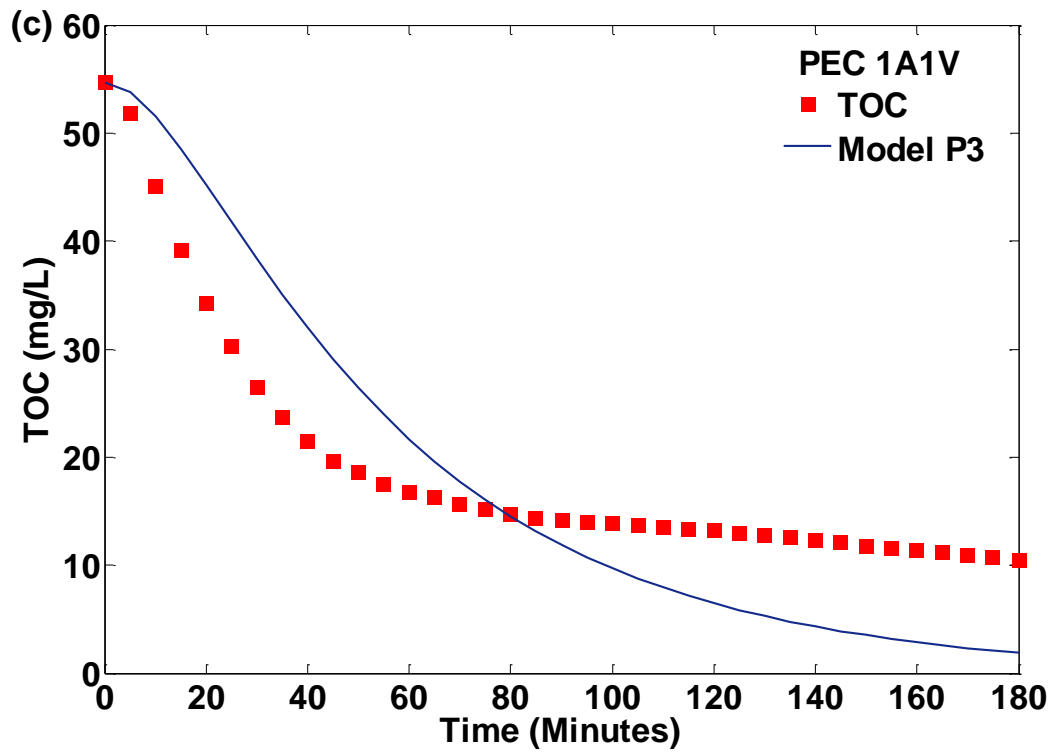
Figure 5-4. TOC reduction kinetics during SDS degradation by PEC processes at 1V: (a) P_1; (b) P_2; (c) P_3; (d) P_4, taken from the **Eq.5-4** (P1); **Eq.5-10** (P2); **Eq.5-19** (P3)**, Eq. 5-27** (P4)**.**

This can be explained that the model P_1 was not enough kinetic parameters (only 2) to describe the whole kinetics of TOC reduction during the degradation of SDS. Meanwhile, the model P_2 and model P_3 could not present the nature of SDS molecule, which is easily hydrolyzed in water owing to its hydrophilic head group. Indeed, the hydrolysis of SDS to form dodecanol is the first priority when dissolving SDS in water. In other words, the proposed model P_4 model was selected to describe the TOC reduction kinetics for all testing conditions in both EC and PEC processes. Accordingly, the TOC reduction during SDS degradation by PEC and EC processes with applied voltage from 1 V to 3 V is shown in **Figure 5-5.**
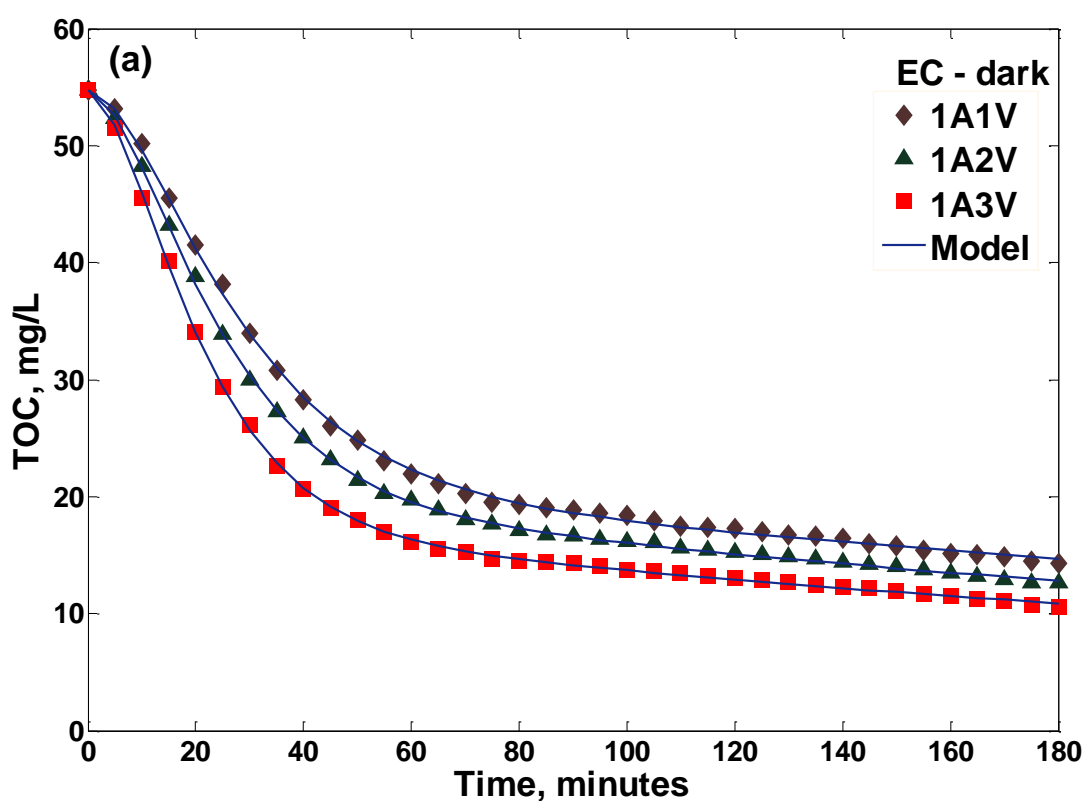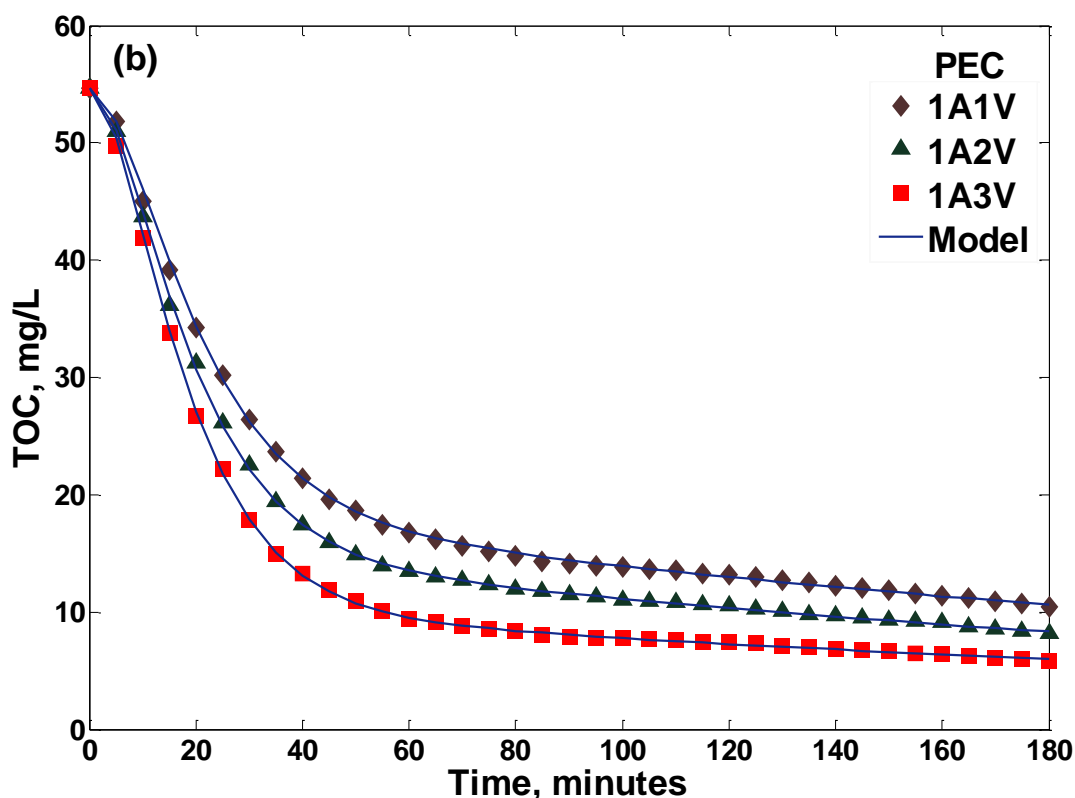
Figure 5-5. TOC reduction during SDS degradation by (a) EC and (b) PEC
processes with different applied voltage.

It should be noted that the initial TOC was 54 mg/L, which was more than the
carbon quantity corresponding to 100 mg/L SDS. The difference was a result of
impurity on SDS, which has been well-documented in the literature [240].
Comparing to the degradation of SDS molecules (**Figure 5-3**), TOC kinetics in all
case was slower (k_0 is much larger than k_1, k_2, k_3). Moreover, the sharp change in
TOC curves after 60 minutes revealed two distinguishable steps. Within the first
hour, TOC was reduced quickly, which corresponded well to the completed
removal of SDS. Afterward, the TOC followed a gradual decline. The change
reflected the dominant role of partial oxidation after the formation of dodecanol.
The intermediates, products of partial oxidation, have much slower oxidation rates.
Quantitatively, the kinetics constants reflect the relative rates of oxidation. The
direct oxidation dodecanol to carbon dioxide was far larger than others ($k_1 > k_2$ and
k_3 in all conditions). It is noteworthy that PEC had higher constants than EC − dark
in all testing conditions: k_1 was almost double, while k_2, k_3 were approximately 1.5
times higher. Thus, the PEC presented a better decomposition of generated SDS

derivatives compared to EC – dark process. Contrasting to SDS degradation, TOC removal was evidently enhanced by light.

To verify the obtained modeling, the 95 % confidence interval [241] of the fitting parameters were calculated for all systems (**Table 5-2a - Table 5-2c**). Apparently, the errors were negligible for all k values (< 10 %). The good agreement between theoretical and experimental results and the small confidence interval confirm the appropriateness of the proposed mechanism.

Table 5-2. Kinetic coefficients and their 95% confidence interval parameters of TOC reduction kinetics with testing conditions from 1 V – 3 V.

a - 1A 1V				
Constants (min^{-1})	**PEC**	**95% CI**	**EC - dark**	**95% CI**
$k_1 \times 10^{-2}$	7.43	7.17 - 7.69	3.78	3.65 - 3.90
$k_2 \times 10^{-2}$	3.62	3.40- 3.84	2.29	2.12 - 2.47
$k_3 \times 10^{-3}$	3.31	3.08 - 3.54	2.28	2.00 - 2.57

b - 1A 2V				
Constants (min^{-1})	**PEC**	**95% CI**	**EC - dark**	**95% CI**
$k_1 \times 10^{-2}$	8.22	8.02 - 8.42	4.55	4.46 – 4.64
$k_2 \times 10^{-2}$	3.04	2.90 - 3.19	2.50	2.39 – 2.62
$k_3 \times 10^{-3}$	3.60	3.39 - 3.81	2.71	2.54 - 2.88

c -1A 3V				
Constants (min^{-1})	**PEC**	**95% CI**	**EC - dark**	**95% CI**
$k_1 \times 10^{-2}$	10	9.82 – 10.17	5.69	5.57– 5.81
$k_2 \times 10^{-2}$	2.26	2.17 – 2.35	2.57	2.45 – 2.68
$k_3 \times 10^{-3}$	3.27	3.04 – 3.50	2.84	2.65 – 3.02

In addition to the kinetics, overall TOC removal efficiency after 180 minutes of treatment was defined as the following equation:

$$\% \, removal = \frac{TOC_0 - TOC_t}{TOC_0} 100 \qquad \text{5-28}$$

Where, TOC_0, TOC_t is the initial and transient TOC concentration (mg/L) respectively.

The higher the bias, the larger SDS was removed in both of two processes (**Table 5-2a, 5-2b, and 5-2c**). Apparently, at high bias applied crossing electrodes, the rate constants of completed oxidizing reactions were higher as a result of a large amount of current carrier (photoelectrons) passes through the anode, and photocurrent excited holes and electrons used to oxidize organics. Moreover, 90% and 80 % TOC was removed after three treatment hours at 3 V applied via PEC and EC – dark process, respectively. Likewise, TOC removal efficiency of the PEC process was 7% and 8% higher in than EC – dark with 1 V and 2 V respectively. This divergence illustrated explicitly the higher efficiency of the PEC process in removing more stable organics. These results also confirm the rationality of the k variation between two processes. After the first treatment hour, polar molecules (SDS) were rapidly removed by both of two processes by adsorbing onto the oppositely charged α-Fe_2O_3 surface. However, degradation of intermediate products, i.e. dodecanol or acids, was strongly driven by the PEC process, which has more oxidizing radical species.

Table 5-3. Overall SDS degradation efficiency after 180 minutes.

Process	Efficiency (%)		
	1 A, 1 V	1 A, 2 V	1 A, 3 V
EC – dark	73	77	80
PEC	80	85	90

5.2.5. Verification of the intermediate products

The solution samples were analyzed via FTIR spectrum (**Figure 5-6**). The disappearance of SDS molecules and the appearance of intermediates were verified qualitatively. In the 3000-2800 cm^{-1} region, the spectrum of SDS was dominated by the asymmetric and symmetric stretching bands of $-$ CH$_3$ and $-$ CH$_2$ of the hydrocarbon tail [242]. The adsorption band from 3200 to 3500 cm^{-1} was linked to the stretching of $-$ OH from the intermolecular hydrogen bond, particularly $-$ OH bonded (3329 cm^{-1}) and free alcohol (3461 cm^{-1}) [243]. While, the adsorption at 1561 cm^{-1} was owing to the bending mode of $-$ CH$_2$ $-$, whereas the weak band at 1220 cm^{-1} corresponds to a $-$ CH$_3$ deformation [244]. From 1220 to 950 cm^{-1}, the spectrum exhibits several distinct asymmetric and symmetric stretching bands of $-$ OSO$_3$. The strong doublet at 1220 and 1061 cm^{-1} corresponds to asymmetric S$-$O stretching, conversely the peaks at 1061 and 979 cm^{-1} result from symmetric S$-$O stretching. The correlation between symmetry and IR spectra of sulfate complexes has been well established [245].
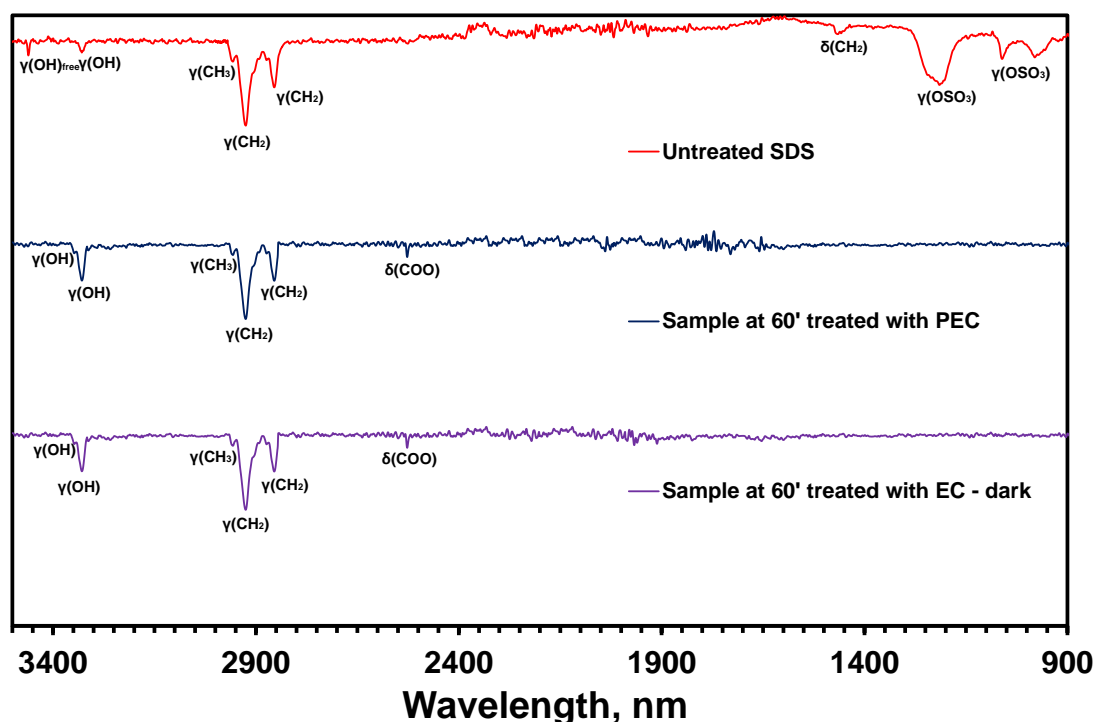
Figure 5-6. FTIR spectrum of initial SDS, and treated solution with PEC, and EC $-$ dark at 1 V at 60 minutes.

The peaks corresponding to $-OSO_3$ group were not observed after one hour of treatment with both PEC and EC – dark. Meanwhile, the presence of alcohol with peaks in the region from 3200 to 3500 cm^{-1} was still detected. Furthermore, new peaks at 2531 cm^{-1} reflecting the appearance of carboxylic acids and their derivatives (2500 – 3300 cm^{-1}) [245] were recognized. The same results were also found from the two processes at other voltage values against time i.e., 2 V and 3 V. In summary, the spectrum profiles confirm the kinetics modelling: (i) $-SO_3$ group of SDS was completely removed within 1 hours, and (ii) intermediates with hydroxyl and carboxylic groups were formed.

5.3.   Summary

Overall, SDS was completely degraded after the first hour of treatment by both photoelectrochemical (PEC) and electrochemical in dark (EC – dark) processes. While, only 1% SDS was removed by physical adsorption on α-Fe_2O_3 surface. The different ordinary equation kinetic model developed successfully described the kinetics of both SDS removal and TOC reduction. Further, the mechanisms of EC and PEC reactions for TOC reduction in this study were similar to those of Chapter 4 presented. These results once again confirm the rationality of the proposed models for degradation of organics from laundry water by EC and PEC methods.

Chapter 6   Conclusions and Recommendations

6.1.   Conclusions

In this study, α-Fe$_2$O$_3$ thin films were successfully synthesized by the sol-gel spin coating method. The α-Fe$_2$O$_3$ nano-tuft nanostructure was obtained after annealing the deposited sample at 450 ^{0}C for 2 hours in the furnace. The organic compounds from synthetic laundry water were removed by the EC and PEC processes on these α-Fe$_2$O$_3$ thin films with applied voltage from 1 V to 3 V. It was found that the PEC exhibited higher efficiency than the EC process in removing organic pollutants. Accordingly, approximately 53 % and 47 % TOC were removed by PEC and EC process at 1 A, 3 V respectively. Further, it was found that the kinetics of organic degradation from laundry water occurred via two mechanisms: (i) completed oxidation to form CO_2 and water; and (ii) break-down to shorter chains. The remaining organics are expectedly less surface active and consequently less harmful than the original compounds. The lumped kinetic model well fitted the experimental data. The stability of the α-Fe$_2$O$_3$ anodes was also investigated. The PEC process had the more noticeable impact on α-Fe$_2$O$_3$ films more than EC process owing to the larger adsorption capacity and higher catalysis activity under solar illumination. However, nanostructured anode used in this study exhibits a good stable under bias applied over the treating time.

Also in this study, α-Fe$_2$O$_3$ nanoflake structure were obtained by annealing the deposited film at 450 ^{0}C for 8 hours. Sodium dodecyl sulfate was completely degraded after the first hour of treatment by both the PEC and EC – dark processes on α-Fe$_2$O$_3$ anode. It was found that sodium dodecyl sulfate removal was dominated by the applied current due to its ionic nature. The PEC and EC processes also removed 90% and 80% TOC from the SDS solution respectively. The remaining organics contain hydroxyl and carboxylic groups, which are expectedly less surface active and consequently less harmful than SDS. The proposed numerical model successfully described the experimental data. Accordingly, the degradation of SDS includes the hydrolysis of SDS to form alcohols in water and both partial and completed decomposition these alcohols to generate intermediates

or carbon dioxide respectively. The quantitative and qualitative results confirmed the proposal mechanism and modeling assumptions.

Overall, all the results present the economical and environmentally friendly methods for the degradation of organics from domestic laundry wastewater that can be applied in Australia at a household level. The methods can also be used for rural areas in developing countries, where centralized wastewater treatment and electricity are not available.

6.2. Recommendations

This study explores the removal of organics and sodium dodecyl sulfate from laundry water by the electrochemical (EC) and photoelectrochemical (PEC) processes on α-Fe_2O_3 nanostructure. Based on the results of this study, the following recommendations are offered for future research works:

- Use flow through reactors running for few hours per day. This study used a non - continuous reactor for testing on the lab scale. Thus, for practical applications, the larger and continuous reactor should be investigated.

- Degrade other kinds of wastewater by using the processes from this study. These presented techniques should also be tested for treatment of black water (such as wastewater from toilets).

- Supply power for the processes by using solar panels. By investigating this step, the operating cost of the PEC and EC processes can be considerably reduced.

- The presented methods can be combined with other methods such as adsorption or bio-membrane to achieve the desirable efficiency.

References

1. Kivaisi, A.K., *The potential for constructed wetlands for wastewater treatment and reuse in developing countries: a review.* Ecological Engineering, 2001. **16**(4): p. 545-560.

2. Massoud, M.A., A. Tarhini, and J.A. Nasr, *Decentralized approaches to wastewater treatment and management: Applicability in developing countries.* Journal of Environmental Management, 2009. **90**(1): p. 652-659.

3. Burkhard, R., A. Deletic, and A. Craig, *Techniques for water and wastewater management: a review of techniques and their integration in planning.* Urban Water, 2000. **2**(3): p. 197-221.

4. Jeppesen, B., *Domestic greywater re-use: australia's challenge for the future.* Desalination, 1996. **106**(1): p. 311-315.

5. *Living in the environment principles, connections, and solutions.* Reference & Research Book News, 2006. **15**.

6. Qadir, M., et al., *The challenges of wastewater irrigation in developing countries.* Agricultural Water Management, 2010. **97**(4): p. 561-568.

7. Levine, A.D. and T. Asano, *Peer reviewed: recovering sustainable water from wastewater.* Environmental Science & Technology, 2004. **38**(11): p. 201A-208A.

8. Finley, S., S. Barrington, and D. Lyew, *Reuse of domestic greywater for the irrigation of food crops.* Water, Air, and Soil Pollution, 2009. **199**(1-4): p. 235-245.

9. Butkovskyi, A., et al., *Electrochemical conversion of micropollutants in grey water.* Environmental Science & Technology, 2013: p. 1893–1901.

10. Ahmad, J. and H. El-Dessouky, *Design of a modified low cost treatment system for the recycling and reuse of laundry waste water.* Resources, Conservation and Recycling, 2008. **52**(7): p. 973-978.

11. Banat, I.M., R.S. Makkar, and S. Cameotra, *Potential commercial applications of microbial surfactants.* Applied Microbiology and Biotechnology, 2000. **53**(5): p. 495-508.

12.   Schouten, N., et al., *Selection and evaluation of adsorbents for the removal of anionic surfactants from laundry rinsing water.* Water Research, 2007. **41**(18): p. 4233-4241.

13.   Park, Y., et al., *Removal of cobalt, strontium and cesium from radioactive laundry wastewater by ammonium molybdophosphate–polyacrylonitrile (AMP–PAN).* Chemical Engineering Journal, 2010. **162**(2): p. 685-695.

14.   Cserháti, T., E. Forgács, and G. Oros, *Biological activity and environmental impact of anionic surfactants.* Environment International, 2002. **28**(5): p. 337-348.

15.   Ying, G.-G., *Fate, behavior and effects of surfactants and their degradation products in the environment.* Environment International, 2006. **32**(3): p. 417-431.

16.   Poyatos, J.M., et al., *Advanced oxidation processes for wastewater treatment: State of the art.* Water, Air, and Soil Pollution, 2010. **205**(1-4): p. 187-204.

17.   Chong, M.N., et al., *Recent developments in photocatalytic water treatment technology: A review.* Water Research, 2010. **44**(10): p. 2997-3027.

18.   Shi, Y., et al., *Novel α-Fe_2O_3/CdS cornlike nanorods with enhanced photocatalytic performance.* ACS Applied Materials & Interfaces, 2012. **4**(9): p. 4800-4806.

19.   Andreas Kay, IIkay Cersar, and M. Gratzel, *New benchmark for water photooxidation by nanostructured α-Fe_2O_3 films.* Journal of the American Chemical Society, 2006. **128**(49): p. 15714-15721.

20.   Sun, W., et al., *Facile synthesis of surface-modified nanosized α-Fe_2O_3 as efficient visible photocatalysts and mechanism insight.* The Journal of Physical Chemistry C, 2013. **117**(3): p. 1358-1365.

21.   Bourne, P.G., *Water and sanitation: economic and sociological perspectives.* 2013: Elsevier.

22.   Montgomery, M.A. and M. Elimelech, *Water and sanitation in developing countries: including health in the equation.* Environmental Science & Technology, 2007. **41**(1): p. 17-24.

23.   Hanjra, M.A. and M.E. Qureshi, *Global water crisis and future food security in an era of climate change.* Food Policy, 2010. **35**(5): p. 365-377.

24. Rijsberman, F.R., *Water scarcity: Fact or fiction?* Agricultural Water Management, 2006. **80**(1–3): p. 5-22.

25. Huang, Y.-R., et al., *Application of electrolyzed water in the food industry.* Food Control, 2008. **19**(4): p. 329-345.

26. Wilderer, P., *Applying sustainable water management concepts in rural and urban areas: some thoughts about reasons, means and needs.* Water Science & Technology, 2004. **49**(7): p. 7-16.

27. Owlad, M., et al., *Removal of hexavalent chromium-contaminated water and wastewater: a review.* Water, Air, and Soil Pollution, 2009. **200**(1-4): p. 59-77.

28. Brown, V.M., D.H.M. Jordan, and B.A. Tiller, *The effect of temperature on the acute toxicity of phenol to rainbow trout in hard water.* Water Research, 1967. **1**(8-9): p. 587-594.

29. Takeda, N. and K. Teranishi, *Generation of superoxide anion radical from atmospheric organic matter.* Bulletin of Environmental Contamination and Toxicology, 1988. **40**(5): p. 678-682.

30. Xiao, Z., et al., *Enhanced photocatalytic activity of Bi-doped α-Fe$_2$O$_3$.* Journal of Advanced Oxidation Technologies, 2014. **17**(1): p. 93-98.

31. Ge, J., et al., *New bipolar electrocoagulation–electroflotation process for the treatment of laundry wastewater.* Separation and Purification Technology, 2004. **36**(1): p. 33-39.

32. Wang, C.-T., W.-L. Chou, and Y.-M. Kuo, *Removal of COD from laundry wastewater by electrocoagulation/electroflotation.* Journal of Hazardous Materials, 2009. **164**(1): p. 81-86.

33. Showell, M.S., *Powdered detergents / edited by Michael S. Showell*, ed. M.S. Showell. 1998, New York: New York : Marcel Dekker.

34. Ward, M., *Uniliver Unveils new-generation compact detergent powder.* Chem. Week, 1994. **154**(17): p. 15-15.

35. Rahimpour, A., S. Madaeni, and Y. Mansourpanah, *The effect of anionic, non-ionic and cationic surfactants on morphology and performance of polyethersulfone ultrafiltration membranes for milk concentration.* Journal of Membrane Science, 2007. **296**(1): p. 110-121.

36. Falbe, J., *Surfactants in consumer products: Theory, Technology and Application*. 2012: Springer Science & Business Media.

37. Mahvi, A.H., *Removal of anionic surfactants in detergent wastewater by chemicalcoagulation.* Pakistan Journal of Biological Sciences, 2004. **7**(12): p. 2222-2226.

38. Quironga, J.M. and D. Sales, *Experimental variables in biodegradation of surfactant in marine environment.* Bulletin of Environmental Contamination and Toxicology, 1990. **44**(6): p. 851-858.

39. Papadopoulos, A., et al., *An assessment of the quality and treatment of detergent wastewater.* Water Science and Technology, 1997. **36**(2–3): p. 377-381.

40. Sen, T.K., et al., *Removal of anionic surfactant sodium dodecyl sulphate from aqueous solution by adsorption onto pine cone biomass of Pinus Radiate: equilibrium, thermodynamic, kinetics, mechanism and process design.* Desalination and Water Treatment, 2012. **45**(1-3): p. 263-275.

41. Lea, J. and A.A. Adesina, *The photo-oxidative degradation of sodium dodecyl sulphate in aerated aqueous TiO$_2$ suspension.* Journal of Photochemistry and Photobiology A: Chemistry, 1998. **118**(2): p. 111-122.

42. Sammalkorpi, M., M. Karttunen, and M. Haataja, *Ionic surfactant aggregates in saline solutions: sodium dodecyl sulfate (SDS) in the presence of excess sodium chloride (NaCl) or calcium chloride (CaCl$_2$).* The Journal of Physical Chemistry B, 2009. **113**(17): p. 5863-5870.

43. Dutkiewicz, E. and A. Jakubowska, *Effect of electrolytes on the physicochemical behaviour of sodium dodecyl sulphate micelles.* Colloid and Polymer Science, 2002. **280**(11): p. 1009-1014.

44. Mungray, A.K. and P. Kumar, *Occurrence of anionic surfactants in treated sewage: risk assessment to aquatic environment.* Journal of Hazardous Materials, 2008. **160**(2): p. 362-370.

45. Olkowska, E., Z. Polkowska, and J. Namiesnik, *Analytics of surfactants in the environment: problems and challenges.* Chemical Reviews, 2011. **111**(9): p. 5667-5700.

46.   Kıran, I., et al., *Photocatalytic Fenton oxidation of sodium dodecyl sulfate solution using iron-modified zeolite catalyst.* Desalination and Water Treatment, 2013. **51**(28-30): p. 5768-5775.

47.   Laine, D.F. and I.F. Cheng, *The destruction of organic pollutants under mild reaction conditions: A review.* Microchemical Journal, 2007. **85**: p. 183-193.

48.   Hospido, A., et al., *Environmental evaluation of different treatment processes for sludge from urban wastewater treatments: Anaerobic digestion versus thermal processes (10 pp).* The International Journal of Life Cycle Assessment, 2005. **10**(5): p. 336-345.

49.   Rushton, L., *Health hazards and waste management.* British Medical Bulletin, 2003. **68**: p. 183-197.

50.   Elliott, P., et al., *Incidence of cancers of the larynx and lung near incinerators of waste solvents and oils in Great - Britan.* Lancet, 1992. **339**(8797): p. 854-858.

51.   Won, S.W., et al., *Platinum recovery from ICP wastewater by a combined method of biosorption and incineration.* Bioresource Technology, 2010. **101**(4): p. 1135-1140.

52.   El Qada, E.N., S.J. Allen, and G.M. Walker, *Adsorption of basic dyes from aqueous solution onto activated carbons.* Chemical Engineering Journal, 2008. **135**(3): p. 174-184.

53.   Stefanakis, A.I., D.P. Komilis, and V.A. Tsihrintzis, *Stability and maturity of thickened wastewater sludge treated in pilot-scale sludge treatment wetlands.* Water Research, 2011. **45**(19): p. 6441-6452.

54.   Foo, K. and B. Hameed, *Detoxification of pesticide waste via activated carbon adsorption process.* Journal of Hazardous Materials, 2010. **175**(1): p. 1-11.

55.   Liu, Q.-S., et al., *Adsorption isotherm, kinetic and mechanism studies of some substituted phenols on activated carbon fibers.* Chemical Engineering Journal, 2010. **157**(2): p. 348-356.

56.   Zhang, L., et al., *Removal of phosphate from water by activated carbon fiber loaded with lanthanum oxide.* Journal of Hazardous Materials, 2011. **190**(1–3): p. 848-855.

57. Rosu, M., et al., *Surfactant adsorption onto activated carbon and its effect on absorption with chemical reaction.* Chemical Engineering Science, 2007. **62**(24): p. 7336-7343.

58. Schreiber, B., et al., *Adsorption of dissolved organic matter onto activated carbon - the influence of temperature, absorption wavelength, and molecular size.* Water Research, 2005. **39**(15): p. 3449.

59. Snyder, S.A., et al., *Role of membranes and activated carbon in the removal of endocrine disruptors and pharmaceuticals.* Desalination, 2007. **202**(1): p. 156-181.

60. Tamai, H., et al., *Synthesis of extremely large mesoporous activated carbon and its unique adsorption for giant molecules.* Chemistry of Materials, 1996. **8**(2): p. 454-462.

61. Banat, F., et al., *Bench-scale and packed bed sorption of methylene blue using treated olive pomace and charcoal.* Bioresource Technology, 2007. **98**(16): p. 3017-3025.

62. Ahmad, A.A. and B.H. Hameed, *Fixed-bed adsorption of reactive azo dye onto granular activated carbon prepared from waste.* Journal of Hazardous Materials, 2010. **175**(1–3): p. 298-303.

63. Malik, P., *Dye removal from wastewater using activated carbon developed from sawdust: adsorption equilibrium and kinetics.* Journal of Hazardous Materials, 2004. **113**(1): p. 81-88.

64. Bhattacharyya, K.G. and S.S. Gupta, *Adsorption of a few heavy metals on natural and modified kaolinite and montmorillonite: a review.* Advances in Colloid and Interface Science, 2008. **140**(2): p. 114-131.

65. Gürses, A., et al., *Determination of adsorptive properties of clay/water system: methylene blue sorption.* Journal of Colloid and Interface Science, 2004. **269**(2): p. 310-314.

66. Ghosh, D. and K.G. Bhattacharyya, *Adsorption of methylene blue on kaolinite.* Applied Clay Science, 2002. **20**(6): p. 295-300.

67. Li, Z., et al., *Mechanism of methylene blue removal from water by swelling clays.* Chemical Engineering Journal, 2011. **168**(3): p. 1193-1200.

68.   Ferrero, F., *Adsorption of Methylene Blue on magnesium silicate: Kinetics, equilibria and comparison with other adsorbents.* Journal of Environmental Sciences, 2010. **22**(3): p. 467-473.

69.   Wang, S. and Y. Peng, *Natural zeolites as effective adsorbents in water and wastewater treatment.* Chemical Engineering Journal, 2010. **156**(1): p. 11-24.

70.   Wingenfelder, U., et al., *Removal of heavy metals from mine waters by natural zeolites.* Environmental Science & Technology, 2005. **39**(12): p. 4606-4613.

71.   Meng, S., et al., *Influences of environmental factors on Lanthanum/Aluminum-Modified Zeolite Adsorbent (La/Al-ZA) for phosphorus adsorption from wastewater.* Water, Air, & Soil Pollution, 2013. **224**(6): p. 1-8.

72.   Guo, J., C. Yang, and G. Zeng, *Treatment of swine wastewater using chemically modified zeolite and bioflocculant from activated sludge.* Bioresource Technology, 2013. **143**: p. 289-297.

73.   Han, R., et al., *Study of equilibrium, kinetic and thermodynamic parameters about methylene blue adsorption onto natural zeolite.* Chemical Engineering Journal, 2009. **145**(3): p. 496-504.

74.   Misaelides, P., *Application of natural zeolites in environmental remediation: A short review.* Microporous and Mesoporous Materials, 2011. **144**(1): p. 15-18.

75.   Stoquart, C., et al., *Hybrid membrane processes using activated carbon treatment for drinking water: a review.* Journal of Membrane Science, 2012. **411**: p. 1-12.

76.   Boehler, M., et al., *Removal of micropollutants in municipal wastewater treatment plants by powder-activated carbon.* Water Science & Technology, 2012. **66**(10): p. 2115-2121.

77.   Margot, J., et al., *Treatment of micropollutants in municipal wastewater: Ozone or powdered activated carbon?* Science of the Total Environment, 2013. **461**: p. 480-498.

78. Aleboyeh, A., M.E. Olya, and H. Aleboyeh, *Oxidative treatment of azo dyes in aqueous solution by potassium permanganate.* Journal of Hazardous Materials, 2009. **162**(2–3): p. 1530-1535.

79. Li, G., et al., *Decolorization of azo dye Orange II by ferrate(VI)–hypochlorite liquid mixture, potassium ferrate(VI) and potassium permanganate.* Desalination, 2009. **249**(3): p. 936-941.

80. *Handbook of Chemistry and Physics.* 2013, Boca Raton, Florida: Boca Raton, Florida CRC Press.

81. Xu, X.-R., et al., *Decolorization of dyes and textile wastewater by potassium permanganate.* Chemosphere, 2005. **59**(6): p. 893-898.

82. Shen, C., et al., *Fast and highly efficient removal of dyes under alkaline conditions using magnetic chitosan-Fe (III) hydrogel.* Water Research, 2011. **45**(16): p. 5200-5210.

83. Gallard, H. and U. Von Gunten, *Chlorination of natural organic matter: Kinetics of chlorination and of THM formation.* Water Research, 2002. **36**(1): p. 65-74.

84. Dash, S., S. Patel, and B.K. Mishra, *Oxidation by permanganate: synthetic and mechanistic aspects.* Tetrahedron, 2009. **65**(4): p. 707-739.

85. Liu, R., et al., *Treatment of dye wastewater with permanganate oxidation and in situ formed manganese dioxides adsorption: Cation blue as model pollutant.* Journal of Hazardous Materials, 2010. **176**(1–3): p. 926-931.

86. Seol, Y., H. Zhang, and F.W. Schwartz, *A review of in situ chemical oxidation and heterogeneity.* Environmental and Engineering Geoscience, 2003. **9**(1): p. 37-49.

87. Dodd, M.C., M.-O. Buffle, and U. Von Gunten, *Oxidation of antibacterial molecules by aqueous ozone: moiety-specific reaction kinetics and application to ozone-based wastewater treatment.* Environmental Science & Technology, 2006. **40**(6): p. 1969-1977.

88. Yeom, I., et al., *Effects of ozone treatment on the biodegradability of sludge from municipal wastewater treatment plants.* Water Science & Technology, 2002. **46**(4-5): p. 421-425.

89. Martínez, S.B., J. Pérez-Parra, and R. Suay, *Use of ozone in wastewater treatment to produce water suitable for irrigation.* Water Resources Management, 2011. **25**(9): p. 2109-2124.

90. Gogate, P.R. and A.B. Pandit, *A review of imperative technologies for wastewater treatment I: oxidation technologies at ambient conditions.* Advances in Environmental Research, 2004. **8**(3): p. 501-551.

91. Oller, I., S. Malato, and J. Sánchez-Pérez, *Combination of advanced oxidation processes and biological treatments for wastewater decontamination - a review.* Science of the Total Environment, 2011. **409**(20): p. 4141-4166.

92. Singh, M. and R. Srivastava, *Sequencing batch reactor technology for biological wastewater treatment: a review.* Asia-Pacific Journal of Chemical Engineering, 2011. **6**(1): p. 3-13.

93. Skouteris, G., et al., *Anaerobic membrane bioreactors for wastewater treatment: a review.* Chemical Engineering Journal, 2012. **198**: p. 138-148.

94. Lombi, E., et al., *Transformation of four silver/silver chloride nanoparticles during anaerobic treatment of wastewater and post-processing of sewage sludge.* Environmental Pollution, 2013. **176**: p. 193-197.

95. Sarayu, K. and S. Sandhya, *Current technologies for biological treatment of textile wastewater–a review.* Applied Biochemistry and Biotechnology, 2012. **167**(3): p. 645-661.

96. Sperling, M.v., *Biological wastewater treatment in warm climate regions / Marcos von Sperling and Carlos Augusto de Lemos Chernicharo*, ed. C.A.d.L. Chernicharo. 2005, London: London : IWA Publishing.

97. Carrère, H., et al., *Pretreatment methods to improve sludge anaerobic degradability: a review.* Journal of Hazardous Materials, 2010. **183**(1): p. 1-15.

98. Amani, T., M. Nosrati, and T. Sreekrishnan, *Anaerobic digestion from the viewpoint of microbiological, chemical, and operational aspects-a review.* Environmental Reviews, 2010. **18**(NA): p. 255-278.

99. Demirel, B., O. Yenigun, and T.T. Onay, *Anaerobic treatment of dairy wastewaters: a review.* Process Biochemistry, 2005. **40**(8): p. 2583-2595.

100. Diamantis, V.I. and A. Aivasidis, *Comparison of single-and two-stage UASB reactors used for anaerobic treatment of synthetic fruit wastewater.* Enzyme and Microbial Technology, 2007. **42**(1): p. 6-10.

101. Alalayah, W.M., et al., *Bio-hydrogen production using a two-stage fermentation process.* Pakistan Journal of Biological Sciences, 2009. **12**(22): p. 1462.

102. Demirel, B. and O. Yenigün, *Two-phase anaerobic digestion processes: a review.* Journal of Chemical Technology and Biotechnology, 2002. **77**(7): p. 743-755.

103. Trouve, E., V. Urbain, and J. Manem, *Treatment of municipal wastewater by a membrane bioreactor: results of a semi-industrial pilot-scale study.* Water Science & Technology, 2014. **30**(4): p. 151-157.

104. Ren, L., Y. Ahn, and B.E. Logan, *A two-stage microbial fuel cell and anaerobic fluidized bed membrane bioreactor (MFC-AFMBR) system for effective domestic wastewater treatment.* Environmental Science & Technology, 2014. **48**(7): p. 4199-4206.

105. Sipma, J., et al., *Comparison of removal of pharmaceuticals in MBR and activated sludge systems.* Desalination, 2010. **250**(2): p. 653-659.

106. Lloret, L., et al., *Removal of estrogenic compounds from filtered secondary wastewater effluent in a continuous enzymatic membrane reactor. Identification of biotransformation products.* Environmental Science & Technology, 2013. **47**(9): p. 4536-4543.

107. Edalatmanesh, M., M. Mehrvar, and R. Dhib, *Optimization of phenol degradation in a combined photochemical-biological wastewater treatment system.* Chemical Engineering Research and Design, 2008. **86**(11A): p. 1243-1252.

108. Chen, G., *Electrochemical technologies in wastewater treatment.* Separation and Purification Technology, 2004. **38**(1): p. 11-41.

109. Canizares, P., et al., *Coagulation and electrocoagulation of oil-in-water emulsions.* Journal of Hazardous Materials, 2008. **151**(1): p. 44-51.

110. Aoudj, S., et al., *Electrocoagulation process applied to wastewater containing dyes from textile industry.* Chemical Engineering and Processing: Process Intensification, 2010. **49**(11): p. 1176-1182.

111. Mollah, M.Y.A., et al., *Electrocoagulation (EC)—science and applications.* Journal of Hazardous Materials, 2001. **84**(1): p. 29-41.

112. Chen, X., G. Chen, and P.L. Yue, *Separation of pollutants from restaurant wastewater by electrocoagulation.* Separation and Purification technology, 2000. **19**(1): p. 65-76.

113. Kobya, M., O.T. Can, and M. Bayramoglu, *Treatment of textile wastewaters by electrocoagulation using iron and aluminum electrodes.* Journal of Hazardous Materials, 2003. **100**(1): p. 163-178.

114. İrdemez, Ş., et al., *The effects of current density and phosphate concentration on phosphate removal from wastewater by electrocoagulation using aluminum and iron plate electrodes.* Separation and Purification Technology, 2006. **52**(2): p. 218-223.

115. A.T. Kuhn, *Electrolytic decomposition of cyanides, phenols and thiocyanates in effluents streams—a literature review.* Journal of Chemical Technology and Biotechnology, 1971. **21**: p. 29-34.

116. Yavuz, Y., A.S. Koparal, and Ü.B. Öğütveren, *Treatment of petroleum refinery wastewater by electrochemical methods.* Desalination, 2010. **258**(1): p. 201-205.

117. Canizares, P., et al., *Costs of the electrochemical oxidation of wastewaters: a comparison with ozonation and Fenton oxidation processes.* Journal of Environmental Management, 2009. **90**(1): p. 410-420.

118. Drogui P, Blais JF, and M. G, *Review of electrochemical technologies for environmental applications.* Recent Patents on Engineering, 2007. **1**: p. 257-272.

119. Anglada, A., A. Urtiaga, and I. Ortiz, *Contributions of electrochemical oxidation to waste-water treatment: fundamentals and review of applications.* Journal of Chemical Technology and Biotechnology, 2009. **84**(12): p. 1747-1755.

120. Anglada, A., A. Urtiaga, and I. Ortiz, *Contributions of electrochemical oxidation to waste-water treatment: fundamentals and review of applications.* Journal of Chemical Technology and Biotechnology, 2009. **84**(12): p. 1747-1755.

121. Panizza, M., et al., *Electrochemical degradation of methylene blue.* Separation and Purification Technology, 2007. **54**(3): p. 382-387.

122. Zhu, X., J. Ni, and P. Lai, *Advanced treatment of biologically pretreated coking wastewater by electrochemical oxidation using boron-doped diamond electrodes.* Water Research, 2009. **43**(17): p. 4347-4355.

123. Panizza, M. and G. Cerisola, *Application of diamond electrodes to electrochemical processes.* Electrochimica Acta, 2005. **51**(2): p. 191-199.

124. Papastefanakis, N., D. Mantzavinos, and A. Katsaounis, *DSA electrochemical treatment of olive mill wastewater on Ti/RuO$_2$ anode.* Journal of Applied Electrochemistry, 2010. **40**(4): p. 729-737.

125. Chen, J., H. Shi, and J. Lu, *Electrochemical treatment of ammonia in wastewater by RuO$_2$–IrO$_2$–TiO$_2$/Ti electrodes.* Journal of Applied Electrochemistry, 2007. **37**(10): p. 1137-1144.

126. Li, G., et al., *Electrochemically assisted photocatalytic degradation of Acid Orange 7 with β-PbO$_2$ electrodes modified by TiO$_2$.* Water Research, 2006. **40**(2): p. 213-220.

127. S.Anthuvan badu, S.R., S.Sibi and P.Neeraja, *Decolorization of synthetic and real polluted water by indirect electrochemical oxidation process.* Pollution Research Journal, 2012. **31**(1): p. 45-59.

128. Rajkumar, D., J. Guk Kim, and K. Palanivelu, *Indirect electrochemical oxidation of phenol in the presence of chloride for wastewater treatment.* Chemical Engineering & Technology, 2005. **28**(1): p. 98-105.

129. Scialdone, O., *Electrochemical oxidation of organic pollutants in water at metal oxide electrodes: A simple theoretical model including direct and indirect oxidation processes at the anodic surface.* Electrochimica Acta, 2009. **54**(26): p. 6140-6147.

130. Martínez-Huitle, C.A. and S. Ferro, *Electrochemical oxidation of organic pollutants for the wastewater treatment: direct and indirect processes.* Chemical Society Reviews, 2006. **35**(12): p. 1324.

131. Radjenovic, J. and D.L. Sedlak, *Challenges and opportunities for electrochemical processes as next-generation technologies for the treatment of contaminated water.* Environmental Science & Technology, 2015.

132. Swaminathan, M., M. Muruganandham, and M. Sillanpaa, *Advanced oxidation processes for wastewater treatment.* International Journal of Photoenergy, 2013. **2013**.

133. Garcia-Montano, J., et al., *Pilot plant scale reactive dyes degradation by solar photo-Fenton and biological processes.* Journal of Photochemistry and Photobiology A: Chemistry, 2008. **195**(2-3): p. 205-214.

134. Herney-Ramirez, J., M.A. Vicente, and L.M. Madeira, *Heterogeneous photo-Fenton oxidation with pillared clay-based catalysts for wastewater treatment: a review.* Applied Catalysis B: Environmental, 2010. **98**(1): p. 10-26.

135. Brillas, E., I. Sirés, and M.A. Oturan, *Electro-Fenton Process and Related Electrochemical Technologies Based on Fenton's Reaction Chemistry.* Chemical Reviews, 2009. **109**(12): p. 6570-6631.

136. Barb, W.G., et al., *Reactions of ferrous and ferric ions with hydrogen peroxide. Part II. - The ferric ion reaction.* Transactions of the Faraday Society, 1951. **47**: p. 591-616.

137. Bautista, P., et al., *An overview of the application of Fenton oxidation to industrial wastewaters treatment.* Journal of Chemical Technology and Biotechnology, 2008. **83**(10): p. 1323-1338.

138. Du, W.P., Y.M. Xu, and Y.S. Wang, *Photoinduced degradation of orange II on different iron (Hydr)oxides in aqueous suspension: Rate enhancement on addition of hydrogen peroxide, silver nitrate, and sodium fluoride.* Langmuir, 2008. **24**(1): p. 175-181.

139. Pignatello, J.J., D. Liu, and P. Huston, *Evidence for an additional oxidant in the photoassisted Fenton reaction.* Environmental Science & Technology, 1999. **33**(11): p. 1832-1839.

140. Brillas, E., I. Sirés, and M.A. Oturan, *Electro-Fenton process and related electrochemical technologies based on Fenton's reaction chemistry.* Chemical Reviews, 2009. **109**(12): p. 6570-6631.

141. Ntampegliotis, K., et al., *Decolorization kinetics of Procion H-exl dyes from textile dyeing using Fenton-like reactions.* Journal of Hazardous Materials, 2006. **136**(1): p. 75.

142.   Wang, J.L. and L.J. Xu, *Advanced oxidation processes for wastewater treatment: formation of hydroxyl radical and application.* Critical Reviews in Environmental Science and Technology, 2012. **42**(3): p. 251-325.

143.   Elmolla, E.S. and M. Chaudhuri, *Degradation of the antibiotics amoxicillin, ampicillin and cloxacillin in aqueous solution by the photo-Fenton process.* Journal of Hazardous Materials, 2009. **172**(2-3): p. 1476.

144.   Kim, S.M. and A. Vogelpohl, *Degradation of organic pollutants by the photo-fenton-process.* Chemical Engineering & Technology, 1998. **21**(2): p. 187-191.

145.   Hanna, K., T. Kone, and G. Medjahdi, *Synthesis of the mixed oxides of iron and quartz and their catalytic activities for the Fenton-like oxidation.* Catalysis Communications 2008. **9**(5): p. 955-959.

146.   Gonzalez-Bahamon, L.F., et al., *Photo-Fenton degradation of resorcinol mediated by catalysts based on iron species supported on polymers.* Journal of Photochemistry and Photobiology A: Chemistry, 2011. **217**(1): p. 201-206.

147.   Han, F., et al., *Tailored titanium dioxide photocatalysts for the degradation of organic dyes in wastewater treatment: a review.* Applied Catalysis A: General, 2009. **359**(1): p. 25-40.

148.   Bhatkhande, D.S., V.G. Pangarkar, and A. Beenackers, *Photocatalytic degradation for environmental applications - a review.* Journal of Chemical Technology and Biotechnology, 2002. **77**: p. 102-116.

149.   Cabeza, A., et al., *Ammonium removal from landfill leachate by anodic oxidation.* Journal of Hazardous Materials, 2007. **144**(3): p. 715.

150.   Mills, A. and S. Le Hunte, *An overview of semiconductor photocatalysis.* Journal of Photochemistry and Photobiology A: Chemistry, 1997. **108**(1): p. 1-35.

151.   Di Paola, A., et al., *A survey of photocatalytic materials for environmental remediation.* Journal of Hazardous Materials, 2012. **211-212**: p. 3-29.

152.   Gaya, U.I. and A.H. Abdullah, *Heterogeneous photocatalytic degradation of organic contaminants over titanium dioxide: A review of fundamentals, progress and problems.* Journal of Photochemistry and Photobiology C: Photochemistry Reviews, 2008. **9**(1): p. 1-12.

153. Konstantinou, I.K. and T.A. Albanis, *TiO₂-assisted photocatalytic degradation of azo dyes in aqueous solution: kinetic and mechanistic investigations: a review.* Applied Catalysis B: Environmental, 2004. **49**(1): p. 1-14.

154. Pirkanniemi, K. and M. Sillanpää, *Heterogeneous water phase catalysis as an environmental application: a review.* Chemosphere, 2002. **48**(10): p. 1047-1060.

155. Chong, M.N., et al., *Recent developments in photocatalytic water treatment technology: a review.* Water Research, 2010. **44**(10): p. 2997-3027.

156. Bahnemann, D., *Photocatalytic water treatment: solar energy applications.* Solar Energy, 2004. **77**(5): p. 445-459.

157. Daghrir, R., P. Drogui, and D. Robert, *Modified TiO₂ for environmental photocatalytic applications: a review.* Industrial & Engineering Chemistry Research, 2013. **52**(10): p. 3581-3599.

158. Jain, R., et al., *Removal of the hazardous dye rhodamine B through photocatalytic and adsorption treatments.* Journal of Environmental Management, 2007. **85**(4): p. 956-964.

159. Fujishima, A., T.N. Rao, and D.A. Tryk, *Titanium dioxide photocatalysis.* Journal of Photochemistry and Photobiology C: Photochemistry Reviews, 2000. **1**(1): p. 1-21.

160. Arana, J., et al., *TiO₂-photocatalysis as a tertiary treatment of naturally treated wastewater.* Catalysis Today, 2002. **76**(2): p. 279-289.

161. Li, X., et al., *Photocatalytic oxidation using a new catalyst TiO₂ microsphere for water and wastewater treatment.* Environmental Science & Technology, 2003. **37**(17): p. 3989-3994.

162. Thiruvenkatachari, R., S. Vigneswaran, and I.S. Moon, *A review on UV/TiO₂ photocatalytic oxidation process (Journal Review).* Korean Journal of Chemical Engineering, 2008. **25**(1): p. 64-72.

163. Wang, G., et al., *Hydrogen-treated TiO₂ nanowire arrays for photoelectrochemical water splitting.* Nano Letters, 2011. **11**(7): p. 3026-3033.

164.   Liu, Z., et al., *Highly ordered TiO₂ nanotube arrays with controllable length for photoelectrocatalytic degradation of phenol.* The Journal of Physical Chemistry C, 2008. **112**(1): p. 253-259.

165.   Yang, J., et al., *Mechanism of TiO₂-assisted photocatalytic degradation of dyes under visible irradiation: photoelectrocatalytic study by TiO₂-film electrodes.* The Journal of Physical Chemistry B, 2005. **109**(46): p. 21900-21907.

166.   Adewuyi, Y.G., *Sonochemistry in environmental remediation. 2. Heterogeneous sonophotocatalytic oxidation processes for the treatment of pollutants in water.* Environmental Science & Technology, 2005. **39**(22): p. 8557-8570.

167.   Sonawane, R., B. Kale, and M. Dongare, *Preparation and photo-catalytic activity of Fe-TiO₂ thin films prepared by sol–gel dip coating.* Materials Chemistry and Physics, 2004. **85**(1): p. 52-57.

168.   Lu, N., et al., *Fabrication of boron-doped TiO₂ nanotube array electrode and investigation of its photoelectrochemical capability.* The Journal of Physical Chemistry C, 2007. **111**(32): p. 11836-11842.

169.   An, Y., et al., *A photoelectrochemical immunosensor based on Au-doped TiO₂ nanotube arrays for the detection of α-synuclein.* Chemistry-A European Journal, 2010. **16**(48): p. 14439-14446.

170.   Choi, W., A. Termin, and M.R. Hoffmann, *The role of metal ion dopants in quantum-sized TiO₂: correlation between photoreactivity and charge carrier recombination dynamics.* The Journal of Physical Chemistry, 1994. **98**(51): p. 13669-13679.

171.   Chen, D., et al., *Carbon and nitrogen Co-doped TiO₂ with enhanced visible-light photocatalytic activity.* Industrial & Engineering Chemistry Research, 2007. **46**(9): p. 2741-2746.

172.   Zhang, S., et al., *Synthesis, characterization of Cr-doped TiO₂ nanotubes with high photocatalytic activity.* Journal of Nanoparticle Research, 2008. **10**(5): p. 871-875.

173.   Chang, S.-m. and R.-a. Doong, *Characterization of Zr-doped TiO₂ nanocrystals prepared by a nonhydrolytic sol-gel method at high*

temperatures. The Journal of Physical Chemistry B, 2006. **110**(42): p. 20808-20814.

174. Janisch, R., P. Gopal, and N.A. Spaldin, *Transition metal-doped TiO_2 and ZnO - present status of the field.* Journal of Physics: Condensed Matter, 2005. **17**(27): p. R657.

175. Liu, Y., et al., *Novel TiO_2 nanocatalysts for wastewater purification-tapping energy from the sun.* Water Practice & Technology, 2006. **1**(04).

176. Chen, L.-C., et al., *Enhanced visible light-induced photoelectrocatalytic degradation of phenol by carbon nanotube-doped TiO_2 electrodes.* Electrochimica Acta, 2009. **54**(15): p. 3884-3891.

177. Zaleska, A., *Doped-TiO_2: a review.* Recent Patents on Engineering, 2008. **2**(3): p. 157-164.

178. Wu, G., et al., *Synthesis and characterization of carbon-doped TiO_2 nanostructures with enhanced visible light response.* Chemistry of Materials, 2007. **19**(18): p. 4530-4537.

179. Chakrabarti, S. and B.K. Dutta, *Photocatalytic degradation of model textile dyes in wastewater using ZnO as semiconductor catalyst.* Journal of Hazardous Materials, 2004. **112**(3): p. 269-278.

180. Ghaly, M.Y., et al., *ZnO/spiral-shaped glass for solar photocatalytic oxidation of Reactive Red 120.* Arabian Journal of Chemistry.

181. Daneshvar, N., D. Salari, and A.R. Khataee, *Photocatalytic degradation of azo dye acid red 14 in water on ZnO as an alternative catalyst to TiO_2.* Journal of Photochemistry and Photobiology A: Chemistry, 2004. **162**(2–3): p. 317-322.

182. Yeber, M.C., et al., *Photocatalytic degradation of cellulose bleaching effluent by supported TiO_2 and ZnO.* Chemosphere, 2000. **41**(8): p. 1193-1197.

183. Cao, S.-W. and Y.-J. Zhu, *Hierarchically nanostructured α-Fe_2O_3 hollow spheres: preparation, growth mechanism, photocatalytic property, and application in water treatment.* The Journal of Physical Chemistry C, 2008. **112**(16): p. 6253-6257.

184. Gupta, A.K. and M. Gupta, *Synthesis and surface engineering of iron oxide nanoparticles for biomedical applications.* Biomaterials, 2005. **26**(18): p. 3995-4021.

185. Xu, P., et al., *Use of iron oxide nanomaterials in wastewater treatment: a review.* Science of the Total Environment, 2012. **424**: p. 1-10.

186. Hu, J.S., et al., *Synthesis of hierarchically structured metal oxides and their application in heavy metal ion removal.* Advanced Materials, 2008. **20**(15): p. 2977-2982.

187. Akhavan, O. and R. Azimirad, *Photocatalytic property of Fe₂O₃ nanograin chains coated by TiO₂ nanolayer in visible light irradiation.* Applied Catalysis A: General, 2009. **369**(1): p. 77-82.

188. Zhong, D.K., et al., *Solar water oxidation by composite catalyst/α-Fe₂O₃ photoanodes.* Journal of the American Chemical Society, 2009. **131**(17): p. 6086-6087.

189. Hahn, N.T., et al., *Reactive ballistic deposition of α-Fe₂O₃ thin films for photoelectrochemical water oxidation.* ACS nano, 2010. **4**(4): p. 1977-1986.

190. Hu, Y.-S., et al., *Pt-doped α-Fe₂O₃ thin films active for photoelectrochemical water splitting.* Chemistry of Materials, 2008. **20**(12): p. 3803-3805.

191. Kleiman-Shwarsctein, A., et al., *Electrodeposition of α-Fe₂O₃ doped with Mo or Cr as photoanodes for photocatalytic water splitting.* The Journal of Physical Chemistry C, 2008. **112**(40): p. 15900-15907.

192. Liu, S., et al., *A mechanism for enhanced photocatalytic activity of silver-loaded titanium dioxide.* Catalysis Today, 2004. **93**: p. 877-884.

193. Zhang, W.-x., *Nanoscale iron particles for environmental remediation: an overview.* Journal of Nanoparticle Research, 2003. **5**(3-4): p. 323-332.

194. Kleiman-Shwarsctein, A., et al., *Electrodeposited aluminum-doped α-Fe₂O₃ photoelectrodes: experiment and theory.* Chemistry of Materials, 2009. **22**(2): p. 510-517.

195. Memar, A., C.M. Phan, and M.O. Tade, *Influence of surfactants on Fe₂O₃ nanostructure photoanode.* International Journal of Hydrogen Energy, 2012. **37**(22): p. 16835-16843.

196.   Chen, J., et al., *α-Fe₂O₃ nanotubes in gas sensor and lithium‑ion battery applications.* Advanced Materials, 2005. **17**(5): p. 582-586.

197.   Wen, X., et al., *Controlled growth of large-area, uniform, vertically aligned arrays of α-Fe₂O₃ nanobelts and nanowires.* The Journal of Physical Chemistry B, 2005. **109**(1): p. 215-220.

198.   Wu, C., et al., *Synthesis of hematite (α-Fe₂O₃) nanorods: diameter-size and shape effects on their applications in magnetism, lithium ion battery, and gas sensors.* Journal of Physical Chemistry B, 2006. **110**(36): p. 17806-17812.

199.   Vayssieres, L., et al., *Controlled aqueous chemical growth of oriented three-dimensional crystalline nanorod arrays: Application to iron(III) oxides.* Chemistry of Materials, 2001. **13**(2): p. 233-235.

200.   Wang, R.M., et al., *Bicrystalline hematite nanowires.* The Journal of Physical Chemistry B, 2005. **109**(25): p. 12245-12249.

201.   Mao, A., et al., *Controlled synthesis of vertically aligned hematite on conducting substrate for photoelectrochemical cells: nanorods versus nanotubes.* ACS Applied Materials & Interfaces 2011. **3**(6): p. 1852-1858.

202.   Fan, H.M., et al., *Shape-controlled synthesis of single-crystalline Fe₂O₃ hollow nanocrystals and their tunable optical properties.* The Journal of Physical Chemistry C, 2009. **113**(22): p. 9928-9935.

203.   Shen, Y., et al., *Surface photovoltage property of magnesium ferrite/hematite heterostructured hollow nanospheres prepared with one-pot strategy.* Colloids and Surfaces A: Physicochemical and Engineering Aspects, 2012. **403**: p. 35-40.

204.   Armelao, L., et al., *Nanocrystalline α-Fe₂O₃ sol-gel thin films: a microstructural study.* Journal of Non-Crystalline Solids, 1995. **193**: p. 435-438.

205.   Woo, K., et al., *Sol-gel mediated synthesis of Fe₂O₃ nanorods.* Advanced Materials, 2003. **15**(20): p. 1761 -1764.

206.   Golden, D.C., et al., *Hydrothermal synthesis of hematite spherules and jarosite: Implications for diagenesis and hematite spherule formation in sulfate outcrops at Meridiani Planum, Mars.* American Mineralogist, 2008. **93**(8-9): p. 1201-1214.

207. Watanable, A. and H. Kozuka, *Photoanodic properties of sol-gel-derived Fe_2O_3 thin films containing dispersed gold and silver particles.* Journal of Physical Chemistry B, 2003. **107**(46).

208. Wang, D.G., et al., *Effects of sol-gel processing parameters on the phases and microstructures of HA films.* Colloids and Surfaces B: Biointerfaces, 2007. **57**(2): p. 237-242.

209. Byrne, D., et al., *A study of drop-coated and chemical bath-deposited buffer layers for vapor phase deposition of large area, aligned, zinc oxide nanorod arrays.* Crystal Growth & Design, 2010. **10**(5): p. 2400-2408.

210. Qian, F., et al., *Core/multishell nanowire heterostructures as multicolor, high-efficiency light-emitting diodes.* Nano Letters, 2005. **5**(11): p. 2287-2291.

211. Glasscock, J.A., et al., *Enhancement of photoelectrochemical hydrogen production from hematite thin films by the introduction of Ti and Si.* The Journal of Physical Chemistry C, 2007. **111**(44): p. 16477-16488.

212. Lin, Y.J., et al., *Nanonet-based hematite heteronanostructures for efficient solar water splitting.* Journal of the American Chemical Society, 2011. **133**(8): p. 2398-2401.

213. Li, Y., et al., *Dopant-free GaN/AlN/AlGaN radial nanowire heterostructures as high electron mobility transistors.* Nano Letters, 2006. **6**(7): p. 1468-1473.

214. Wheeler, D.A., et al., *Nanostructured hematite: synthesis, characterization, charge carrier dynamics, and photoelectrochemical properties.* Energy & Environmental Science, 2012. **5**(5): p. 6682-6702.

215. Wang, H.L. and J.A. Turner, *Characterization of hematite thin films for photoelectrochemical wter slitting in a dual photoelectrode device.* Journal of The Electrochemical Society, 2010. **157**(11): p. F173-F178.

216. Sartoretti, C.J., et al., *Photoelectrochemical oxidation of water at transparent ferric oxide film electrodes.* The Journal of Physical Chemistry B 2005. **109**(28): p. 13685-13692.

217. Perednis, D. and L.J. Gauckler, *Thin film deposition using spray pyrolysis.* Journal of Electroceramics, 2005. **14**(2): p. 103-111.

218. Yang, H., et al., *Electronic and optical properties of new multifunctional materials via half-substituted hematite: first principles calculations.* RSC Advances, 2012. **2**(28): p. 10708-10716.

219. Liu, Y., Y.-X. Yu, and W.-D. Zhang, *Photoelectrochemical properties of Ni-doped Fe₂O₃ thin films prepared by electrodeposition.* Electrochimica Acta, 2012. **59**: p. 121-127.

220. Wu, X.-J., et al., *Electrochemical synthesis and applications of oriented and hierarchically quasi-1D semiconducting nanostructures.* Coordination Chemistry Reviews, 2010. **254**(9): p. 1135-1150.

221. Gilles, S.-J., . *Automated quantitative and isotopic (13C) analysis of dissolved inorganic carbon and dissolved organic carbon in continuous-flow using a total organic carbon analyser.* Rapid Communications in Mass Spectrometry, 2003. **17**(5): p. 419-428.

222. Koga, M., et al., *Rapid determination of anionic surfactants by improved spectrophotometric method using methylene blue.* Analytical Sciences, 1999. **15**(6): p. 563-568.

223. Belkacemi, K., F.ç. Larachi, and A. Sayari, *Lumped kinetics for solid-catalyzed wet oxidation: a versatile model.* Journal of Catalysis, 2000. **193**(2): p. 224-237.

224. Zhang, Q. and K.T. Chuang, *Lumped kinetic model for catalytic wet oxidation of organic compounds in industrial wastewater.* AIChE Journal, 1999. **45**(1): p. 145-150.

225. Cao, C.-Y., et al., *Low-cost synthesis of flowerlike α-Fe₂O₃ nanostructures for heavy metal ion removal: adsorption property and mechanism.* Langmuir, 2012. **28**(9): p. 4573-4579.

226. Wang, L. and L. Gao, *Controlled synthesis and tunable properties of hematite hierarchical structures in a dual-surfactant system.* CrystEngComm, 2011. **13**(6): p. 1998-2005.

227. Bejankiwar, R., et al., *Electrochemical degradation of 1,2-dichloroethane (DCA) in a synthetic groundwater medium using stainless-steel electrodes.* Water Research, 2005. **39**(19): p. 4715-4724.

228. Quan, X., et al., *Photoelectrocatalytic degradation of pentachlorophenol in aqueous solution using a TiO₂ nanotube film electrode.* Environmental Pollution, 2007. **147**(2): p. 409-414.

229. Roni Penna, Matan Hadarib, and Eran Friedlera, *Evaluation of the effects of greywater reuse on domestic wastewater quality and quantity.* Urban Water Journal, 2012. **9**(4): p. 137–148.

230. Paria, S. and K.C. Khilar, *A review on experimental studies of surfactant adsorption at the hydrophilic solid–water interface.* Advances in Colloid and Interface Science, 2004. **110**(3): p. 75-95.

231. Naman, S.A., Z.A.A. Khammas, and F.M. Hussein, *Photo-oxidative degradation of insecticide dichlorovos by a combined semiconductors and organic sensitizers in aqueous media.* Journal of Photochemistry and Photobiology A: Chemistry, 2002. **153**(1–3): p. 229-236.

232. Pelizzetti, E. and C. Minero, *Mechanism of the photo-oxidative degradation of organic pollutants over TiO₂ particles.* Electrochimica Acta, 1993. **38**(1): p. 47-55.

233. Bethell, D., et al., *The hydrolysis of C₁₂ primary alkyl sulfates in concentrated aqueous solutions. Part 1. General features, kinetic form and mode of catalysis in sodium dodecyl sulfate hydrolysis.* Journal of the Chemical Society, Perkin Transactions 2, 2001(9): p. 1489-1495.

234. Reddy, M., et al., *α-Fe₂O₃ nanoflakes as an anode material for Li-ion batteries.* Advanced Functional Materials, 2007. **17**(15): p. 2792-2799.

235. Zaghbani, N., A. Hafiane, and M. Dhahbi, *Separation of methylene blue from aqueous solution by micellar enhanced ultrafiltration.* Separation and Purification Technology, 2007. **55**(1): p. 117-124.

236. Hayashi, K., *A rapid determination of sodium dodecyl sulfate with methylene blue.* Analytical Biochemistry, 1975. **67**(2): p. 503-506.

237. Gao, X. and J. Chorover, *Adsorption of sodium dodecyl sulfate (SDS) at ZnSe and α-Fe₂O₃ surfaces: Combining infrared spectroscopy and batch uptake studies.* Journal of Colloid and Interface Science, 2010. **348**(1): p. 167-176.

238. Bandala, E.R., et al., *Degradation of sodium dodecyl sulphate in water using solar driven Fenton-like advanced oxidation processes.* Journal of Hazardous Materials, 2008. **151**(2–3): p. 578-584.

239. Hosseini, F., et al., *Biodegradation of anionic surfactants by isolated bacteria from activated sludge.* International Journal of Environmental Science & Technology, 2007. **4**(1): p. 127-132.

240. Hines, J.D., *The preparation of surface chemically pure sodiumn - dodecyl sulfate by foam fractionation.* Journal of Colloid and Interface Science, 1996. **180**(2): p. 488-492.

241. Devore, J., *Probability and statistics for engineering and the sciences*, ed. N. ed. 2015, Pearson Education: Boston, MA, USA: Cengage Learning.

242. Viana, R.B., A.B.F. da Silva, and A.S. Pimentel, *Adsorption of sodium dodecyl sulfate on Ge substrate: The effect of a low-plarity solvent.* International Journal of Molecular Sciences, 2012. **13**(7): p. 7980-7993.

243. Andrade, G.I., et al., *Small-angle X-ray scattering and FTIR characterization of nanostructured poly (vinyl alcohol)/silicate hybrids for immunoassay applications.* Journal of Materials Science, 2008. **43**(2): p. 450-463.

244. Mansur, H.S., et al., *FTIR spectroscopy characterization of poly (vinyl alcohol) hydrogel with different hydrolysis degree and chemically crosslinked with glutaraldehyde.* Materials Science and Engineering: C, 2008. **28**(4): p. 539-548.

245. Nakamoto, K., *Infrared and Raman Spectra of Inorganic and Coordination Compounds*, in *Handbook of Vibrational Spectroscopy*. 2006, John Wiley & Sons, Ltd.

APENDIX

A.1. MATLAB codes

- **PEC 1 A, 1 V:**


```matlab
function y = pec1v(beta,t)

global K0 K1 K2 K3 %K5


K0 = 0.07808474;
K1 = beta(1);
K2 = beta(2);
K3 = beta(3);


options = odeset('RelTol',1e-4,'AbsTol',[1e-4 1e-4 1e-5]);

[T,Y]=ode45(@odefun1,t,[54.70605163 0 0],options);

Ysynthetic(:,1)=Y(:,1)+Y(:,2)+Y(:,3);

y=Ysynthetic';

%clear K1 K2 K3 K4 K5
```
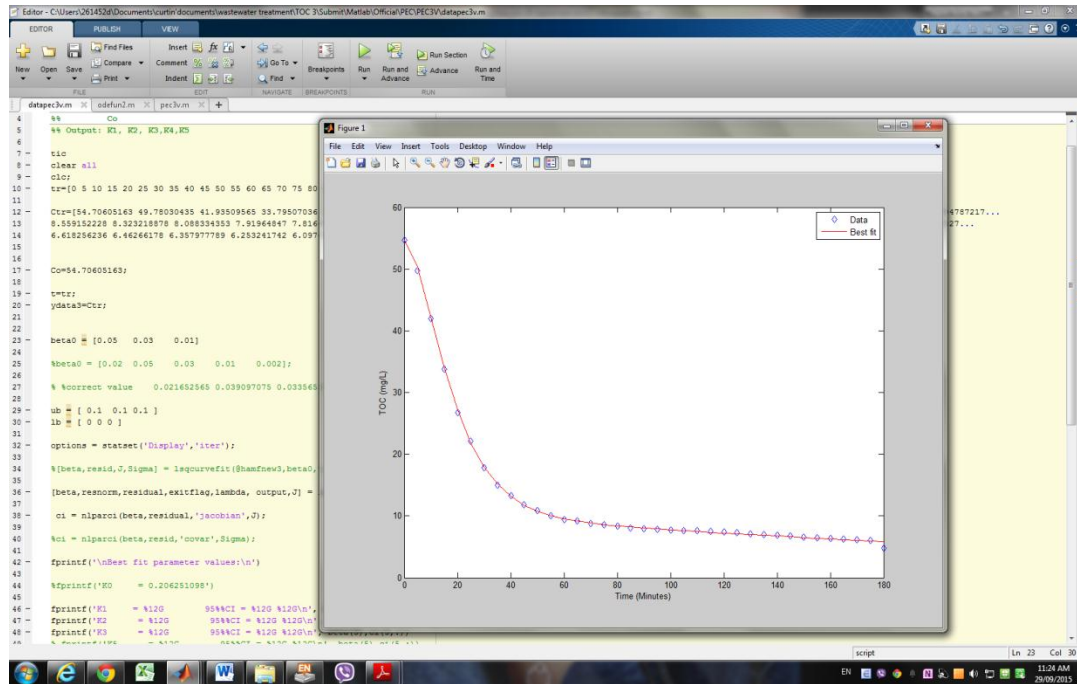
```matlab
function dy=odefun1(t,y)

    global K0 K1 K2 K3
    dy=zeros(3,1);
    dy(1)=-K0*y(1);
    dy(2)=K0*y(1)-(K1+K2)*y(2);
    dy(3)=K2*y(2)-K3*y(3);

    %%matrix(i, 0) = matrix(i - 1, 0) + dt
    % % dadt = -(k1 + k2) * matrix(i - 1, 1)  ' SDS k1+k2=k0
    % % dbdt = k2 * matrix(i - 1, 1) - k3 * matrix(i - 1, 2) - k4 * matrix(i - 1, 2)
    % % dcdt = k4 * matrix(i - 1, 2) - k5 * matrix(i - 1, 3)
```
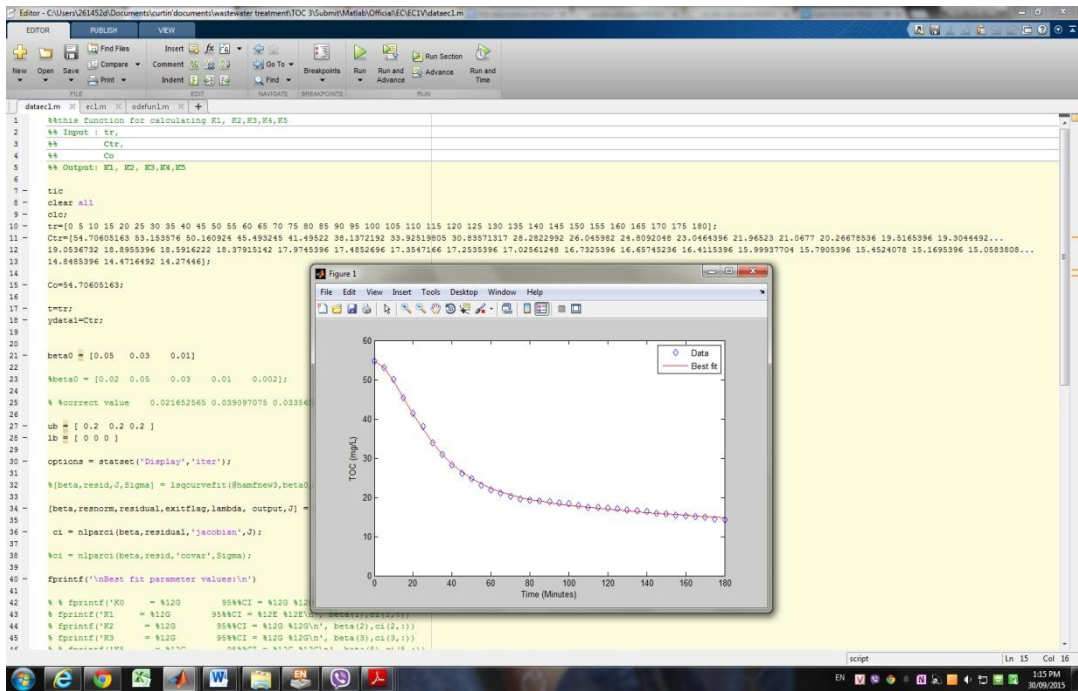
- **PEC 1 A, 2 V :**


```matlab
function y = pec2v(beta,t)

    global K0 K1 K2 K3 %K5


    K0 = 0.089576513;
    K1 = beta(1);
    K2 = beta(2);
    K3 = beta(3);


    options = odeset('RelTol',1e-4,'AbsTol',[1e-4 1e-4 1e-5]);

    [T,Y]=ode45(@odefun,t,[54.70605163 0 0],options);

    Ysynthetic(:,1)=Y(:,1)+Y(:,2)+Y(:,3);

    y=Ysynthetic';

    %clear K1 K2 K3 K4 K5
```



```matlab
function dy=odefun(t,y)

    global K0 K1 K2 K3
    dy=zeros(3,1);
    dy(1)=-K0*y(1);
    dy(2)=K0*y(1)-(K1+K2)*y(2);
    dy(3)=K2*y(2)-K3*y(3);

    %%matrix(i, 0) = matrix(i - 1, 0) + dt
    % % dadt = -(k1 + k2) * matrix(i - 1, 1)   ' SDS k1+k2=k0
    % % dbdt = k2 * matrix(i - 1, 1) - k3 * matrix(i - 1, 2) - k4 * matrix(i - 1, 2)
    % % dcdt = k4 * matrix(i - 1, 2) - k5 * matrix(i - 1, 3)
```

- **PEC 1 A, 3 V:**


```matlab
function y = pec3v(beta,t)

    global K0 K1 K2 K3 %K5


    K0 = 0.089576513;
    K1 = beta(1);
    K2 = beta(2);
    K3 = beta(3);


    options = odeset('RelTol',1e-4,'AbsTol',[1e-4 1e-4 1e-5]);

    [T,Y]=ode45(@odefun2,t,[54.70605163 0 0],options);

    Ysynthetic(:,1)=Y(:,1)+Y(:,2)+Y(:,3);

    y=Ysynthetic';

    %clear K1 K2 K3 K4 K5
```

```matlab
function dy=odefun2(t,y)

global K0 K1 K2 K3
dy=zeros(3,1);
dy(1)=-K0*y(1);
dy(2)=K0*y(1)-(K1+K2)*y(2);
dy(3)=K2*y(2)-K3*y(3);

%%matrix(i, 0) = matrix(i - 1, 0) + dt
% % dadt = -(k1 + k2) * matrix(i - 1, 1)   ' SDS k1+k2=k0
% % dbdt = k2 * matrix(i - 1, 1) - k3 * matrix(i - 1, 2) - k4 * matrix(i - 1, 2)
% % dcdt = k4 * matrix(i - 1, 2) - k5 * matrix(i - 1, 3)
```

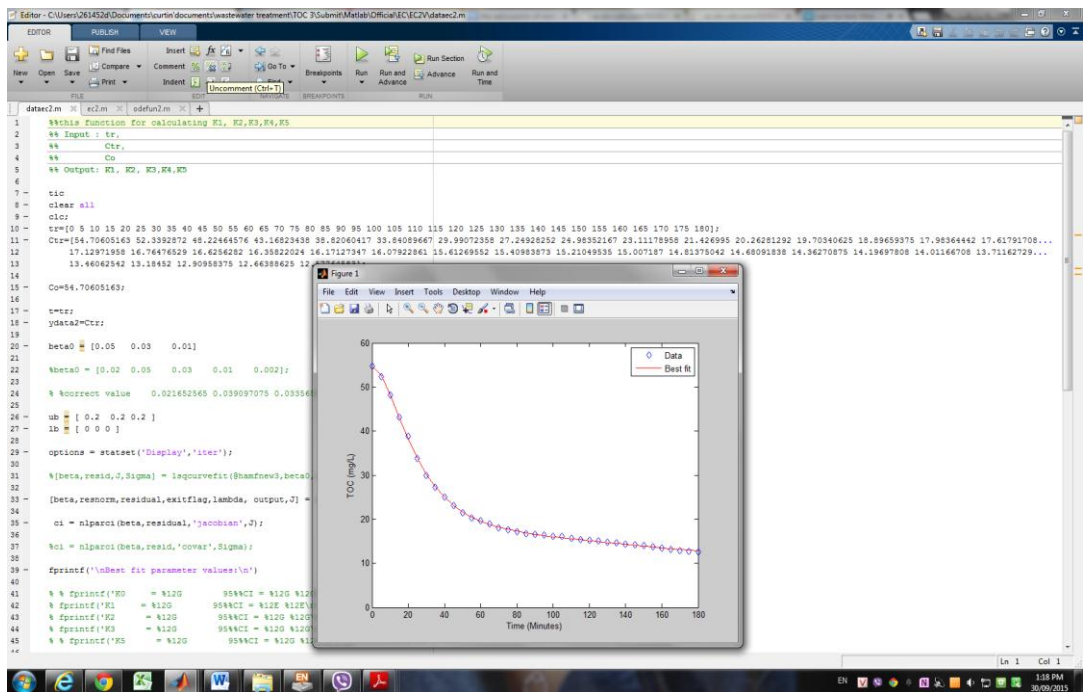- **EC 1 A, 1 V:**

```matlab
function dy=odefun1(t,y)

    global K0 K1 K2 K3
    dy=zeros(3,1);
    dy(1)=-K0*y(1);
    dy(2)=K0*y(1)-(K1+K2)*y(2);
    dy(3)=K2*y(2)-K3*y(3);

    %%matrix(i, 0) = matrix(i - 1, 0) + dt
    % % dadt = -(k1 + k2) * matrix(i - 1, 1)   ' SDS k1+k2=k0
    % % dbdt = k2 * matrix(i - 1, 1) - k3 * matrix(i - 1, 2) - k4 * matrix(i - 1, 2)
    % % dcdt = k4 * matrix(i - 1, 2) - k5 * matrix(i - 1, 3)
```

```matlab
function y = ec1(beta,t)

    global K0 K1 K2 K3 %K5


    K0 = 0.07556124;
    K1 = beta(1);
    K2 = beta(2);
    K3 = beta(3);


    options = odeset('RelTol',1e-4,'AbsTol',[1e-4 1e-4 1e-5]);

    [T,Y]=ode45(@odefun1,t,[54.70605163 0 0],options);

    Ysynthetic(:,1)=Y(:,1)+Y(:,2)+Y(:,3);


    y=Ysynthetic';

    %clear K1 K2 K3 K4 K5
```

- **EC 1 A, 2V:**

Editor - C:\Users\261452d\Documents\curtin'documents\wastewater treatment\TOC 3\Submit\Matlab\Official\EC\EC2V\ec2.m

```matlab
function y = ec2(beta,t)

global K0 K1 K2 K3 %K5


K0 = 0.086799675;
K1 = beta(1);
K2 = beta(2);
K3 = beta(3);


options = odeset('RelTol',1e-4,'AbsTol',[1e-4 1e-4 1e-5]);

[T,Y]=ode45(@odefun2,t,[54.70605163 0 0],options);

Ysynthetic(:,1)=Y(:,1)+Y(:,2)+Y(:,3);

y=Ysynthetic';

%clear K1 K2 K3 K4 K5
```
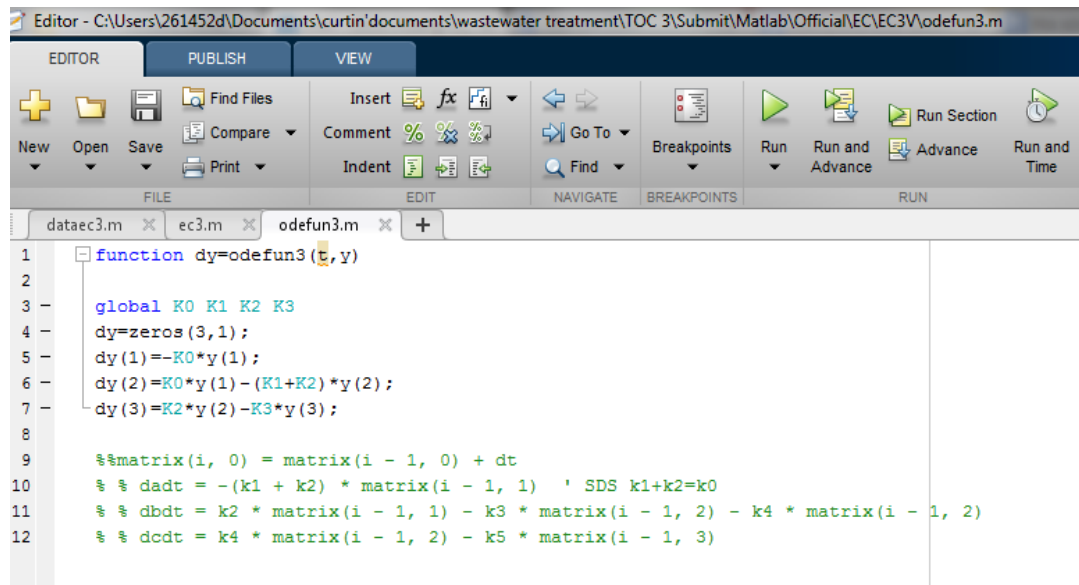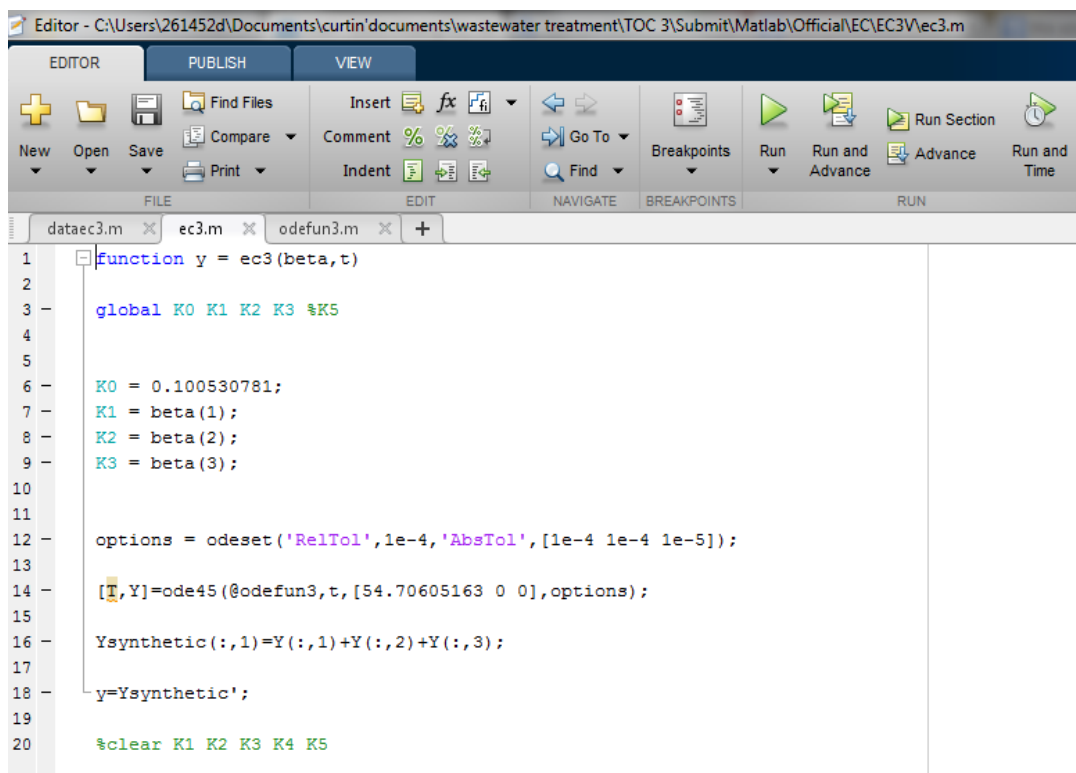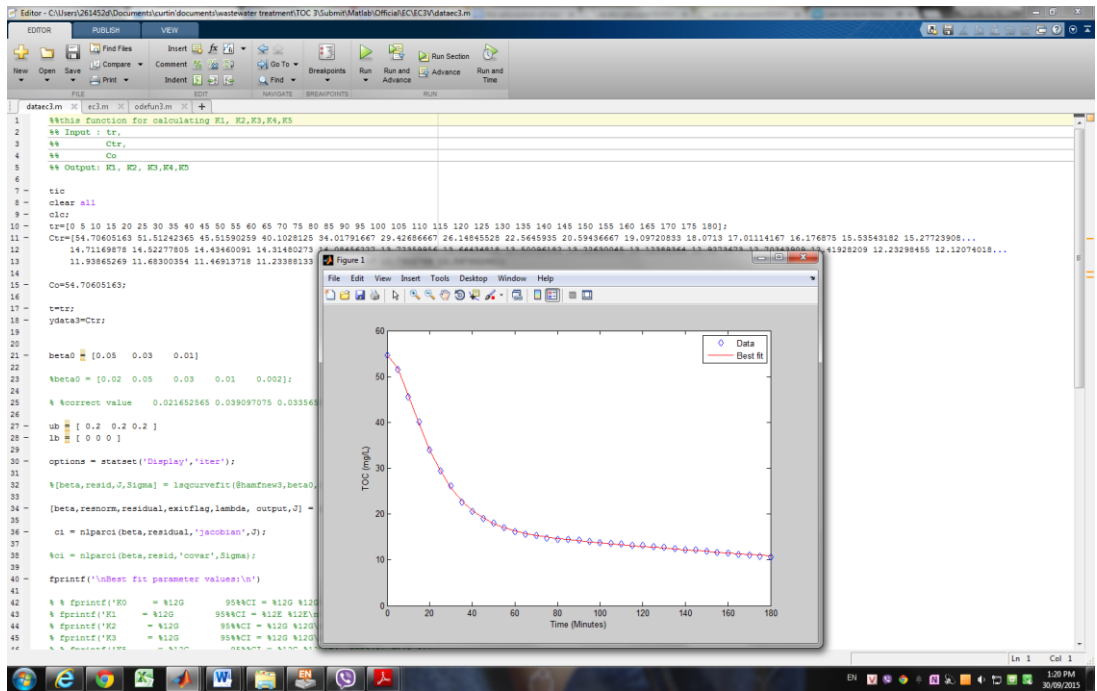
- EC 1 A, 3 V:


```matlab
function dy=odefun3(t,y)

  global K0 K1 K2 K3
  dy=zeros(3,1);
  dy(1)=-K0*y(1);
  dy(2)=K0*y(1)-(K1+K2)*y(2);
  dy(3)=K2*y(2)-K3*y(3);

  %%matrix(i, 0) = matrix(i - 1, 0) + dt
  % % dadt = -(k1 + k2) * matrix(i - 1, 1)   ' SDS k1+k2=k0
  % % dbdt = k2 * matrix(i - 1, 1) - k3 * matrix(i - 1, 2) - k4 * matrix(i - 1, 2)
  % % dcdt = k4 * matrix(i - 1, 2) - k5 * matrix(i - 1, 3)
```



```matlab
function y = ec3(beta,t)

  global K0 K1 K2 K3 %K5


  K0 = 0.100530781;
  K1 = beta(1);
  K2 = beta(2);
  K3 = beta(3);


  options = odeset('RelTol',1e-4,'AbsTol',[1e-4 1e-4 1e-5]);

  [T,Y]=ode45(@odefun3,t,[54.70605163 0 0],options);

  Ysynthetic(:,1)=Y(:,1)+Y(:,2)+Y(:,3);

  y=Ysynthetic';

  %clear K1 K2 K3 K4 K5
```

A.2. Fourier transform infrared spectroscopy

EC - DARK 1A1V

PEC - 1A2V

PEC - 1A1V

Wavelength, nm

EC - DARK - 1A3V

Legend: 0', 15', 30', 45', 50', 55', 60', 65', 70', 75', 80', 90', 120', 180'

Wavelength, nm

EC - DARK - 1A2V

Legend: 0', 15', 30', 45', 50', 55', 60', 65', 70', 75', 80', 90', 120', 180'

PEC - 1A3V